

**Wind driven circulation in large shallow lakes
Implications for Taihu Lake**

Liu, S.

DOI

[10.4233/uuid:ba4563e2-2a45-4443-9c5f-8903b0881236](https://doi.org/10.4233/uuid:ba4563e2-2a45-4443-9c5f-8903b0881236)

Publication date

2020

Document Version

Final published version

Citation (APA)

Liu, S. (2020). *Wind driven circulation in large shallow lakes: Implications for Taihu Lake*. [Dissertation (TU Delft), Delft University of Technology]. <https://doi.org/10.4233/uuid:ba4563e2-2a45-4443-9c5f-8903b0881236>

Important note

To cite this publication, please use the final published version (if applicable).
Please check the document version above.

Copyright

Other than for strictly personal use, it is not permitted to download, forward or distribute the text or part of it, without the consent of the author(s) and/or copyright holder(s), unless the work is under an open content license such as Creative Commons.

Takedown policy

Please contact us and provide details if you believe this document breaches copyrights.
We will remove access to the work immediately and investigate your claim.

Wind driven circulation in large shallow lakes

Implications for Taihu Lake

Wind driven circulation in large shallow lakes

Implications for Taihu Lake

Dissertation

for the purpose of obtaining the degree of doctor
at Delft University of Technology
by the authority of the Rector Magnificus prof.dr.ir. T.H.J.J. van der Hagen
chair of the Board for Doctorates
to be defended publicly on
Monday 13 July 2020 at 12:30 o'clock

by

Sien LIU

Master of Science in Civil Engineering, Technology University of Delft, Delft, the
Netherlands
born in Nanjing, China,

This dissertation has been approved by the promotor[s].

Composition of the doctoral committee:

| | |
|------------------------|-----------------------------------|
| Rector Magnificus, | chairman |
| Prof. dr. M.J.F. Stive | TU Delft, promotor |
| Prof. dr. Z. Wang | TU Delft and Deltares, promotor |
| Dr. Q. Ye | TU Delft and Deltares, copromotor |

Independent members:

| | |
|---------------------------------|------------------|
| Prof. dr. ir. A.M. Heemink | TU Delft |
| Prof. dr. ir. A.E. Mynett | IHE and TU Delft |
| Prof. dr. ir. W.S.J. Uijttewaai | TU Delft |
| Dr. T.A. Bogaard | TU Delft |



Keywords: large shallow lakes; Delft3D, hydrodynamic circulation; wind-induced current; water age; river networks

Printed by: Gildeprint

Front & Back: Numerical model grid of Taihu Lake and its Basin overlapped on satellite image. (Image Landsat/copernicus).

Copyright © 2020 by S. Liu

ISBN 978-94-6402-381-7

An electronic version of this dissertation is available at

<http://repository.tudelft.nl/>.

Contents

| | |
|---|-------------|
| Summary | ix |
| Samenvatting | xiii |
| 1 Introduction | 1 |
| 1.1 Background context | 2 |
| 1.2 Problem definition and research objectives | 2 |
| 1.3 Outline | 4 |
| 2 Literature study | 7 |
| 2.1 Introduction of large shallow lakes | 8 |
| 2.2 Wind influence on large shallow lakes | 8 |
| 2.3 Challenges for large shallow lakes | 9 |
| 2.3.1 Eutrophication | 9 |
| 2.3.2 Climate change | 10 |
| 2.4 Why Taihu Lake is so specific | 12 |
| 2.4.1 Location and history | 12 |
| 2.4.2 Anthropogenic challenge | 13 |
| 2.4.3 Spatial heterogeneity. | 14 |
| 2.5 Summary | 14 |
| 3 Horizontal Circulation Patterns in a Large Shallow Lake Introduction | 17 |
| 3.1 Introduction | 18 |
| 3.2 Regional settings | 19 |
| 3.2.1 Study area | 19 |
| 3.2.2 Fluvial discharge | 20 |
| 3.2.3 Meteorological settings | 21 |
| 3.3 Methodology. | 22 |
| 3.3.1 Numerical model | 22 |
| 3.3.2 Model setup | 24 |
| 3.3.3 Model calibration | 24 |
| 3.4 Results | 26 |
| 3.4.1 Effects of wind: steady wind | 26 |
| 3.4.2 Effects of historical wet/dry seasons: | 27 |
| 3.4.3 Effects of wind speed | 30 |
| 3.4.4 Vertical variation in flow field | 30 |
| 3.4.5 Unsteady wind | 32 |

| | | |
|----------|--|-----------|
| 3.5 | Discussion | 35 |
| 3.5.1 | Numerical sensitivity. | 35 |
| 3.5.2 | Velocity vorticity: key indicator of hydrodynamic circulation | 37 |
| 3.5.3 | Transport due to horizontal circulation. | 40 |
| 3.5.4 | Is large-scale water transfer effective? | 44 |
| 3.6 | Conclusion | 48 |
| 4 | Hydrodynamic Circulation, Water Age and Water Quality Implication | 49 |
| 4.1 | Introduction | 50 |
| 4.2 | Theoretical background | 51 |
| 4.3 | Methodology. | 52 |
| 4.3.1 | Numerical model description | 52 |
| 4.3.2 | Age calculation in Delft3D | 53 |
| 4.3.3 | Model setup | 54 |
| 4.3.4 | Scenarios | 54 |
| 4.4 | Results | 57 |
| 4.4.1 | Spatial and temporal distribution of WA | 57 |
| 4.4.2 | Wind speed and direction effects. | 60 |
| 4.4.3 | Discharge effects | 61 |
| 4.5 | Discussion. | 62 |
| 4.5.1 | Various transport time scales | 62 |
| 4.5.2 | Wind change due to climate change. | 64 |
| 4.5.3 | Implication of water age on shallow lake management. | 64 |
| 4.6 | Conclusions | 65 |
| 5 | Interaction between river networks and lakes | 67 |
| 5.1 | Introduction | 68 |
| 5.1.1 | Urbanization of Taihu Lake. | 68 |
| 5.1.2 | Water and Energy Status in Taihu Basin. | 69 |
| 5.1.3 | Wuxi City: a typical city in the megalopolis of Taihu Basin | 70 |
| 5.1.4 | Water-energy nexus | 72 |
| 5.2 | Methodology. | 74 |
| 5.2.1 | Water-energy nexus model | 74 |
| 5.2.2 | D-Flow Flexible Mesh | 75 |
| 5.3 | Nexus scenarios | 76 |
| 5.4 | Hydrodynamic and water quality model | 81 |
| 5.4.1 | Model setup | 81 |
| 5.4.2 | Model calibration and validation. | 82 |
| 5.4.3 | Hydrodynamic and water quality scenarios | 82 |
| 5.5 | Results | 85 |
| 5.5.1 | Nexus evaluation | 85 |
| 5.5.2 | River network results | 87 |

| | |
|--|------------|
| 5.6 Discussion | 88 |
| 5.6.1 Water demand implication | 88 |
| 5.6.2 Hydrodynamics of the river network | 89 |
| 5.7 Conclusions | 90 |
| 6 Conclusions and recommendations | 93 |
| 6.1 Synthesis | 94 |
| 6.2 Recommendations | 96 |
| A Appendix | 99 |
| A.1 Experiment setup | 100 |
| A.1.1 Flume layout | 100 |
| A.1.2 Instruments | 102 |
| References | 107 |
| Curriculum Vitæ | 123 |
| List of Publications | 125 |
| Acknowledgements | 127 |

Summary

Providing multi-functional services including industry, agriculture, navigation and recreation, and usually locating at highly populated areas, large shallow lakes plays a significant role in the rapid urbanization process. A series of problems have occurred due to urbanization including water quality degradation, flood intensity increase, ecological and environmental issues etc. One of the most important threat comes from eutrophication, as it deteriorates water quality, introduces harmful algal blooms, harms lake ecosystems, affecting human health and hinders social-economic development. Eutrophication, from Greek word *eutrophos*, by definition from dictionary is a state of lakes and ponds to be "rich in mineral and organic nutrients that promote a proliferation of algae and aquatic plants, resulting in a reduction of dissolved oxygen". One of the typical example is Taihu Lake, which locates at the southeast part of China. As the 3rd largest shallow lake in China with urbanization rate over 80% in its basin, Taihu Lake faces severe eutrophication problems, which threatens drinking water safety for over 4 million people.

Prior to this study, researches of Taihu Lake's eutrophication problem are mainly devoted to chemical, biological and ecological aspects, while research efforts for hydrodynamics that transport and mix nutrient in the lake is scarce. Therefore it is hardly found in literature why the consequently ecological and biological pattern varies temporally and spatially in large shallow lake. Moreover, knowledge of wind effects on lake scale circulation and further water quality implication with influence of physical factors including tributary discharge, precipitation and topographical contour are unclear. To improve the understanding of wind effects on large shallow lakes, the present study is aimed at quantitatively describing the spatial and temporal varying wind induced hydrodynamics with its water quality effects of large shallow lakes. Special attention was paid to Taihu Lake and Taihu Basin, of which the underlying physics related to wind induced hydrodynamics, implication of wind induced hydrodynamics to shallow lake system and response to external changing environment of climate change and urbanization are analyzed.

To investigate the rich structure of spatial and temporal varying hydrodynamic circulation (i.e. direction, intensity and position) in Taihu Lake with complex geometry and irregular shape and to quantify wind induced changes in hydrodynamic circulations (volume exchange between sub basins and vertical variations) on spatial scales, we first define hydrodynamic circulation in large shallow lakes spatially heterogeneous large-scale movement of water, and velocity vectors and particle tracers are used to indicate the hydrodynamic circulation patterns. A three-dimensional, numerical Delft3D model of Taihu Lake, driven by steady and/or unsteady wind, river discharge, rainfall and evaporation is setup. The model is calibrated with observed water level of 5 monitoring stations, showing its capability for prediction. Stable circulation pattern is found to form after 2 days with steady wind, where

the overall hydrodynamic circulation structure, i.e. direction, intensity and position, is determined by wind direction, wind speed and initial water level. Vertical variations of horizontal velocity are found to be related to the relative shallowness of water depth. Volume exchange between sub-basins, influenced by wind speed and initial water level, differs due to the complex topography and irregular shape. With unsteady wind, these findings are still valid to a high degree. Vorticity of current velocity, as the key indicator of hydrodynamic circulation is determined by wind direction, bathymetry gradient and water depths while the maximum change of velocity vorticity happens when wind direction and bathymetry gradient are perpendicular to each other. Furthermore, Lagrangian-based tracer tests are used to assess emergency pollution/leakage effects and to evaluate water transfer effects, suggesting the model's potential to serve as an operational management tool model. The water transfer project shows that even a large scale water transfer (about 1/5 volume of total lake volume in 138 days from Yangtze River) does not alter the hydrodynamic circulation and volume exchanges between sub basins significantly, but it succeeds to transport and mix the imported Yangtze River water to the majority of Taihu Lake area.

To provide quantitative comparison of nutrient load from different parts of the catchment river networks and investigating meteorological influence on the advection and mixing process of nutrient from tributary discharge inside Taihu Lake, concept of water age is adopted in this study as indicator of transport time. First, the inflow tributaries are divided into three groups based on upstream catchment subbasins and the boundary condition of the hydrodynamic model, to represent nutrient inflow from different external sources. Then, a water quality model with hydrodynamic information from last chapter is setup and water age movement is simulated. Results show that for all three groups of inflow discharge, water age distribution show spatial and temporal heterogeneity, influenced by distance to the tributary boundaries and total discharge through tributary boundary for each group. Wind effects, from both wind speed and wind direction, is significant in changing water age distribution, meaning the nutrient flux is strongly modified by wind. Other than that, tributary discharge show smaller influence on water age distribution. Further, wind speed change effects due to climate change is modelled and results show other than encouraging of internal nutrient release, declined wind speed also causes external nutrient to stay longer inside Taihu Lake, both of which are exacerbate current eutrophication status.

Finally, influence of urbanization of Taihu Basin water environment is studied, using Wuxi city as an example. The Water-Energy-Nexus method is adopted to study the water resource allocation and water environment in adjacent river network with the consideration of energy in Wuxi city. First, at the Wuxi city scale, based on history water consumption data, water availability, and master water resource management plan, 10 scenarios are designed and analysed with The Water Evaluation And Planning system (WEAP) based on assumptions of urbanization development, industrial structure adjustment, agricultural development, Yangtze River delta megalopolis development, and multi water use efficiency improvement. Then the WEAP model results are used as the input of hydrodynamic and water quality

model D-FLOW Flexible Mesh (DFM), to simulate and study effects of changing water and energy allocation pattern on the environment of river network using particle tracking model. The DFM model uses a combination of quadrilateral and triangular mesh mode and covers both Taihu Lake and surrounding river network, with special refinement near Wuxi city. Results analysis show the total water demand increase due to rapid urbanization and industrial development, while increase of water use efficiency helps to decrease the total water demand. Specially, water use efficiency for energy production and industry has significant effect on water demand in the long run. Wastewater treatment plant effluent is predicted to increase with urbanization, but with high water efficiency scenarios using the integrated planning of urbanization development, the impact on the hydrodynamic and water environment of the whole system can be mitigated to the utmost extent.

In summary, this thesis presents a series of studies focusing on wind induced hydrodynamic circulation in large shallow lake, with the implication of Taihu Lake from lake scale hydrodynamic study, to lake scale water quality implication, and to basin scale implication. The proposed modelling approach could serve as a basis and provide information on lake scale wind effects on hydrodynamic circulation and catchment scale urbanization implication on water environment for management and planning of Taihu Lake and Taihu Basin.

Samenvatting

Grote ondiepe meren spelen een belangrijke rol in snelle urbanisatie-processen en bieden multifunctionele diensten, waaronder industrie, landbouw, navigatie en recreatie, en bevinden zich meestal in dichtbevolkte gebieden. Een typisch voorbeeld is het meer van Taihu, dat zich in het zuidoostelijke deel van China bevindt en wordt gekenmerkt door zijn typische, onregelmatige vorm. Er zijn een aantal problemen opgetreden als gevolg van verstedelijking, waaronder verslechtering van de waterkwaliteit, een verhoogde overstromings-intensiteit en algemene ecologische en milieukwesties (enz.). Een van de belangrijkste bedreigingen is eutrofiëring, omdat het de waterkwaliteit verslechtert, schadelijke algenbloei introduceert, de ecosystemen van het meer beschadigt, de menselijke gezondheid beïnvloedt en de sociaal-economische ontwikkeling belemmert. Eutrofiëring, van het Griekse woord *eutrophos*, is per definitie een staat van meren en plassen die "rijk zijn aan minerale en organische voedingsstoffen die een proliferatie van algen en waterplanten bevorderen, wat resulteert in een vermindering van opgeloste zuurstof". Het meer van Taihu is het op twee na grootste ondiepe meer in China met een urbanisatie percentage van meer dan 80% in haar bekken. Het heeft een ernstig eutrofiërings-probleem, dat de veiligheid van het drinkwater voor meer dan 4 miljoen mensen bedreigt.

Voorafgaand aan dit proefschrift waren studies naar het eutrofiëringsprobleem van het meer van Taihu vooral gericht op chemische, biologische en ecologische aspecten, terwijl onderzoek naar de hydrodynamica in het meer schaars is. Er is nauwelijks literatuur naar de redenen waarom de ecologische en biologische patronen in dit grote ondiepe meer in tijd en ruimte variëren. De kennis van windeffecten op de circulatie en de implicaties voor de waterkwaliteit onder invloed van fysische factoren, zoals afvoer van zijrivieren, neerslag en topografische contouren, ontbreken. Om het begrip van windeffecten op grote ondiepe meren te verbeteren, is deze studie gericht op de kwantitatieve beschrijving van de ruimtelijke en temporele variatie van door wind geïnduceerde hydrodynamica en de effecten hiervan op de waterkwaliteit van grote ondiepe meren. Speciale aandacht werd besteed aan zowel het meer van Taihu als het Taihu-bassin, waarbij de onderliggende fysica met betrekking tot door wind geïnduceerde hydrodynamica, de implicatie van door wind geïnduceerde hydrodynamica op een ondiep merenstelsel en de reactie op klimaatverandering en verstedelijking werden geanalyseerd. Om de rijke structuur van ruimtelijke en temporele variërende hydrodynamische circulatie (dwz richting, intensiteit en positie) in het meer van Taihu (met zijn complexe geometrie en onregelmatige vorm) te onderzoeken en om de door wind veroorzaakte veranderingen in hydrodynamische circulaties (volume-uitwisseling tussen sub-bassins en verticale variaties) op ruimtelijke schaal te kwantificeren, wordt eerst de hydrodynamische circulatie in grote ondiepe meren gedefinieerd als een ruimtelijk heterogene

grootschalige beweging van water, met behulp van snelheidsvectoren en deeltjes traceerders om de hydrodynamische circulatiepatronen aan te geven. Een driedimensionaal model, Delft3D, van meer van Taihu, aangestuurd door constante en / of wisselvallige wind, rivierafvoer, neerslag en verdamping, is opgezet. Het model is gekalibreerd met de waargenomen waterniveaus bij 5 meetstations, daarmee het vermogen tot voorspelling aantonend. Modelresultaten tonen aan dat een stabiel circulatiepatroon wordt gevormd na 2 dagen met constante wind, waarbij de algehele hydrodynamische circulatie-structuur, dwz richting, intensiteit en positie, wordt bepaald door windrichting, windsnelheid en aanvankelijk waterniveau. Verticale variaties van horizontale snelheid zijn gerelateerd aan de relatieve ondiepte van de waterdiepte. Uitwisseling van volume tussen de sub-bassins, beïnvloed door windsnelheid en aanvankelijk waterniveau, verschilt vanwege de complexe topografie en de onregelmatige vorm. Bij wisselvallige wind zijn deze bevindingen nog steeds in hoge mate geldig. Vorticititeit van huidige snelheid, als de belangrijkste indicator van hydrodynamische circulatie, wordt bepaald door windrichting, bathymetrie-gradiënt en waterdiepten, terwijl de maximale verandering van snelheids-vorticititeit optreedt wanneer windrichting en bathymetrie-gradiënt loodrecht op elkaar staan. Verder worden op Lagrangian gebaseerde traceertesten gebruikt om vervuiling / lekkage-effecten in situaties van crisis te beoordelen en om wateroverdrachtseffecten te evalueren, wat suggereert dat het model kan dienen als een operationeel managementinstrument. De simulatie van wateroverdracht laat zien dat zelfs een grootschalige wateroverdracht (ongeveer 1/5 volume van het totale volume van het meer in 138 dagen vanaf de Yangtze Rivier) de hydrodynamische circulatie en volume-uitwisselingen tussen de sub-bassins niet significant verandert, maar er in slaagt om het geïmporteerde Yangtze rivierwater in het grootste deel van het Taihu Lake-gebied te transporteren en te vermengen.

Om een kwantitatieve vergelijking van nutriënten uit verschillende delen van de stroomgebieden van het rivierennetwerk te verkrijgen en om meteorologische invloeden op het advectie- en mengproces van nutriënten uit de afvoer van de zijtakken in het meer van Taihu te onderzoeken, is in deze studie het concept van 'watertijd' aangenomen als indicator. Ten eerste is de instroming uit de zijtakken verdeeld in drie groepen op basis van de bekkens in de stroomopwaartse stroomgebieden en de grensvoorwaarden van het hydrodynamische model, om de instroom van voedingsstoffen uit verschillende externe bronnen weer te geven. Ten tweede wordt een waterkwaliteitsmodel met hydrodynamische informatie opgesteld en wordt de beweging van de 'watertijd' berekend. Resultaten tonen in het geval van alle drie afvoer van instroom groepen aan, dat de watertijd distributie een ruimtelijke en temporele heterogeniteit vertoont, beïnvloed door de afstand tot de buitengrens van de zijrivier en door de totale afvoer via de buitengrens van de zijtakken voor elke groep. Windefecten van zowel windsnelheid als windrichting zijn significant bij het veranderen van de watertijdsdistributie, wat betekent dat de voedingsinflux sterk wordt gewijzigd door wind. Bovendien vertoont afvoer uit de zijrivieren een kleinere invloed op de verdeling van de watertijd. Voorts wordt de daling van de windsnelheid gemodelleerd als gevolg van klimaatverandering. Naast de toename in het vrijkomen van meer interne voedingsstoffen, heeft een daling

van de de windsnelheid ook tot gevolg dat externe voedingsstoffen langer in het meer van Taihu blijven, welke beide de huidige eutrofiëring verergeren. Ten slotte wordt de invloed van de verstedelijking van het water milieu van het Taihu Basin bestudeerd, met de stad Wuxi als voorbeeld. De 'Water-Energy-Nexus' methode wordt gebruikt om de toewijzing van waterbronnen en het watermilieu in aangrenzende riviernetwerken te bestuderen met het oog op de productie van energie. Ten eerste worden op de schaal van de stad Wuxi, op basis van historische water verbruiksgegevens, waterbeschikbaarheid en het masterplan voor het waterbeheer van de stad, 10 scenario's ontworpen en geanalyseerd. Het 'water-evaluatie- en planningssysteem' (WEAP) wordt gebruikt, gebaseerd op veronderstellingen van de ontwikkeling van urbanisatie in de megalopool van de Yangtze Rivier delta, met name industriële reconstructie, ontwikkeling van de landbouw en de verbetering van de efficiency van multifunctioneel watergebruik. Vervolgens worden de resultaten van het WEAP-model gebruikt als input voor het hydrodynamische- en waterkwaliteitsmodel 'D-FLOW Flexible Mesh' (DFM) om de effecten van veranderende water- en energietoewijzingspatronen op de omgeving van het riviernetwerk te simuleren met behulp van een model dat de deeltjes traceert. Het DFM-model maakt gebruik van een combinatie van vierhoekige en driehoekige mazen en omvat zowel het meer van Taihu als het omliggende riviernetwerk, met verfijnde details in de buurt van de stad Wuxi. Analyse van de resultaten toont aan dat de totale vraag naar water toeneemt als gevolg van snelle urbanisatie en industriële ontwikkeling, terwijl een toename van de efficiëntie van het watergebruik bijdraagt aan vermindering van de totale vraag naar water. In het bijzonder heeft de efficiëntie van watergebruik voor energieproductie en voor industrieel gebruik op de lange termijn een aanzienlijk effect op de vraag naar water. Rioleringsinstallaties zullen toenemen met verstedelijking, maar met een hoog efficiënt watergebruik-scenario met een geïntegreerde planning van stedelijke ontwikkeling, kan het effect op de hydrodynamische- en water omgeving van het gehele systeem tot in het uiterste beperkt worden.

Samenvattend presenteert dit proefschrift een reeks studies gericht op door de wind geïnduceerde hydrodynamische circulatie in een groot ondiep meer, namelijk het meer van Taihu, met de implicatie van hydrodynamisch onderzoek op de waterkwaliteit op de schaalgrootte van een meer tot de waterkwaliteit op de schaalgrootte van een bassin. Deze modelmatige aanpak van de implicaties op de effecten van wind op de schaal van een meer op de hydrodynamische circulatie, en de verstedelijking op de schaal van een geheel stroomgebied op het water milieu zou een basis en informatief uitgangspunt kunnen zijn voor het beheer en de planning van het meer van Taihu en het Taihu Basin.

1

Introduction

1.1. Background context

Urbanization, by definition, is a “complex socio-economic process that transforms the built environment, converting formerly rural into urban settlements, while also shifting the spatial distribution of a population from rural to urban areas.” (Nations, 2018) Urbanization has been a major theme and a global challenge during the 20th century. The urban population worldwide has grown more than four-fold, from around 800 million to an estimated 4.2 billion between (the years of) 1950 and 2018 (Nations, 2018).

Large shallow lakes, especially those located in highly urbanized areas, provide multi-functional services for industry, agriculture, navigation and recreation, unfortunately they often suffer from severe eutrophication problems (Janssen et al., 2014; Paerl et al., 2011b; Smith et al., 1999). The increased population due to urbanization causes rising sewage effluent and excess nutrients load (Le et al., 2010).

The large shallow Taihu Lake and its Basin, considered to have the fastest urbanization rate and the highest urbanization level, face a series of challenges due to urbanization, including water quality degradation, flood intensity increase, ecological and environmental issues etc. One of the best-known events is the algae bloom in 2007 which caused significant financial and environmental losses (Qin et al., 2010). Increased attention has been paid to these issues by government and society, since Taihu Lake plays a significant role in the social-economic development of the country, and many studies about the recovery procedure have been published (Deng et al., 2015b; Guo, 2007; Qin et al., 2019; Xu et al., 2015b).

Due to the shallowness, large shallow lakes, compared to deep lakes, are more sensitive to wind, evaporation and human interference (Gulati2008, Leira2008, Nutz2018). Thus, understanding how human activity and climate change modify the lake is important.

1.2. Problem definition and research objectives

The question that arises is what role wind plays in the dynamics in both Taihu Lake and (the whole) Taihu Basin. For the last several decades, more attention was paid to the ecological behavior with the changing nutrient availability, but the wind-induced hydrodynamics that mix and transport nutrients received less consideration. As a consequence, less attention was paid to the reasons why the consequently ecological and biological pattern varies temporally and spatially in the large shallow lake.

To quantitatively describe the wind induced hydrodynamics of large shallow lakes, especially for Taihu Lake, is challenging since the spatial scale of the horizontal and vertical directions is hugely different. Besides, although the spiderweb like river networks inside Taihu Basin are very complex, the implication of the wind is also influenced by human activities and climate change.

The main objective of this study is to improve our understanding of the physical processes of wind driven circulation in large shallow lakes at different temporal and spatial scales.

Specifically, for Taihu Lake, we aim to investigate (1) the underlying physics related to wind induced hydrodynamics, and (2) the implication of wind induced hydrodynamics for a shallow lake system. In particular this research focuses on 3 different research questions as discussed below:

(1)What is the effect of wind on the spatial and temporal hydrodynamic circulation pattern in Taihu Lake?

Insight into the wind-induced large scale hydrodynamic circulation is essential for the understanding of the whole shallow lake ecosystems, as it has a key role as the dynamic driver of the system. However, the wind induced large-scale circulation is usually poorly understood since more attention has been given to the water quality and to the biological and ecological aspects of large shallow lakes.

In this study, hydrodynamic circulation in shallow lakes is defined as the spatially heterogeneous large-scale movement of water. To quantitatively examine the large-scale hydrodynamic circulation induced in Taihu Lake, numerical tools are adopted. A three-dimensional Delft3D model is designed to investigate the rich structure of spatially and temporally varying hydrodynamic circulation (i.e. direction, intensity and position) in a large shallow lake with a complex geometric and irregular shape. In particular, the implication of anthropologic effects on wind-induced hydrodynamics is researched.

On a smaller scale, wind-induced waves and currents play more extensive roles in the air-water, water-sediment interactions and the mixing processes inside water columns, and in turn affect the nutrient cycling and the water quality. A flume experiment is adopted to investigate the smaller scale circulation in shallow lakes.

Previously, this type of experiment focused more on only the vertical circulation but less on the situation when both vertical and horizontal circulations occur. Thus, we modified the flume to create a horizontal circulation inside the flume; influence of wind speed, fetch lengths, and water depth are examined.

Additionally, due to the fast changing environment, caused mainly by anthropogenic activities and climate change, the implication of wind driven circulations are further examined with the following 2 research objectives.

(2)What is the implication of wind induced hydrodynamic circulation on the water quality?

The external nutrient input is assumed a significant contributor for the nutrient balance in shallow lakes. Serving as point-sources for the lake, the external nutrients from river inlets also accumulate the diffusive nutrient release from all over the catchment. After they enter Taihu Lake, the incoming nutrients are transported and mixed with circulating water and further influence the ecosystems of the lake.

Numerical tools designed to answer the first research objective were developed with the adoption of a transport time scale, the so-called "water age." The analysis of the model results shows how wind induced hydrodynamics are causing the spatial and temporal variability in nutrient distributions inside the lake.

(3)What main hydrodynamic, water quality implications can be observed under the changing environment with wind induced hydrodynamic circulation on the catchment scale tributary systems of Taihu Lake?

Due to fast urbanization, the population along Taihu Lake and its catchment area is booming and in turn causes the adaption of an energy industry pattern. By adopting the so-called “water-energy nexus” approach, the study gives insight into the amount of water consumption, effluent disposal, the related water quality and the ecological implications of the whole catchment water system, including both Taihu Lake and the adjacent river networks with a D-Flow Flexible Mesh model.

1.3. Outline

The major aim of this research is to describe the influence of wind on large shallow lakes water systems. The structure of this thesis reflects the objectives shown above.

Chapter 1 presents an introduction to this study, specifically an introduction to the study site. The main objective of this research is presented, followed by specific research questions.

Chapter 2 gives a general review about the state of the art of large shallow lake research, providing detailed information about the challenges for shallow lake systems and, specifically for shallow lakes in Jiangsu Province, China.

Chapter 3 describes the large-scale hydrodynamic circulation induced by wind forcing; a Delft3D numerical model is setup, calibrated and used to analyse wind influence for both horizontal and vertical structure of large-scale hydrodynamic circulation in the large shallow Taihu Lake. The calibrated model is further applied to discuss the effectiveness of the famous water transfer project.

Chapter 4 presents a water age study application, which is an extension of wind induced hydrodynamic circulation. Water circulation inside the lake is discussed and analyzed.

Chapter 5 gives insight into a large spatial scale water circulation/change/interaction between Taihu Lake and the surrounding river networks using D-Flow Flexible Mesh models.

Chapter 6 synthesizes the key findings of this study and gives recommendations for further research.

The Appendix introduces a series of flume experiments, which are designed for the smaller-scale hydrodynamics induced by wind. An innovative flume modification is presented.

The outline of this thesis is visualized in Figure 1.1.

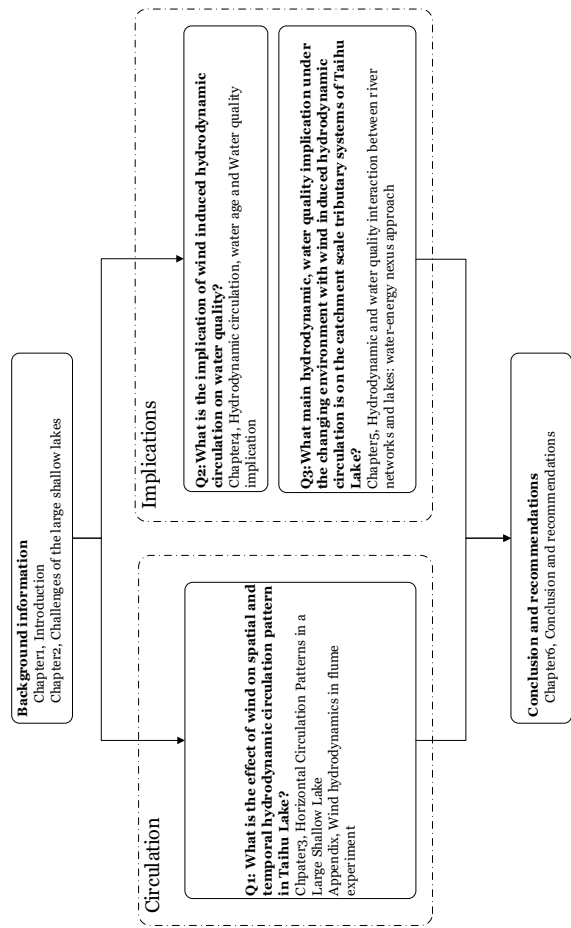


Figure 1.1: Thesis outline

2

Literature study

2.1. Introduction of large shallow lakes

Large shallow lakes, usually defined as large lakes which are usually well-mixed and non-stratified for long periods of time, as having intensive water-sediment interactions, and with a larger possibility to be colonized by macrophytes (Scheffer, 2004). Most of these lakes have an averaged depth of less than 3m, but a surface area larger than 100km². Compared to deep lakes, the water-sediment interaction of a large shallow lake potentially contributes more to the ecosystem.

Due to the shallowness, large shallow lakes are fundamentally different from deep lakes. Since the 1980s, large numbers of researches have been carried out to better understand the dynamics of the large shallow lakes and to be able to manage the lakes more efficiently (Beklioglu et al., 2016).

Large shallow lakes are usually located in populated areas, providing for various purposes, including agriculture, industry, residence, urban development and entertainment, etc. It is crucial to sustain a healthy state of the lake as the foundation of socio-economic development in the catchment area.

2.2. Wind influence on large shallow lakes

Water circulations in large shallow lakes play key roles in the development of the water environment and ecosystem, as it is related to physical processes, such as sediment resuspension, nutrient transporting and mixing, which influence the biological process like phytoplankton growth by altering the light penetration conditions, nutrient availability etc. (Madsen et al., 2001). For large shallow lakes, the major energy input of water circulation is from the surface air-water interaction.

Wind itself, as an environmental factor, has a spatial and temporal heterogeneity. With large scales of space and time, wind influences on large shallow lakes could even change the alternative stable states (Beklioglu et al., 2006; Liu, 2013; Scheffer et al., 2001).

Through surface shear stress, wind transfers momentum from air to water, which generates waves, currents and turbulence (Józsa, 2014; Wüest and Lorke, 2003). These processes together determine the spatial and temporal distribution of phytoplankton and further stimulate the algae bloom. Many studies have been carried out to show the linkage of the physical processes with the biological processes.

Waves induced by wind with various intensities, duration and fetch lengths are considered to be relevant for algae bloom (Qin et al., 2007; Wu et al., 2013; Zheng et al., 2015). With a low wind condition with smaller waves, cyanobacteria are horizontally migrated through waves and currents, while during a high wind speed condition, e.g. a typhoon period, the vertical migration of cyanobacteria is influenced due to strong mixing (Cao et al., 2006). However, during a high wind speed period, wind waves enhance the bottom sediment resuspension and increase the sediment and nutrient concentration in the water column. As a consequence the light availability for submerged plants will decrease, thereby benefiting large cells of phytoplankton by the decrease of sedimentation (Zhou et al., 2015). Thus, increased wind waves, to a certain extent, alter the competence between sub-

merged macrophytes and phytoplankton and benefit the dominance of phytoplankton, which finally causes the shift between alternative stable states in large shallow lakes (Janssen et al., 2017).

Turbulence induced by wind could substantially shift the competitive balance between phytoplankton species (Huisman et al., 2004; Peters, 2006). The wind induced enhanced turbulence benefits the large cells, like diatoms, over the small cells, such as *Microcystis*, in the competition for nutrients (Prairie et al., 2012). Also, due to vertical mixing induced by turbulence, the competition for light between the large non-motile diatoms, chlorophytes and buoyant cyanobacteria is changed. The gas-vacuolated cyanobacteria gain advantage under less dynamic conditions by floating to the upper layer for light and nutrients (Oliver, 1994). This advantage is diminished in a highly turbulent environment, whereas non-motile diatoms, chlorophytes, show better adaption with a fluctuating light availability (Huisman et al., 2004).

Turbulence also influences the feeding rate of herbivorous zooplankton (Zhou et al., 2015). Predators, like herbivorous zooplankton, as a food source, generally prefer large cells of diatoms and chlorophytes. Although turbulence increases the chance of an encounter between them, it decreases the capture rate of the predator (Pécseli et al., 2014). In this way, turbulence also contributes to the dominance of diatoms and chlorophytes. Previous studies in the literature also show the dependence of dominant species on local physiological conditions, hydrodynamics and nutrient availability (Romero et al., 2012).

2.3. Challenges for large shallow lakes

2.3.1. Eutrophication

One of the most prominent issues for large shallow lakes is eutrophication. Eutrophication, from the Greek word *eutrophos*, is defined as a state of lakes and ponds to be “rich in mineral and organic nutrients that promote a proliferation of algae and aquatic plants, resulting in a reduction of dissolved oxygen.” (Morris and Others, 1969)

Eutrophication has become a big challenge for large shallow lakes, where an increasing urbanization is taking place. The threat of eutrophication affects the drinking water supply, public health and food security, and is increasingly gaining the attention of the government and the public. Wastewater production is increasing in urbanized areas due to a booming population. While over 80% of the wastewater produced worldwide is reported to be directly discharged into the environment without treatment (Connor et al., 2017), for large shallow lakes wastewater is not the only source of pollution, but also diffuse sources of pollution from accumulated nutrients from agriculture, aquaculture, rural habitation, and soil erosion through surface river networks and Lacustrine Groundwater Discharge (LGD) are threatening the shallow lake ecosystem (Le et al., 2010; Lewandowski et al., 2015).

The eutrophication phenomenon observed could be categorized as 1) natural eutrophication and 2) cultural eutrophication. The cultural eutrophication is accelerated by human activities worldwide (Schindler, 2012). Due to a fast urbanization

rate, population, industry and agriculture around lake areas are booming, causing a dramatic increase in the industrial, agricultural and urban water use, leading to an increased volume of waste water disposal. In turn, the nitrogen and phosphorus input into the system have doubled and tripled, respectively, compared to pre-industrial time (Poikane et al., 2019).

The influence of algae bloom on nature and society is tremendous; in lakes, the proliferations of biomasses could induce oxygen depletion during the degradation process, accompanied with possible toxic emissions and biomass accumulation over a water surface. In turn, massive death of aquatic flora and fauna is caused and the biodiversity is threatened. People around lakes have to suffer from a deteriorated and bad smelling water quality (CO_2 , H_2S , CH_4 etc.) (Le Moal et al., 2019; Smith et al., 2015). Aside from these direct biological influences, indirect influences including environmental damage, socio-economic threats and human health risks deserve equal attention. In May 2007, a massive algae bloom took place in Taihu Lake due to excess nutrient enrichment, leaving over 2 million people without drinking water for over 1 week time (Qin et al., 2010). Not to mention the damage to tourism and the local aquaculture industry. Similar situations also happened in Lake Erie (USA) in August 2014, where 400,000 people were short of drinking water supplies (Smith et al., 2015).

Dealing with eutrophication is no easy task. There is no single solution that is applicable to all conditions. Even a successfully implemented method could make little contribution to other similar cases (Bishop et al., 2008). Several strategies or approaches have been applied to mitigate the influence of the eutrophication problem (Rastogi et al., 2015).

The methods used in these projects included a chemical method, such as using algaecides, inhibitors or flocculants to directly eliminate the existing phytoplankton, with the risk of inevitably contaminating the water body (Hullebusch et al., 2002; Jančula and Maršálek, 2011; Murray-Gulde et al., 2002); physical methods, like diluting the eutrophic lake water with clear water (Liu et al., 2018) and bottom sediment dredging (Murakami, 1984; Zhang et al., 2010); biological methods, such as bio manipulation (Moss et al., 1996; Sierp et al., 2009); or ecological methods, such as restoring macrophytes (Hilt et al., 2006; Moss et al., 1996; Qiu et al., 2001; Strand and Weisner, 2001).

2.3.2. Climate change

Climate change is also a challenge for large shallow lakes from physical, chemical and biological perspectives. Several studies show the earth is getting warmer due to an exponential rise of anthropogenic greenhouse gas emissions, like CO_2 (Allen and Ingram, 2002; Oki, 2006). Some regions experience an even higher increase in temperature in some seasons than the global average, and scientists are highly convinced that higher average temperatures will occur over land than over the oceans (Allen et al., 2018). In turn, the hydrological cycles, the atmospheric and meteorological condition changes, all will finally lead to the deterioration of the water quality (Nazari-Sharabian et al., 2018).

Climate impact on large shallow lakes includes both direct and indirect features

given the physio-biological conditions (Whitehead et al., 2009). The meteorological factors of temperature, precipitation, wind and light availability could alter, which would seriously affect the environmental conditions, especially the trophic state of large shallow lakes (Jeppesen et al., 2014). These changes are believed to amplify the symptoms of known mechanisms and alter the ecological response related to eutrophication, including biomass production, nutrient loads, sediment resuspension and nutrient releasing etc. (Le Moal et al., 2019; Mooij et al., 2005).

Temperature change is directly linked to physical and chemical properties, including water temperature, pH, solubility and diffusion rates of large shallow lakes. Water temperature is closely related to air temperature, and considered as stimulation of algae growth (Jeppesen et al., 2009). Literature shows cyanobacteria, a group of bacteria commonly living in large shallow lakes, has accelerated its growth rate with temperatures over 25°C (Peperzak, 2003). In turn, the time of algae growth starts earlier and the duration of the growth is longer. Higher water temperatures also benefit the phytoplankton growth by stimulating microbial activity in the bottom sediment, which increases the release rate of inner phosphorus. Besides, higher temperatures change several physical factors of the lake water, including decreasing the viscosity, which causes higher nutrient concentrations near the water surface (Chung et al., 2009); and decreasing the degradation coefficients of water (Moss et al., 2003). In summary, the temperature increase will stimulate the growth of phytoplankton and, finally, algae bloom.

Precipitation is another important meteorological factor that matters to large shallow lakes and which is altered by climate change, affecting the hydrological regimes, including water cycle, water level, water quality and runoff. The climate change effect on precipitation is predicted to be uneven between different locations (Babiker et al., 2018). Around the equatorial Pacific region and some high-latitude areas, the annual mean precipitation has a large probability to increase, while in some mid-latitude and subtropical areas, the change is opposite. Thus, extreme precipitation events are more likely to occur in the higher latitude areas, resulting in more eroded sediment concentration into the lake water. Further, increased rain water would mobilize and accumulate nonpoint source pollution and deteriorate the final receiving lake water body (King et al., 2007; Reckien et al., 2017). On the contrary, areas with less precipitation are incapable to dilute pollution, causing higher nutrient concentrations and, in the end, cause an increased probability of eutrophication (Whitehead et al., 2009). Moreover, the variability of precipitation would expose the inefficiency of governance and infrastructure of large shallow lake management in many areas, especially within relatively poor areas (Reckien et al., 2017).

As the major momentum input for large shallow lakes, the global wind pattern changes with locations due to climate change. Wind effects on large shallow lakes, including wind waves, currents and turbulence, will also change. Higher wind speed induces higher sediment resuspension and accelerates internal nutrient release with a better mixing of nutrient in the water column, eventually causing degradation of the water quality (citepGons1986, Hamilton1997, Qin2007, Søndergaard1992, Wu2015a, Zhu2014a).

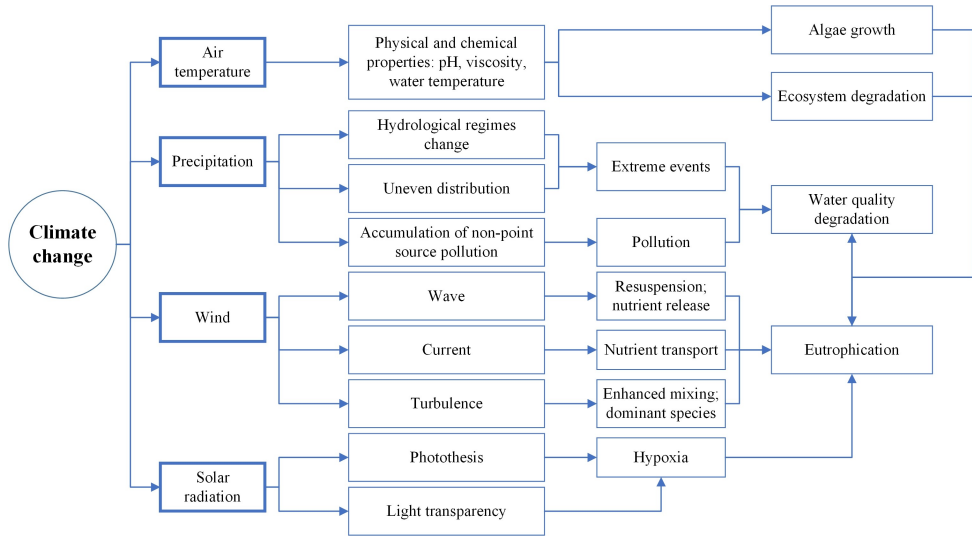


Figure 2.1: Climate change effect on large shallow lakes

Another crucial factor influencing large shallow lakes is solar radiation. As an energy source in photosynthesis, solar radiation variability is closely connected with climate change (Frey et al., 2011). Spatial and temporal distribution of solar radiation is crucial for the growth of aquatic species, including phytoplankton growth and macrophytes, etc. If insufficient solar energy is provided, plants obtain oxygen from water, causing a low DO concentration and stimulate eutrophication (Scavia et al., 2014). Since an eutrophication condition would lower the transparency, a decrease in the growth of submerged macrophytes would take place and phytoplankton would gain dominance in large shallow lakes, leading to the shift of alternative stable states (Janssen et al., 2014; Scheffer et al., 2001). However, excess solar radiation is also harmful to algae growth. The algae growth would decrease from the maximum value once the solar radiation is larger than the critical value (Häder et al., 2007; Williamson et al., 2014).

2.4. Why Taihu Lake is so specific

2.4.1. Location and history

In the southwestern part of China and with a surface area of 2338km^2 , Taihu Lake is the largest shallow lake in Jiangsu Province and the 3rd largest shallow lake in China (Hu, 2016; Li et al., 2013b). The average depth of Taihu Lake is 1.9m where the maximum depth is 3.1m . Located between Jiangsu and Zhejiang Province, Taihu Lake is only around 100km from Shanghai.

There are hundreds of large rivers at different latitudes in the world. However, the most splendid early civilizations were born on the banks of rivers at the 30-degree north latitude. The four major early civilizations, i.e. the Ancient Egypt

Table 2.1: Ten largest shallow lakes in Jiangsu Province

| Name | Location | Surface Area(km ²) | $Z_{max}(m)$ | $Z_{mean}(m)$ | $l_{max}(km)$ | $w_{max}(km)$ |
|---------------|------------------|--------------------------------|--------------|---------------|---------------|---------------|
| TAIHU 太湖 | 31°15'N 120°15'E | 2338 | 3.1 | 1.9 | 68 | 56 |
| HONGZE 洪泽湖 | 33°23'N 118°31'E | 1577 | 4.8 | 1.4 | 60 | 60 |
| GAOYOU 高邮湖 | 32°53'N 119°15'E | 675 | 2.4 | 1.4 | 48 | 28 |
| LUOMA 骆马湖 | 34°7'N 118°11'E | 260 | 5.5 | 2.7 | 27 | 20 |
| SHIJIU 石白湖 | 31°28'N 118°51'E | 210 | 2.4 | 1.7 | 22 | 14 |
| GE 隔湖 | 31°35'N 119°48'E | 147 | 1.9 | 1.1 | 22 | 9 |
| YANGCHENG 阳澄湖 | 31°25'N 120°45'E | 119 | 3 | 1.9 | 17 | 8 |
| BAIMA 白马湖 | 33°14'N 119°7'E | 108 | 1.8 | 0.9 | 18 | 11 |
| TAO 洮湖（长荡湖） | 31°35'N 119°35'E | 89 | 2 | 1.1 | 16 | 8 |
| SHAobo 邵伯湖 | 32°35'N 119°26'E | 63 | 1.4 | 1.1 | 17 | 6 |

civilization on the Nile River; the Babylonian civilization on the Euphrates River in Mesopotamia; the Indus Valley civilization on the Indus River, as well as the ancient Chinese civilization on the Yangtze River are all included. The different ethnicities created the same glory, which is an intriguing phenomenon.

Situated in the Yangtze River delta, Taihu Lake is also the birthplace of one of the earliest civilizations. The record of human activities in the basin could be traced back to the Neolithic Age (Cailin et al., 2000). Evidence shows the footprint of the Majingbang (5000 BC to 3300 BC) and the Liangzhu cultures (3400 BC to 2250 BC), where ancient Chinese people started to cultivate rice, domesticate livestock and engage in fishery. To this day, this region still bears the name of “Yu Mi Zhi Xiang,” which means the land of fish and rice.

The typical climate is believed to have contributed to the development of civilization near Taihu Lake. Taihu Lake has a typical monsoon climate with moderate temperatures and the weather is characterized by a prevailing southeast wind in the summer and a northwest wind during the winter (Li et al., 2013b; Qin et al., 2010). The climate is primarily influenced by the subtropical highs, while the regional precipitation is regulated mainly by the summer monsoon circulations (Zhang et al., 2005).

Around Taihu Lake hundreds of shallow lakes lie scattered in Jiangsu Province. The ten largest ones are listed in Table 2.1, where Taihu Lake and Hongze Lake are respectively the 3rd and 4th largest shallow lakes in China. These large shallow lakes, possessing multi critical functions in the socio-economic development, are facing environmental challenges.

Taking Hongze Lake as an example; it is located in the western region of Jiangsu Province and it is serving as the first of regulating lakes along the Eastern Route of the South-to-North Water Diversion Project (SNWDP-ER). The SNWDP-ER transfers the Yangtze River water to the water deficient northern part of China. Hongze Lake is a potential drinking water source for the residents along this water diversion project. However, due to the accumulated nutrients from upstream Huai River, Hongze Lake also faces the threat of eutrophication (Jin et al., 2005; Ren et al., 2014).

As prototype of a typical lake in Jiangsu Province, Taihu lake represents the

characteristics that all lakes share: the lakes in Jiangsu Province share the same climate, serve the same function, and face the same threats. Thus, for a better understanding of the environmental mechanism and a more effective recovery approach, the study on the “typical lake” is essential. Among all the lakes, Taihu Lake, attracting the most attention and having the largest surface area, is the best choice as a study case.

2.4.2. Anthropogenic challenge

Increasing anthropogenic pressure has changed the trophic state of Taihu Lake from its pristine oligotrophic state to eutrophic state. (Janssen et al., 2014). Population in Taihu Basin grew exponentially ever since 1850, a 300% increase to 40 million in the beginning of the 21st century (Ellis, 1997). Consecutively, the fast development of industry, agriculture and aquaculture in this area has increased the amount of waste water load and nutrient input. In recent years, industry wastewater treatment has become a topic of serious consideration. Taking Wuxi city as example, around 2000 chemical plants were shut down after 2007 for the restoration of Taihu Lake water quality, but diffuse pollution sources, due to municipal, agricultural and aquaculture uses, as well as accumulated nutrients in the sediment, still threatens the lake.

River networks in Taihu Basin are complex and play an important role in transporting wastewater or runoff from municipal, industrial and agricultural use. The tributary discharge into Taihu Lake serves as a point source of nutrients, accumulating diffuse sources of nutrients in the catchment, and induces critical ecological and sanitary issues (WANG et al., 2007). As a consequence of the rapid development of urbanization, rivers are overloaded with pollutants. The pollutants are transported with tributaries discharges into the lake, resulting in a deterioration of water quality and a potential threat to the public health (Su et al., 2014; Wu et al., 2015; Yao et al., 2015).

In order to deal with flooding threat, the embankments of the rivers within the river networks connecting Taihu Lake are enhanced with concrete structures and locks are built. These hydraulic structures strongly influence the natural water level fluctuations and cut off the connection of the lake with its surrounding wetlands (Yang and Liu, 2010).

2.4.3. Spatial heterogeneity

Taihu Lake provides a good example to study the response to and implication of a changing environment. Ongoing urbanization in the surrounding basin area has already caused significant increases in its nutrient concentration. The pristine state concentration for nutrient loads of phosphorus and nitrogen is under $0.4\text{g}/\text{m}^2/\text{yr}$ and $8\text{g}/\text{m}^2/\text{yr}$ respectively. While in 2012, these values have more than doubled to $0.93\text{g}/\text{m}^2/\text{yr}$ and $19\text{g}/\text{m}^2/\text{yr}$ (Janssen et al., 2017; Shuwen et al., 2011; Xu et al., 2015a). The result of the excessive nutrient load is the proliferation of cyanobacteria, which eventually causes the algae bloom and threatens the public health and drinking water security of millions of people.

There is strong spatial heterogeneity in the environmental status of Taihu Lake.

Due to the higher elevation of the western part of the lake, the tributaries with inflow discharge are mostly located at the northern and western boundaries. Every year, a large amount of nutrients enters the lake with inflow discharge, leading to a higher nutrient concentration in the west. Consequently, Taihu Lake is divided into 2 parts, namely the grass-type zone in the west and the algae-type zone in the northern and western part. Algae bloom break out more frequently in the algae-type zone, while due to the hydrophytes the water quality is better in the grass-type zone (Yang et al., 2019). In addition, nutrient release due to sediment resuspension and extreme meteorological events are strongly correlated with algae bloom.

2.5. Summary

Large shallow lakes are usually located in populated areas and provide multiple functions; in particular they are an important foundation of social economic development. As the main momentum input, wind plays a crucial rule on the environmental status of large shallow lakes. Through surface shear stress, wind generates waves, currents and turbulence and in turn alters the nutrient status, light availability and dominance of species of phytoplankton in large shallow lakes. Previous studies have emphasized eutrophication and climate effects, which are the two major challenges that large shallow lakes are facing. These challenges present the change of large shallow lakes due to external forcing.

Taihu Lake, located in the economically booming southeastern part of China, is a typical large shallow lake. Scattered in the Taihu Lake catchment are hundreds of shallow lakes. Together with Taihu Lake, they face the same challenges due to a fast paced urbanization. Taihu Lake also shows spatial heterogeneity due to its specific geographical features. The typical location, the urban development and its environmental status, makes Taihu Lake to the perfect case to study the response of a large shallow lake to the changing world.

3

Horizontal Circulation Patterns in a Large Shallow Lake Introduction

This chapter has been published in: Liu, S.; Ye, Q.; Wu, S.; Stive, M.J.F. Horizontal Circulation Patterns in a Large Shallow Lake: Taihu Lake, China. *Water* 2018, 10, 792.

3.1. Introduction

Large shallow lakes, especially those located in highly developed areas, provide multi-functional services for industry, agriculture, navigation and recreation, but unfortunately they often suffer severe eutrophication problems (Janssen et al., 2014; Paerl et al., 2011a; Smith et al., 1999). In general, population density around these lakes is high (Chen et al., 2014; Codd et al., 2005; Paerl et al., 2011a), which leads to an additional high waste water and associated nutrients load (Le et al., 2010). These issues have triggered increasing attention for the restoration of the water quality and ecological status of large, shallow lakes. The shallowness of lakes is usually emphasized, since the total volume of water is usually small, and shallow lakes are more sensitive to the effects of wind, evaporation and human interference, compared to the deep lakes (Gulati et al., 2008; Leira and Cantonati, 2008; Nutz et al., 2018).

There are two common approaches for shallow lake restoration nowadays, one rather effective approach is to control the source, thus to decrease the total nutrient load (Jeppesen et al., 2007; Paerl et al., 2011b), while the other approach is to increase the hydrodynamic circulation (Pastorok et al., 1981). Especially in densely populated areas, source control almost reaches the limit of the present technology, whereas enhancing the hydrodynamic circulation might offer an important contribution to improve the water quality of shallow lakes. However, comparing research on hydrodynamics in oceans, coastal zones, rivers and deep lakes (Zarzuelo et al., 2015), only limited attention has been paid to the hydrodynamics on large shallow lakes. In fact, thorough qualitative studies on horizontal circulation patterns of large shallow lakes are rather scarce, and quantitative studies are even more surprisingly rare. Especially due to their shallowness, the dominant hydrodynamic processes and the corresponding ecosystem in shallow lakes differ very much from that in deeper lakes (Cooke et al., 2016; Dake and Harleman, 1969). In deep lakes and reservoirs, due to the large depth, the temperature profile is determined by thermal stratification and mixing that dominates the hydrodynamics, especially the vertical exchange (Cooke et al., 2016). While in large shallow lakes stratification is seldom observed and which results in substantially different processes.

In large shallow lakes, i.e. with a mean depth < 3m (Cooke et al., 2016), water quality and eutrophication problems are closely related to advection and diffusion processes driven predominantly by wind forcing (Fragoso et al., 2011; QIAN et al., 2011; You et al., 2007). Momentum transferred by the wind via surface shear stresses generates waves, currents and associated turbulence (Józsa, 2014; Wüest and Lorke, 2003). While these processes are essentially three dimensional, the shallowness allows for a depth-averaged, two dimensional representation for some process features (Boegman et al., 2001; Fenocchi et al., 2016; Hulot et al., 2017; Zhang et al., 2008). Currents induced by wind forcing with velocities at the 10 cm/s scale can lead to lake-wide horizontal circulation patterns with the potential of creating vertical circulations such as Langmuir circulations (Wüest and Lorke, 2003). Furthermore, momentum transferred to the bottom will stir up sediment and keep it suspended by turbulence (Hu et al., 2006; You et al., 2007). During the suspension and resuspension of sediments, pollutions and nutrients attached to the

sediment are released into water column and then transported and mixed by the large scale circulation (Chengxin et al., 2004; Gulati et al., 2008; Yu et al., 2014). Thus, the spatial and temporal large-scale, shallow lake horizontal circulation is essential for system understanding before we move to water quality and aquatic ecosystem issues.

In this paper the focus is therefore on the spatiotemporal wind driven circulations in Taihu Lake, an unusual, extremely shallow and geometrically complex lake including bays and islands (Figure 3.1). Enhanced anthropogenic emissions in recent years, have had a huge impact on water quality and strongly motivated the eutrophication (Qin et al., 2010). Quite some studies have been carried out to seek solutions for the water quality issue of Taihu Lake. One of the most famous engineering interventions is the water transfer project, which diverts water from the Yangtze River of better water quality but more suspended sediment through to the lake, to dilute the excess nutrients and pollutions in the lake water. However, whether the water transfer project has succeeded in improving the general water quality in Taihu Lake remains unclear since a positive influence could only be observed in some parts of the lake (Hu et al., 2008; Li et al., 2011a). These facts indicate that a better understanding of the hydrodynamics of Taihu Lake is urgently required for future water quality management and restoration of the lake ecosystem.

In this chapter, numerical models are used to study the hydrodynamics and water quality of Taihu Lake under steady and unsteady wind conditions. Even though, over 20 studies have been carried out using two or three dimensional numerical models before this study, their focus was either on the resulting water quality index or on the ecological status, and none of them dedicated to a thorough, quantitative description of (wind induced) large scale hydrodynamic circulation itself, nor to the implication of hydrodynamic circulation to the environment or the ecology in this lake (Hu et al., 2016, 2006; Zhang et al., 2013).

In this research, hydrodynamic circulation in shallow lakes is defined as the spatially heterogeneous large-scale movement of water. Velocity vectors and particle tracers are used to indicate the hydrodynamic circulation patterns. Time scales are usually from days, weeks to seasons and spatial scales can be a few kilometers. Thus, barotropic seiches (1 day), wind-driven short waves (seconds) and other processes of a smaller time scale are not included in this study.

The overall goal of this study is to gain a better understanding of the wind-induced hydrodynamics and thereby to provide essential knowledge for the design and implementation of future lake restoration measurements, using state-of-the-art numerical models as a quantitative assessment tool.

Thus, our objectives in this study are to: 1. Investigate the rich structure of spatial and temporal varying hydrodynamic circulation (i.e. direction, intensity and position) in a large shallow lake with complex geometry and irregular shape; 2. Quantify wind induced changes in hydrodynamic circulations (volume exchange between sub basins and vertical variations) on spatial scales; 3. Discuss implications of anthropogenic effects, such as large-scale water transfer, on hydrodynamic circulations.

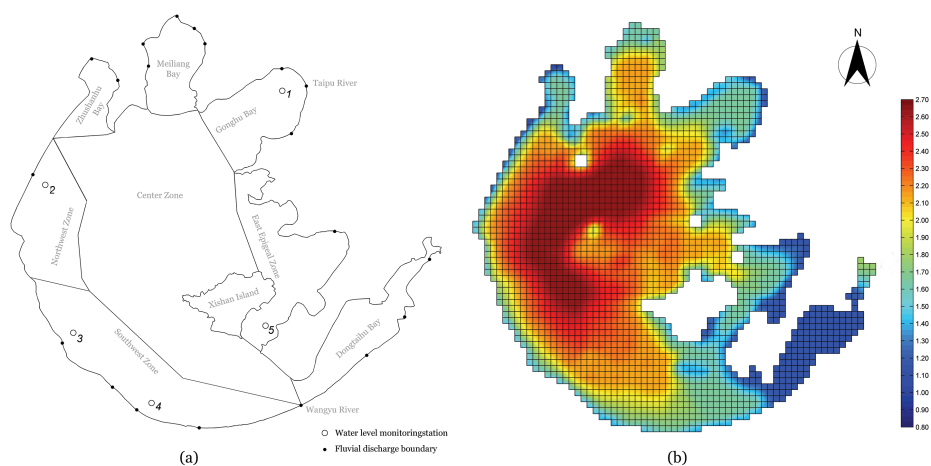


Figure 3.1: (a) Eight Subzones, boundary discharge locations, cross-sections and positions of 5 monitoring stations. (b) Grid and depth used in numerical models

3.2. Regional settings

3.2.1. Study area

Taihu Lake is the 3rd largest shallow lake in China with a surface area of 2338 km^2 (Hu et al., 2016; Li et al., 2013b). It is confronted with severe eutrophication problems. Adverse meteorological conditions and increasing waste loads in combination with the typical geometry of Taihu Lake, with the deepest part no more than 3m (Figure 3.1(b)), cause frequent blooming of algae with a disastrous impact on the ecosystem. Due to its geographical location in the Yangtze River floodplain, the Taihu Basin belongs to the most populated and economically most developed regions in China (Hu et al., 2006). The lake provides services such as water supply, flood control, navigation and recreation etc. In the area, there are over 150 river tributaries connecting to Taihu Lake. Some of these are very seasonal. Here we schematized all these branches into 20 discharge boundaries (Figure 3.1(a)). Based on the lake's geometrical and hydrological features and ecological functions, Taihu Lake is divided into eight sub basins, namely Gonghu Bay, Meiliang Bay, Zhushan Bay, Northwest Zone, Southwest Zone, Dongtaihu Bay, East Epigeal Zone and Centre Zone (Li et al., 2013b, 2011a).

Like other large shallow lakes, the hydrodynamics of Taihu Lake are more prone to be altered by wind forcing, evaporation, precipitation and human interference, etc. The dominant wind direction over the lake area in summer is southeasterly and reverses in wintertime, both directions having a large fetch length. Average wind speeds range from 3.5m/s to 5m/s (Hu et al., 2006).

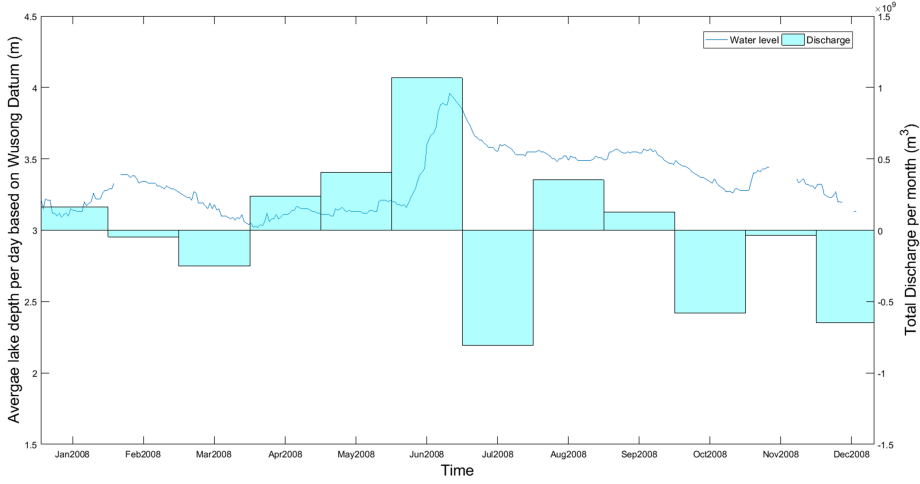


Figure 3.2: Monthly discharge data (bars, positive values represent inflow discharge) and average daily water level (red line) of Taihu Lake in 2008

3.2.2. Fluvial discharge

In situ, monthly averaged discharge data of the 20 discharge boundaries, schematically representing over 150 river tributaries connected to Taihu Lake, are provided by the Taihu Basin Authority. Due to the higher altitude of the mountainous area to the west of Taihu Lake, most of the inflow boundaries are located in the north-western part of the lake. The water transferred from the Yangtze River is injected via Taipu River at the north-east of the lake and further effluent flow goes through the Wangyu River (Figure 3.1(a)). Monthly total discharges and corresponding average total water depths in 2008 are shown in Figure 3.2.

3.2.3. Meteorological settings

The meteorological factors, namely wind, precipitation and evaporation, play significant roles in altering the hydrodynamics and water quality status of the lake. The momentum transferred from wind and water quantity variations due to precipitation and evaporation have a large influence on the consequent hydrodynamic condition. For this model research, time-series data of 10m U- and V-wind speed, precipitation and evaporation is obtained from the NOAA website with a frequency of 4 times a day. Specially for the wind speed, the data are generated onshore, so a correction of 1.2 is applied (cf. Coastal Engineering Manual). The wind shear stress over the lake surface drives the momentum transfer from wind to water. The magnitude of the wind shear stress in this study is approximated by equation (3.1):

$$\tau_s = \rho_a C_D |U_w| U_w \quad (3.1)$$

where ρ_a is the air density which is chosen 1 kg/m^3 , C_D is wind drag coefficient, and U_w is the wind velocity vector which is measured 10m above the water surface.

Table 3.1: Mass balance check in 2008 of Taihu Lake using a box model

| Water Mass Balance Check | Units: 10^9m^3 |
|-------------------------------|--------------------------|
| Total volume of Taihu Lake | 4.400 |
| Inflow from discharge inlets | 11.400 |
| Outflow from discharge inlets | 11.416 |
| Rainfall volume | 4.907 |
| Surface evaporation volume | 5.186 |
| Error of mass balance | 0.294 |
| Relative error* | 6.69% |

The magnitude of the wind drag coefficient depends on the wind speed (e.g. Smith and Banke 1975(Smith and Banke, 1975) etc.). At a free surface the boundary conditions of the numerical model for momentum transfer are:

$$\begin{aligned} \left. \frac{\nu_v}{H} \frac{\partial u}{\partial \sigma} \right|_{\sigma=0} &= \frac{1}{\rho} |\overline{\tau_s}| \cos(\theta) \\ \left. \frac{\nu_v}{H} \frac{\partial v}{\partial \sigma} \right|_{\sigma=0} &= \frac{1}{\rho} |\overline{\tau_s}| \sin(\theta) \end{aligned} \quad (3.2)$$

Where ν_v the vertical eddy viscosity, u and v are the horizontal velocity components, H is water depth, θ is the angle between the wind stress vector and the local direction of the grid-line.

The yearly total amounts of the discharge, precipitation and evaporation volume are calculated for the year 2008 and used as input for the mass balance check (Table 3.1). The total volume of Taihu Lake is derived from bathymetry data. Total inflow and outflow discharge are the summation of data of the 20 tributaries around Taihu Lake. Rainfall and evaporation volumes are calculated from the daily meteorological data from NOAA.

*The relative error is the ratio of error of mass balance of lake volume and the total volume of the lake.

3.3. Methodology

3.3.1. Numerical model

The open source three-dimensional, shallow water numerical model Delft3D, developed by Deltares, is used in this study. Delft3D consists of various modules, covering different physical processes, ranging from flow, sediment transport, morphology to water quality, aquatic ecology and particle tracking etc. The model has been extensively applied worldwide in the fields of hydrodynamics, sediment transport, morphology and water quality in fluvial, lacustrine, estuarine and coastal environments. In this study, the model is used to simulate the hydrodynamics of the lake for the purpose of illustrating the spatial and temporal large-scale hydrodynamic circulation of Taihu Lake induced by the wind shear stress and the discharge from the tributary rivers given the complex geometry and shallow bathymetry of the lake.

In the horizontal direction orthogonal curvilinear co-ordinates is adopted by Delft3D and here σ co-ordinated system is adopted for the 3D simulation in vertical. Based on shallow water and Boussinesq assumption, Delft3D solves the Navier Stokes equation for the incompressible fluid. In the vertical momentum equation, the vertical acceleration is neglected, while the vertical velocity is obtained from the continuity equation.

The depth-averaged continuity equation in ξ - and η -directions is

$$\frac{\partial \zeta}{\partial t} + \frac{I}{\sqrt{G_{\xi\xi}}\sqrt{G_{\eta\eta}}} \frac{\partial \left[(d + \zeta) U \sqrt{G_{\eta\eta}} \right]}{\partial \xi} + \frac{1}{\sqrt{G_{\xi\xi}}\sqrt{G_{\eta\eta}}} \frac{\partial \left[(d + \zeta) V \sqrt{G_{\xi\xi}} \right]}{\partial \eta} = Q \quad (3.3)$$

Where ζ and d are the water level above and below some horizontal plane of reference (datum); t is time; $G_{\xi\xi}$ and $G_{\eta\eta}$ are coefficients used to transform curvilinear to rectangular coordinates; U and V are depth-averaged velocity in ξ -direction and η -direction; Q is the contributions per unit area due to the discharge or withdrawal of water, precipitation and evaporation:

$$Q = H \int_{-1}^0 (q_{in} - q_{out}) d\sigma + P - E \quad (3.4)$$

with q_{in} and q_{out} the local sources and sinks of water per unit of volume (1/s), respectively, P the non-local source term of precipitation and E the non-local sink term due to evaporation. At the free surface there may be a source due to precipitation or a sink due to evaporation.

The momentum equation in ξ - and η -direction are given by:

$$\begin{aligned} \frac{\partial u}{\partial t} + \frac{u}{\sqrt{G_{\xi\xi}}} \frac{\partial u}{\partial \xi} + \frac{v}{\sqrt{G_{\eta\eta}}} \frac{\partial u}{\partial \eta} + \frac{w}{d+\zeta} \frac{\partial u}{\partial \sigma} - \frac{v^2}{\sqrt{G_{\xi\xi}}\sqrt{G_{\eta\eta}}} \frac{\partial \sqrt{G_{\eta\eta}}}{\partial \xi} + \frac{uv}{\sqrt{G_{\xi\xi}}\sqrt{G_{\eta\eta}}} \frac{\partial \sqrt{G_{\eta\eta}}}{\partial \xi} \\ -fv = -\frac{1}{\rho_0\sqrt{G_{\xi\xi}}} P_\xi + F_\xi + \frac{1}{(d+\zeta)^2} \frac{\partial}{\partial \sigma} \left(\nu_v \frac{\partial u}{\partial \sigma} \right) + M_\xi \end{aligned} \quad (3.5)$$

and

$$\begin{aligned} \frac{\partial v}{\partial t} + \frac{u}{\sqrt{G_{\xi\xi}}} \frac{\partial v}{\partial \xi} + \frac{v}{\sqrt{G_{\eta\eta}}} \frac{\partial v}{\partial \eta} + \frac{w}{d+\zeta} \frac{\partial v}{\partial \sigma} - \frac{uv}{\sqrt{G_{\xi\xi}}\sqrt{G_{\eta\eta}}} \frac{\partial \sqrt{G_{\eta\eta}}}{\partial \xi} + \frac{u^2}{\sqrt{G_{\xi\xi}}\sqrt{G_{\eta\eta}}} \frac{\partial \sqrt{G_{\eta\eta}}}{\partial \xi} \\ +fv = -\frac{1}{\rho_0\sqrt{G_{\eta\eta}}} P_\eta + F_\eta + \frac{1}{(d+\zeta)^2} \frac{\partial}{\partial \sigma} \left(\nu_v \frac{\partial v}{\partial \sigma} \right) + M_\eta \end{aligned} \quad (3.6)$$

Where u and v are flow velocity in ξ -direction and η -direction; f is the Coriolis factor; ρ_0 is the reference water density; P_ξ and P_η are the gradient hydrostatic pressure in ξ -direction and η -direction; F_ξ and F_η are turbulent momentum flux in ξ -direction and η -direction; σ is depth; ν_v is vertical eddy viscosity; M_ξ and M_η are the source or sink of momentum in ξ -direction and η -direction.

The transport equation in Delft3D for orthogonal curvilinear co-ordinates in hor-

horizontal and σ co-ordinates in vertical in a conservative form is:

$$\frac{\partial(d+\zeta)c}{\partial t} + \frac{1}{\sqrt{G_{\xi\xi}}\sqrt{\sigma_{\eta\eta}}} \left\{ \frac{\partial[\sqrt{G_{\xi\xi}}(d+\zeta)uc]}{\partial \xi} + \frac{\partial[\sqrt{G_{\xi\xi}}(d+\zeta)vc]}{\partial \eta} \right\} + \frac{\partial\omega c}{\partial \sigma} =$$

$$\frac{d+\zeta}{\sqrt{G_{\xi\xi}}\sqrt{G_{\eta\eta}}} \left\{ \frac{\partial}{\partial \xi} \left(D_H \frac{\sqrt{G_{\eta\eta}}}{\sqrt{G_{\xi\xi}}} \frac{\partial c}{\partial \xi} \right) + \frac{\partial}{\partial \eta} \left(D_H \frac{\sqrt{G_{\xi\xi}}}{\sqrt{G_{\eta\eta}}} \frac{\partial c}{\partial \eta} \right) \right\} + \frac{1}{d+\zeta} \frac{\partial}{\partial \sigma} \left(D_V \frac{\partial c}{\partial \sigma} \right) - \lambda_d(d+\zeta)c + S \quad (3.7)$$

Where D_H is horizontal diffusion coefficient, D_V is vertical diffusion coefficient, λ represents the first order decay process and S is the source and sink terms per unit area due to boundary discharge and free surface exchange.

3.3.2. Model setup

A Cartesian rectangular computational grid is used with a grid resolution of 1000m and a total grid number of 9660. For three-dimensional scenarios, 5 vertical sigma layers are defined uniformly. For Taihu Lake, the deepest point of the lake appears in the lake's center area at 2.66m, while the shallow points are located close to shorelines, having a typical depth of 0.8m. The reference scenario simulates the hydrodynamics of the lake over the entire year of 2008. The simulation time step is based on the Courant-Friedrichs-Lewy (CFL) number and the grid size. To ensure model stability and accuracy, the time step is set to be 5min. The output time step for observation points is 60mins.

3.3.3. Model calibration

The numerical model calibration uses meteorological data and boundary river discharge data for the entire year of 2008. For bottom roughness, we use the Chzy formula with the roughness coefficient assumed constant at $65m^{1/2}s^{-1}$ for the entire lake. Horizontal viscosity is set to be $0.002m^2s^{-1}$ based on literature (Falconer et al., 1991). For vertical turbulent transport process, a standard $k - \varepsilon$ turbulence model is used. For model calibration, in situ measurements of water levels from 5 monitoring stations across the lakes (for locations see Figure 3.1; data source TBA) are compared to the simulated results in Figure 3.3. These 5 monitoring stations are respectively Wangting station, Dapukoua station, Jiapu station, Xiaomeikou station and Xishan station. Water levels were observed once a day at each station with occasional interruptions. Figure 3.3 shows that, although the 5 monitoring stations are located in different parts of the lake, the water levels show very similar trends. Considering the water level difference, due to wind setup over the largest fetch length in Taihu Lake with constant 5m/s wind is 5cm scale, and given the comparison of tributary discharge and average water level trends (Figure 3.2) with the mass balance check result (Table 3.1), water levels in Taihu Lake are predominately modulated by tributary discharge, precipitation and evaporation. The water levels had a slight increase until mid-February and reached an annual peak value at the beginning of July, then gradually fell to 0 at the end of the year. The highest water level of the whole lake reaches around 1m while the lowest water level is around 0m at the beginning of April. A summary of the quantitative model performance

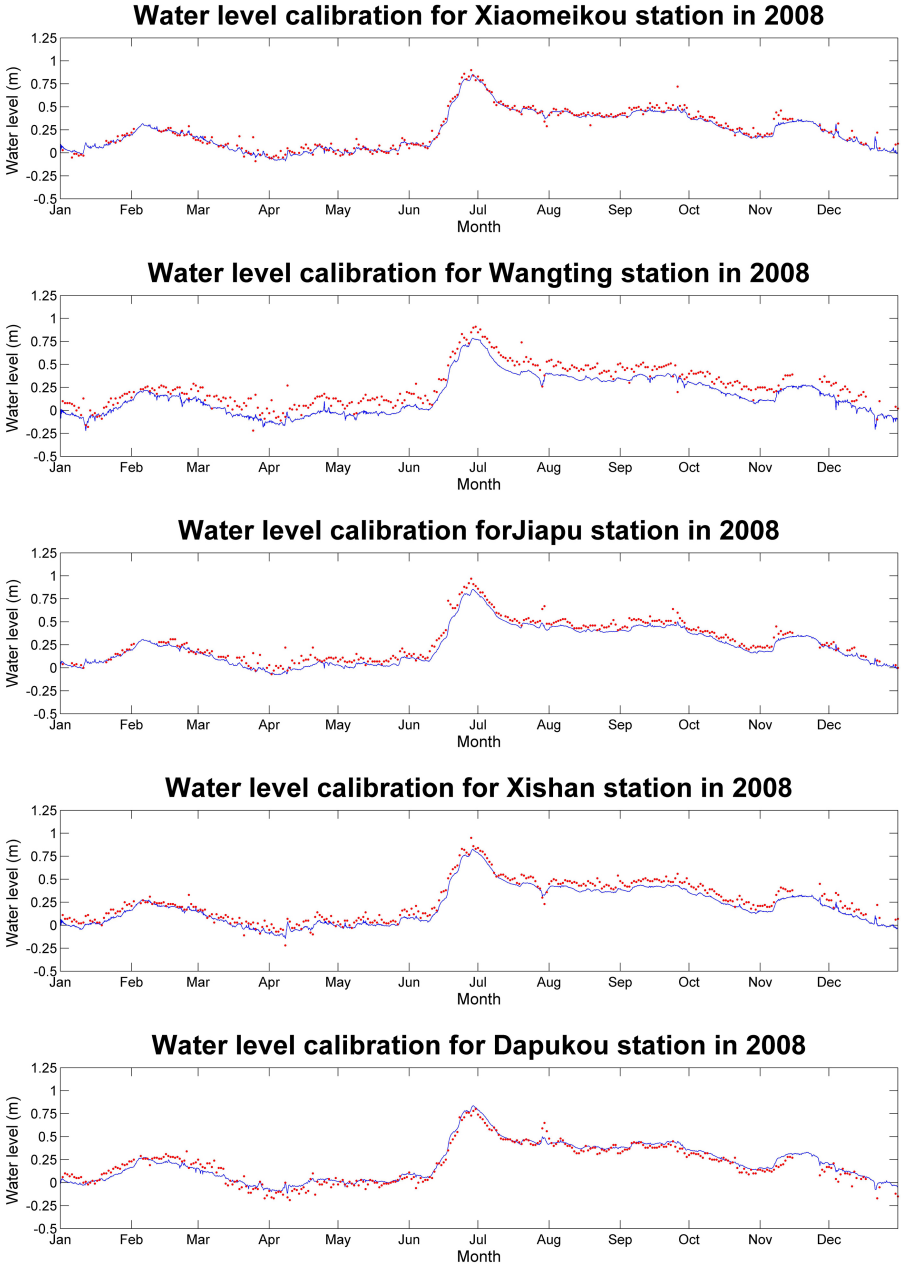


Figure 3.3: In situ measured and modeled water level for 5 monitoring stations in 2008, water levels are based on Wusong Datum. Measured level are shown with points and model results are shown with solid lines

indicators is listed in Table 3.2.

Table 3.2: Model performance indicators for calibration scenario

| Model performance indicator | Dapukou | Jiapu | Xiaomeikou | Xishan | Wangtingtai |
|-------------------------------|------------|------------|------------|------------|-------------|
| RMS error (cm) | 11.1 | 8.6 | 7.2 | 5.1 | 5.4 |
| Error Range (cm) | -16.5-15.8 | -18.4-20.9 | -31.1-11.6 | -29.6-22.8 | -41.7-11.6 |
| Mean Absolute Error (cm) | 4.3 | 4.0 | 5.9 | 7.5 | 9.6 |
| Agreement index ¹ | 0.88 | 0.89 | 0.84 | 0.79 | 0.75 |
| Model efficiency ² | 0.93 | 0.94 | 0.89 | 0.84 | 0.77 |

¹ The Nash-Sutcliffe index of efficiency from (Nash and Sutcliffe 1970(Nash and Sutcliffe, 1970));

² The index of agreement from (Willmott 1981(Willmott, 1981)).

Model performance indicators indicate that the simulation results and in situ measurement for each observation station differ only a few centimeters, which demonstrates that the model well reflects the water level trend due to the influence of various sources, including tributary discharge, precipitation and evaporation. The largest variance between modelled and measured water level is in Wangtingtai Station, potentially because of the irregular lake margin near the station. Further sensitivity analysis shows that variation of other parameters, like bottom roughness, contributes little to the water level model results.

3.4. Results

3.4.1. Effects of wind: steady wind

Besides the fluvial discharge for the tributaries into the lake, wind forcing is an important momentum source driving hydrodynamic circulations. Wind data analysis and literature show that the prevailing wind comes from the southeast in summer and from the northwest in winter. Since Taihu Lake is located in a typical monsoon climate zone characterized by prevailing southeast wind in summer and northwest wind in winter, the wind direction is relatively consistent at a time-scale of days (Li et al., 2013b; Qin et al., 2010). The average wind speed is 5m/s. To find the wind influence on the hydrodynamic circulation, we used a steady wind of 5m/s and 10m/s wind speed from the prevailing summer and winter wind directions. Depth averaged circulation gyre patterns, volume exchange rates between sub basins and the big lake and vertical variations are examined. With a constant wind, the depth-averaged hydrodynamic circulation gyres and surface water level slope in the lake takes around 2 days to reach a rough steady state. Thus, a relative stable hydrodynamic circulation gyres pattern can be achieved (Figure 3.4).

In the three northern sub basins, the structures of hydrodynamic circulation are similar, where two half-sub-basin-size scale circulation gyres from opposite directions are formed. The directions of the inner circulation gyres are clockwise for northwest wind and counter-clockwise for southeast wind. Along the entrance line of all three sub basins, a strong eastern-western direction current with a relatively large velocity exists. With constant northwest wind, the flow goes eastwards, while with the southeast wind, the flow reverses. In the East Epigeal Zone, except for the eastern corner, a near-shore current with high velocity flows near the eastern

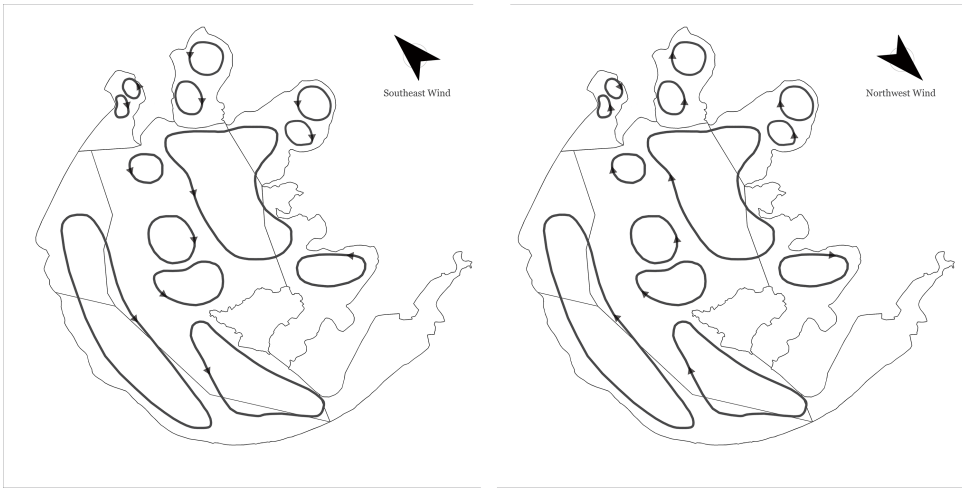


Figure 3.4: Depth averaged circulation gyres for northwest and southeast wind

margin of Taihu Lake in the same direction as the wind. In the eastern corner, a circulation gyre appears. For the northwest wind, the gyre is clockwise, while for the southeast wind it is counter-clockwise. In the Centre Zone of the lake, 5 smaller scale circulations occur due to the combination effects of a strong current in the southwest and the topographic limitation of Xishan Island. Near the entrance of Dongtaihu Bay, at the southern margin of the lake, the current direction is opposite to the east-west component of the wind direction. An elongated-shaped circulation crossing the Northwest Zone, the Southwest Zone with a high current velocity is observed. The direction of this circulation gyre is clockwise with southeast wind and counter clockwise with northwest wind. The rich structure of the steady hydrodynamic circulation is caused by the combined effects of the irregular shaped sub basins and the overall complex geometry. In the shallower margin of the lake parallel to the wind direction, the flow direction is the same as the wind. In the deeper central zone of the lake, there are currents with a smaller velocity flowing opposite to the wind direction. Two main circulation gyres are stable and consistent throughout the lake, one is in the southwestern part of the lake near the western margin, the other one is around the Center Zone and Xishan Island. The latter one is the largest hydrodynamic circulation at the scale of the lake size and is connected with all the other sub basins around the Taihu Lake. Sediments, nutrients and other suspended matters in the water could be transported from one sub basin to another with this hydrodynamic circulation, hence it is very crucial for the transport and mixing in the lake. Volume exchange between sub basins is the accumulated discharge through cross-sections which defines the borders between sub basins. To quantitatively study the initial water level influence on volume exchange between the sub basins in Taihu Lake, the 9 cross-sections can be categorized into two types, one type connects a semi-closed sub basin, for example the entrance cross-section of Meiliang Bay; the other type links two sub basins with an entrance cross section and

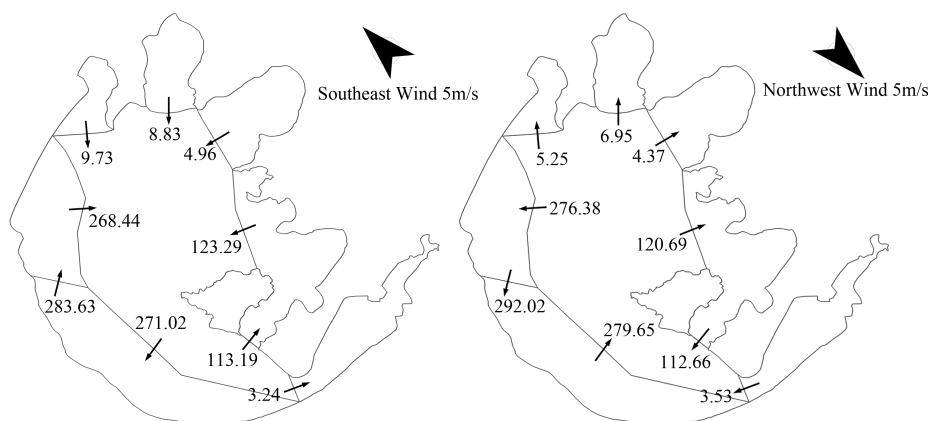


Figure 3.5: Volume exchange between sub basins with constant wind. Unit of numbers shown in the figure is m^3/s .

a linking cross-section, for example the cross-sections between Eastepigeal Zone and the Center Zone. Note that the small total volume exchange rate at the first type of cross-section is due to the combined, but usually reversed, effect of surface and bottom flux. A net volume exchange across the first type of cross-section is usually small due to the topographic limitation and semi-closed sub basin shape, while across the second type of cross-section the volume exchange is much larger. Directions of volume exchange are directly related to wind direction (Figure 3.5)

3.4.2. Effects of historical wet/dry seasons:

To study the effects of the historical wet/dry season impact, the different initial water level of the whole lake is used on the hydrodynamic circulation. The observed water level of 5 monitoring stations shows a maximum water level difference of around 1m with the highest water level in summer (Figure 3.2). Accordingly, the initial water level of 1m and 0m is included in numerical simulations. Model results show that with a constant wind, the difference in initial water level contributes little to the depth-averaged hydrodynamic circulation patterns. Current velocity varies with initial water depth, but the direction and shape of the hydrodynamic circulation patterns remain unchanged. However, the effect of initial water level with constant wind is more significant in the volume exchange between sub basins (Figure 3.6).

Effects of the initial water level on the total volume exchange at the two types of cross-sections are different. For the first type of cross-sections, volume exchange rates decrease with a higher initial water level, while for the second type of cross-section the trend is opposite. These phenomena can be explained by the boundary and bottom limitations. For the first type of cross-section, the semi-closed sub basin is restricted in the back by the closed boundaries around it as well as the narrower entrance, consequently the circulation flux is trapped and harder to result

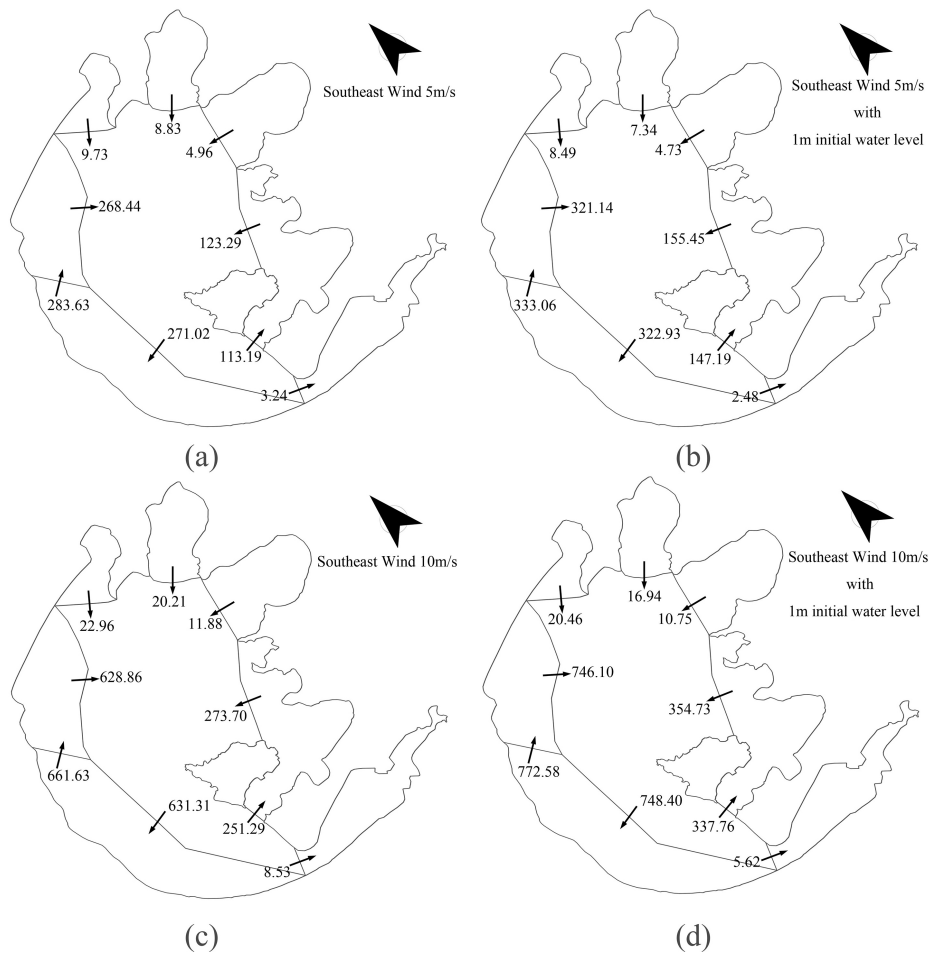


Figure 3.6: Volume exchange rates between each sub basins with southeast wind. Unit of numbers shown in the figure is m^3/s .

in an exchange with a higher initial water level. While for the second type of cross-section, the boundary influence for the sub basins behind it is relatively smaller and the bottom influence becomes less due to the larger water depth. A higher initial water depth can weaken the bottom restrictions even more and thus induce higher volume exchange rates.

Studying the volume exchange rate at cross-sections indicates the difference between water exchange efficiency during summer and winter time, which is of significant importance for water quality issues. In summer, the water level of the lake is roughly 1m higher than that in winter. For the same wind speed, water in semi-closed sub basins is harder to exchange than in the winter, while for relatively open sub basins the water exchange is enhanced.

3.4.3. Effects of wind speed

Similar to initial water level, changes of wind speed do not significantly change the shape of the hydrodynamic circulation. But the effect of wind speed on the net volume exchange between sub basins is significant (Figure 3.6).

Unlike the effect of the initial water level, increase of wind speed will consequently induce the increase of net volume exchange between sub basins. With the same initial water level and wind direction, an increase of the wind speed stimulates the current in the lake, due to the increase of momentum transferred from wind to water, which in turn causes an increase in the net volume exchange.

3.4.4. Vertical variation in flow field

In the literature, vertical variation of hydrodynamic circulation is usually described as a surface flow, following the wind direction, and a compensation flow along the bottom. Due to the complex topography and the irregular shape of Taihu Lake, this simple conclusion is not universally valid for every sub basin within the lake. The details of vertical flow structure will be discussed in this section. The existence of the complex geometry and the irregular boundary shape yield a rich three-dimensional flow structure in Taihu Lake. Figure 3.7 shows the simulated surface and bottom layer horizontal circulation field with a constant 5m/s southeast wind.

The hydrodynamic circulation patterns of the surface and the bottom layers are different in various locations. The major flow direction difference occurs in the center zone of the lake where the water depth is relatively larger. Surface layer currents follow the wind direction, while at the bottom the direction is reversed. Also, at some locations in the deepest area, for example near the borderline of the southwest zone and the center zone, there are entire water columns from surface to bottom flowing against the wind direction with the largest flow velocities in the bottom layer.

For the shallower part, i.e. along the western margin of the lake, borders of the three sub basins in the north, as well as the entire Epigeal Zone and Dongtaihu Bay, unlike the conclusions from previous studies, the current in the entire water column follows the same direction, but the surface flow has a larger velocity.

For the three northern sub basins where the algae bloom problem is most severe, the three dimensional hydrodynamic circulation is more complex due to the narrow

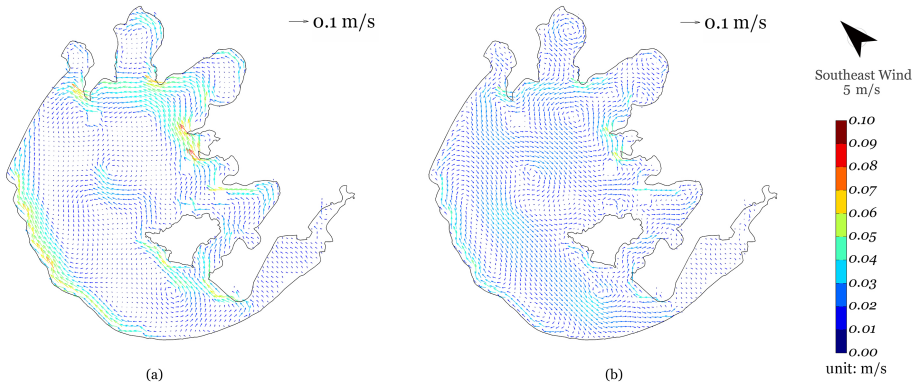


Figure 3.7: Surface and bottom horizontal hydrodynamic circulation pattern with southeast wind, with (a) the surface layer velocity field, (b) the bottom layer velocity field.

constrictions at the entrance. Figure 3.8 shows, as an example, the zoomed in surface and bottom horizontal circulation pattern in Meiliang Bay, where most of the surface flow vectors follow to the wind direction while the bottom current direction is opposite to the wind direction.

The hydrodynamic circulation of Meiliang Bay could be interpreted as a scaled down version of the whole of Taihu Lake. The deepest part of Meiliang Bay is in the center while area near the margin it is shallower. Especially the western part of the entrance is shallower than the eastern part. Along the shallower northeastern and southwestern margin of the basin, current directions are similar to wind direction with a larger surface velocity than the bottom velocity, while in the deeper part in the central zone, the flow direction at the bottom reverses. A difference of flow direction at the surface and bottom indicates the presence of a return flow and thus a vertical circulation. The return flow structure is observed after 2 days with wind holding the same direction.

Variations in the horizontal current velocity have a direct impact on the surface and bottom volume exchange rates through the cross-sections. Except for very narrow and very shallow cross-sections, surface and bottom flux directions reverse. Directions of surface or bottom volume exchange correlate with the wind direction. For most cross-sections, surface and bottom volume exchange rates increase with wind speed (Figure 3.9).

The hydrodynamic character of the lake is very similar to the channel shoal system in a fluvial estuary, where the surface water moves in the direction of the driven force and a reverse flow appears in the deeper channel. This phenomenon can also explain the reason why algae consistently accumulate in the sub basins. In the day time of spring summer time toxic algae, such as Cyanophyta, float upward from the bottom for photosynthesis and stay at the surface layer in the day time. During the day, the algae are consistently transported by the surface layer current in the prevailing wind directions to the northern sub basins. Since only water in the

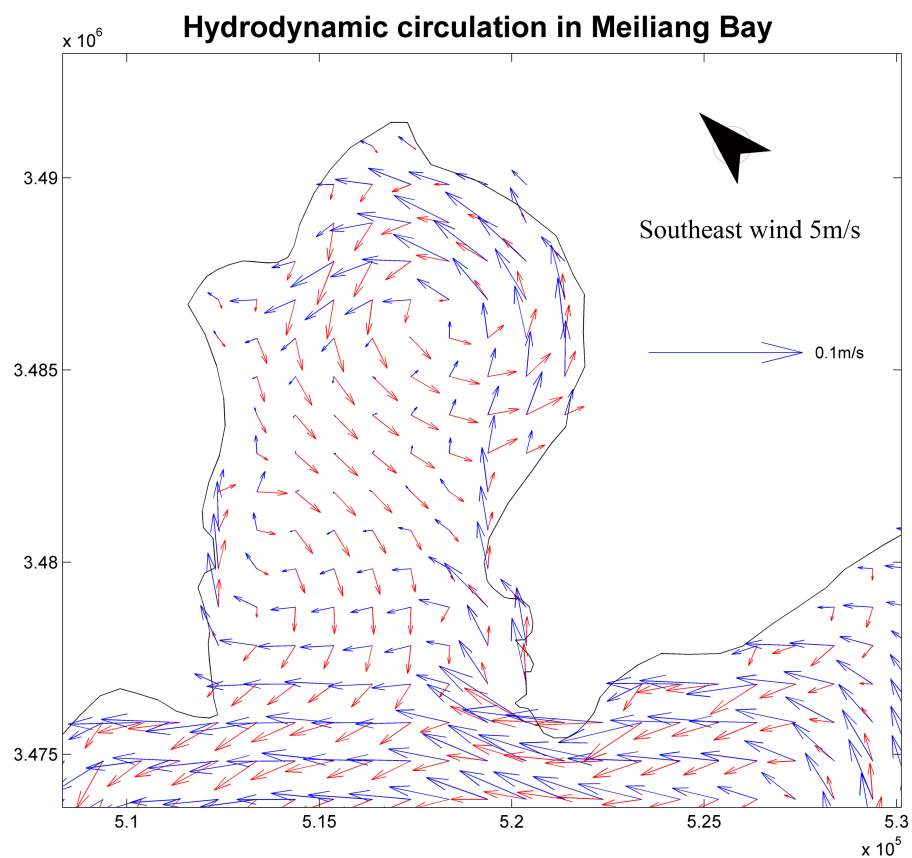


Figure 3.8: Comparison of surface and bottom hydrodynamic circulation pattern of Meiliang Bay of model result of case 2 with 5m/s constant southeast wind. The blue vector indicate the flow pattern on the surface layer and the red vector indicate the bottom layer.

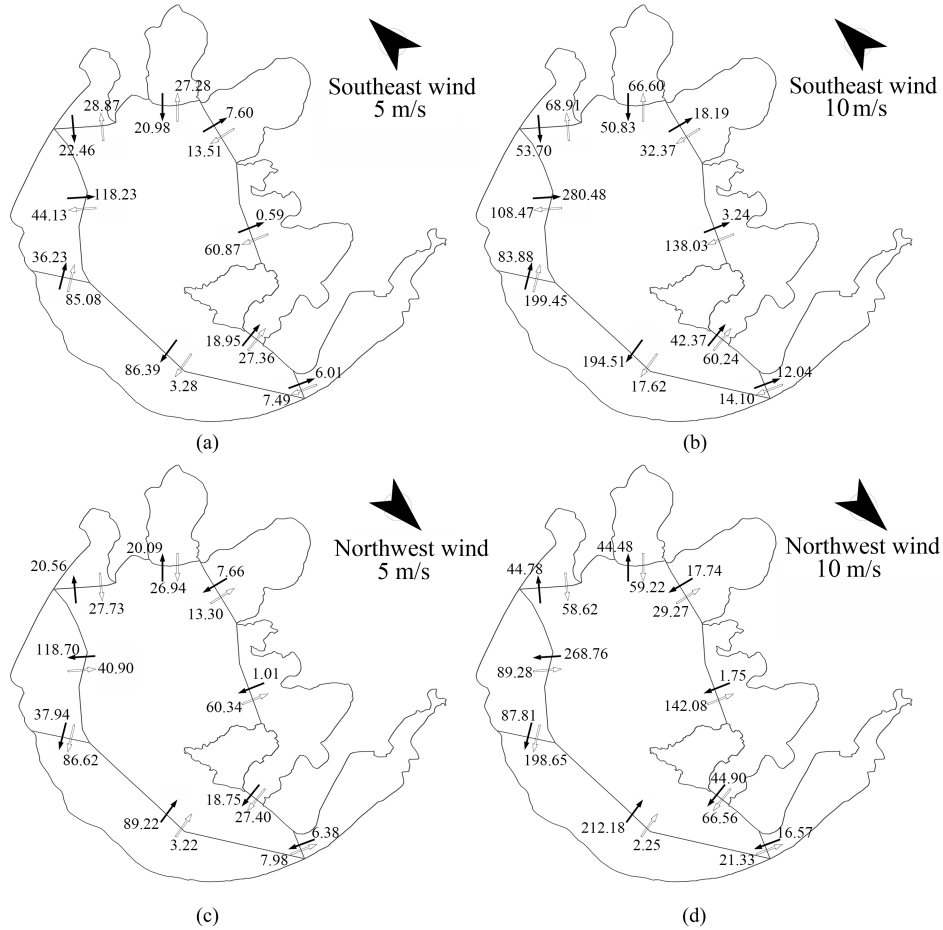


Figure 3.9: Surface and bottom layer flux with constant wind. The hollow arrows represent surface flux while solid arrows are the bottom flux. (a) refers to model result with constant 5m/s southeast wind, (b) refers to model result with constant 10m/s southeast wind, (c) refers to model result with constant 5m/s northwest wind, (d) refers to model result with constant 10m/s northwest wind. Unit of numbers in the figure is m^3/s .

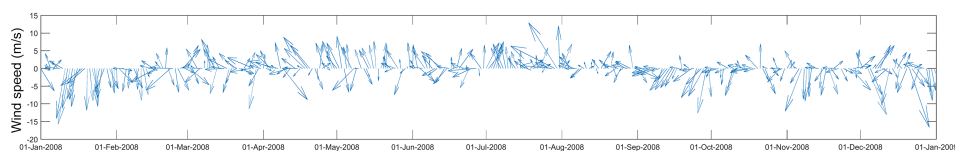


Figure 3.10: Time series of wind vectors of year 2008, with north wind pointing to the top, length of each arrow refers to the wind speed.

3

deeper part has a southern outwards current direction, the algae keep accumulating with the surface water and are captured inside Meiliang Bay, which eventually causes the algae bloom.

3.4.5. Unsteady wind

Hydrodynamic circulation varies with wind scenarios as indicated by model results shown in 3.4.1. In nature, both wind speed and directions are unsteady. However, the prevailing wind directions around Taihu Lake in summer and winter are relatively fixed as shown in Figure 3.10. Observed wind shows that it could blow persistently at one prevailing direction for a couple of days until it changes direction, while the wind speed changes daily.

The shift from a steady hydrodynamic circulation situation to another due to changing wind takes around 2 days. This process usually coincides with a complex and rapid shifting in horizontal hydrodynamic circulation. Major circulation gyres change shape and direction, and so does the water jet along the shallow margin. As discussed in the last section (3.4.4), with the same wind direction the horizontal circulation pattern is fixed regardless of the wind speed, while wind speed is responsible for the varying volume exchange between each sub basin. Using the reference scenario as an example, bottom and surface layer flux through nine cross sections between subzones are shown in Figure 3.4 8. Both the directions and the flux value change with wind directions. For most cross-sections, bottom flux and surface flux have the same direction such as cross-section Eastepigeal 1. However, for cross-sections like the entrance of Meiliang Bay, surface and bottom flux are reversed.

The flux due to unsteady wind can be further understood from the conclusion of the steady wind situation. To illustrate this, Figure 3.12 shows the example of the zoomed in total flux and wind records of the southwest1 cross-section in April 2008.

In a steady wind situation, the stable hydrodynamic circulation occurs after two days of simulation. While in reality, the direction and magnitude of wind change with time, thus the total flux through cross-sections also changes temporally. The magnitude of the total flux increases with a continuous wind blowing from the same direction (17th Apr to 19th Apr in Figure 3.11), while the change of direction of the total flux occurs with wind direction changes (7th Apr to 8th Apr). For unsteady wind, the response of the total flux to wind is relatively fast due to sharp wind changes and it reaches a similar equilibrium as the steady wind.

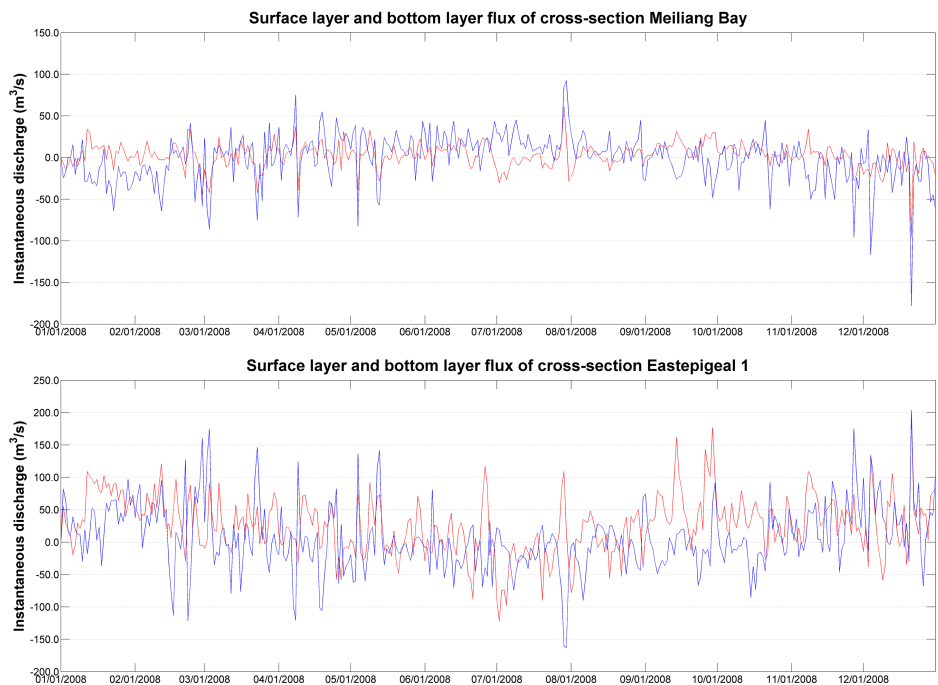


Figure 3.11: Time series of surface and bottom flux of reference scenario (case 1), the red line refers to bottom flux and the blue line refers to the surface flux, unit in the figure is m^3/s .

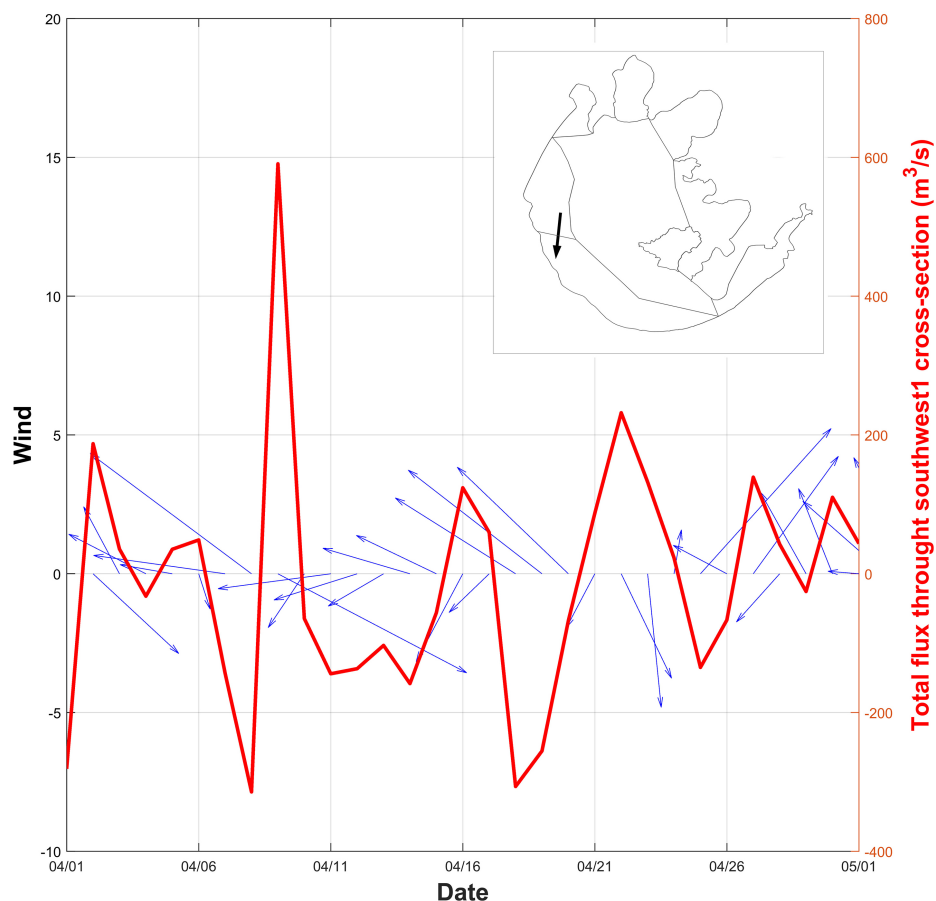


Figure 3.12: Total discharges and corresponding wind vector of southwest 1 cross-section in April 2008. The blue vector represents the wind record and the red line represents the total flux through southwest1 cross-section. Length of the blue wind vector is the magnitude of wind speed. Position and the arrow representing the positive flux are illustrated in the upper right subplot.

To conclude, with unsteady wind conditions, although the stable hydrodynamic circulation may not occur due to a fast varying wind, the volume exchange patterns and cross-section flux changes with a steady wind condition are, to a high degree, still valid.

3.5. Discussion

The influence of wind on the hydrodynamic circulations has been discussed above. The Delft3D simulation model is shown to be able to reproduce the spatial and temporal hydrodynamic circulation patterns in Taihu Lake. However, given the uncertainty in numerical and process input parameters and the unique geomorphology of Taihu Lake, the model results should be carefully scrutinized. To evaluate input errors, a model sensitivity analysis is provided in sections 3.5.1 concerning grid size and bed roughness, respectively. Velocity vorticity, as the key indicator of hydrodynamic circulation, predominantly modulated by wind, depth, bathymetry gradient etc., is discussed through both a theoretical analysis and flat bottom model tests in section 3.5.2. Furthermore, Lagrangian-based tracer tests are used to evaluate emergency pollution/leakage effects in section 3.5.3 and water transfer effects in section 3.5.4.

3.5.1. Numerical sensitivity

Grid size effects

Before model calibration, sensitivity tests have been carried out to test the influence of numerical parameters. One of the major issues is grid size. In this study, the grid size is chosen to be 1000m. A grid size of 500m is utilized in earlier numerical studies of Taihu Lake. To test the influence of grid size on the model's accuracy and efficiency, a 500m grid size model was set up. In both cases, the chosen time step of 10min fulfils the courant number requirement.

Table 3.3: Model behaviour with 500m grid size

| Model performance indicator | Dapukou | Jiapu | Xiaomeikou | Xishan | Wangtingtai |
|-----------------------------|------------|------------|------------|-----------|-------------|
| RMS error (cm) | 7.8 | 8.6 | 8.8 | 8.5 | 8.3 |
| Error Range (cm) | -30.4-13.2 | -31.9-27.3 | -33.8-10.8 | -21.3-7.8 | -33.2-11.1 |
| Mean Absolute Error (cm) | 6.4 | 7.2 | 7.7 | 7.7 | 6.7 |
| Agreement index | 0.83 | 0.79 | 0.80 | 0.79 | 0.81 |
| Model efficiency | 0.86 | 0.82 | 0.83 | 0.84 | 0.84 |

Model performance for the water level at 5 monitoring stations with the finer grid of 500m listed in Table 3.3. The comparison of performance indicators with those in Table 3.3 illustrates that the grid size effect varies with different indicators. For example, for Wangtingtai Station, the Mean Absolute Error increases with grid size while the RMS error shows the opposite result. Other important hydrodynamic circulation model results, such as the horizontal circulation patterns, show little difference. Model performances of both models are equally good, while the coarse grid has an advantage in model efficiency. Thus, the 1000m grid size was chosen.

Bed roughness

The bottom roughness factor is another common tuning parameter in hydrodynamic models. Here in this model, a Chezy coefficient of $65m^{1/2}s^{-1}$ is chosen. Also other values of for the Chezy coefficient were investigated and other bottom roughness formulas were tested. Model results show that the hydrodynamic circulation patterns are not sensitive to the bottom roughness values nor the roughness formulation. However, if the model is further applied to ecology or sediment application, attention should be paid on the bottom roughness since the correlated bed shear stress have a critical impact on the sediment resuspension process.

3.5.2. Velocity vorticity: key indicator of hydrodynamic circulation

Vorticity can be used to describe the spatially varying rotational character of a flow field (Rueda et al., 2005). In this section, we focus on the vorticity of the horizontal velocity field in shallow water as the indicator of hydrodynamic circulation. The appearance of hydrodynamic circulation in the form of vorticity in the lagrangian horizontal velocity field requires driving forces, which can be the wind shear stress gradients due to inhomogeneity of the wind velocity field, existence of submerged and emergent plants, the Coriolis effects and the bathymetry variations. The influence of bathymetry variations is noteworthy compared to the other factors mentioned above (Simionato et al., 2004). In Lake Ontario, Csandy (1973) schematized the study area into a long and narrow lake with parallel depth contours, and proposed the idea of 'topographical gyres', where the depth averaged current direction is identical to wind direction in the shallow area and where it is opposite in the deeper area. This phenomenon was also observed in other shallow lakes around the world (Józsa, 2014; Schoen et al., 2014; Strub and Powell, 1987, 1986). However, these studies mainly focus on long and narrow lakes. For shallow lakes with other shapes and a more rugged topography where lateral differences are more significant, studies are lacking. With different bathymetry and bathymetry gradient, behaviour of hydrodynamic circulation in the lake centre area and the littoral zone varies (Figure 3.4).

In previous studies an analytical solution for the influence of bathymetry on the vorticity has been derived (Józsa, 2014; Laval et al., 2003). Hereby we present a brief review. Assuming a steady state with constant wind, i.e. the time derivative of horizontal velocity is 0, the depth averaged shallow water equations are:

$$\nabla \cdot \mathbf{V} = 0 \quad (3.8)$$

$$\nabla U - fV = -g \frac{\alpha \eta}{\partial x} + \frac{\tau_{s,x} - \tau_{b,x}}{\rho h} + \nu \cdot \Delta U \quad (3.9)$$

$$\nabla V + fU = -g \frac{\alpha \eta}{\partial y} + \frac{\tau_{s,y} - \tau_{b,y}}{\rho h} + \nu \cdot \Delta V \quad (3.10)$$

Where V is the horizontal velocity vector with x component U and y component V , f is the Coriolis factor, g is the gravitational acceleration, η is the surface elevation, h is the total depth, τ_s is the surface wind shear stress, τ_b is the bottom shear

stress, ρ is the density of water, and ν is the horizontal eddy viscosity. ∇ is the Del operator and Δ is the Laplace operator.

Introducing the vorticity of the horizontal velocity, $\zeta = \nabla \times V = \frac{\partial v}{\partial x} - \frac{\partial u}{\partial y}$, and taking the y-derivative of equation 3.9 and x-derivative of equation 3.10, together with equation 3.8, the governing equation for the vorticity becomes:

$$V \cdot \nabla \zeta = -(\zeta + f) \nabla \cdot V + \nabla \times \left(\frac{\tau_s}{\rho h} \right) - \nabla \times \left(\frac{\tau_b}{\rho h} \right) + \nu \Delta \zeta \quad (3.11)$$

The first term on the right hand side represents the vortex stretching, the second term represents the vorticity input from wind, the third term is the vorticity sink due to bottom shear stress and the last term is eddy-viscosity related. Compared to the wind shear stress term, the latter two terms are one or more magnitude smaller, thus they are negligible.

With constant water density, the wind vorticity input term becomes:

$$\nabla \times \left(\frac{\tau_s}{\rho h} \right) = \frac{1}{\rho} \left(\frac{1}{h} \nabla \times \tau_s - \frac{\tau_s}{h^2} \times \nabla h \right) \quad (3.12)$$

The first term in the bracket is related to wind stress curl, with constant wind, this term is 0, and a so called barotropic topographic gyre is generated; the second term represents the velocity gradient influence on the vorticity.

Results from the numerical model also confirm the analysis above. With a constant wind from the northwest, the depth-averaged vorticity is shown in Figure 3.13. In the littoral area, where the total water depth gradient is perpendicular to the wind speed, wind generates a large vorticity value. Along the southwest shore in Taihu Lake, the current direction is the same as the wind, thus it will produce a counter clockwise horizontal circulation. Even in the same gyre, the vorticity is larger with depth becoming smaller. Similar phenomena could be observed in the northeast boundaries of the Lake, the vorticity is negative, which means a clockwise gyre and the shallower part has the larger absolute value of vorticity. For locations where the depth gradient is small, for example Dongtaihu Bay at the southeast part of Taihu Lake, the vorticity is almost zero.

These conclusions can be further illustrated by a numerical test with a flat bottom. Changing the bottom depth to a uniform value of 2m, and maintaining all other parameters, yields model results as shown in Figure 3.14.

With a constant depth, except for the grids near the boundary, depth gradients at all locations are zero. Thus, according to equation 3.9, the velocity vorticity at each layer should be 0 as well, as illustrated in Figure 3.14. Along most of the boundaries, for example the southwest shoreline, the velocities of the surface and bottom layer have the same magnitude but opposite directions, thus the vorticity is positive and negative, respectively. Since the depth-averaged vorticity is the superposition of each layer's vorticity, the values near the boundaries are approaching 0 (see Figure 3.14(c)). It may be concluded, both from the theoretical analysis and the numerical test results above, that the vorticity in the velocity field is related to directions of wind, current and bathymetry gradients, as well as to the value of water depth and

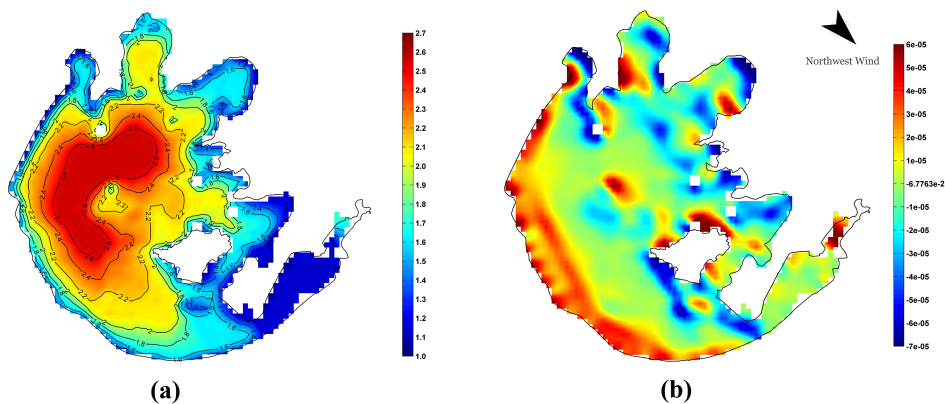


Figure 3.13: (a) Depth contours of Taihu Lake; (b) Depth-averaged vorticity with constant northwest wind.

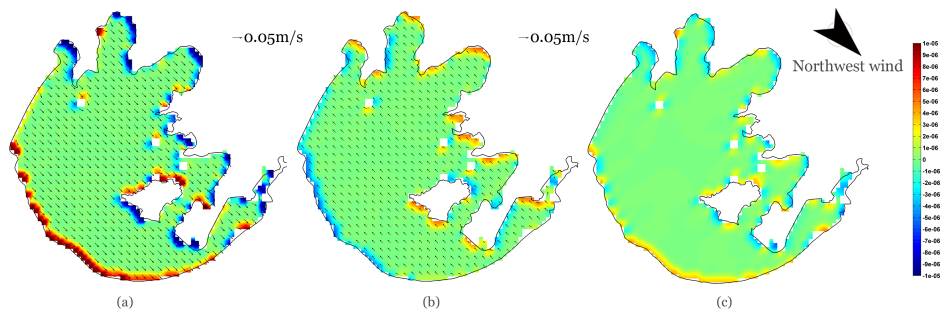


Figure 3.14: Numerical model results of velocity and vorticity with 2m constant depth and constant northwest wind. The vectors represent velocity and coloured patches represent vorticity. (a) Surface layer; (b) Bottom layer; (c) Vorticity of depth averaged velocity.

wind shear stress. When the current velocity is in the same direction as the wind, the major bathymetry influence is the depth gradient and depth itself. Wind has the largest influence on the vorticity when its direction is perpendicular to that of the bathymetry gradient. Wind related vorticity change is larger with a larger wind speed and a smaller water depth.

3.5.3. Transport due to horizontal circulation

Circulation and redistribution of lake water throughout the lake is further illustrated by the model results of the tracer experiment for the first half-year of 2008 with steady wind scenarios. At the beginning of the simulation, tracer concentration all over the lake is 0. After that, tracers are released persistently in the first three months of the simulation at a rate of 5kg/s. Tracers are released at a chosen sub basin for each scenario. Tracer movements well reflect the characteristics of the hydrodynamic circulation under steady wind conditions discussed in section 3.4.1, e.g. when taking the tracer releasing experiment in Eastepigeal as a representative example (Figure 3.15 and Figure 3.16).

With a constant southeast wind, initially tracers move northwards via the shallow east margin of the Epigeal Zone, where the depth-averaged flow velocity in the wind direction is the largest. Subsequently, the tracers penetrate into Gonghu Bay with a counter-clockwise circulation near the entrance of Gonghu Bay (Figure 3.4). After that, tracers move westward with the same circulation pattern and enter the semi-closed sub basins of Meiliang Bay and Zhushan Bay with the smaller sub basin scale circulations. At last, tracers move southwards along the deeper centre and spread out over the lake. The entire time for the advection and diffusion process to fully mix the tracers in the entire lake is around 2 months time. Similarly, with a constant northwest wind, tracers' movements follow the hydrodynamic circulation pattern.

However, as shown in Figure 3.16 on April 30th, the tracer concentration is still high at the southern boundary of the lake, which means that for different locations in the lake, the duration of a high tracer concentration due to redistribution of lake water by wind effects is different. For lake water quality management, it is crucial to assess the temporal influence at a critical spot of a random pollution emission. Thus, altogether 6 important spots are chosen around the lake, including one drinking water intake point (Qin et al. (2010)) and 5 tourist places, as shown in Figure 3.17, to analyse the influence of pollution release in the numerical experiment.

Taking spot A as an example, time series of tracer concentration with different release spots are shown in Figure 3.18. Significant variance in the tracer concentration trend is also the direct result of hydrodynamic circulation, which determines movement of the trajectory of tracers between the interested locations and the release spots. Under the constant southeast wind condition, water from Gonghu Bay, Eastepigeal Zone and Center Zone has the largest influence. Location A is located near the joint point of Meiliang Bay and Gonghu Bay, where a sub basin scale circulation occurs (Figure 3.4). With southeast wind, the circulation gyre will first drive water from inside the Gonghu Bay to point A. Then several days later, water from the Eastepigeal Zone and Center Zone will join this circulation gyre and move towards location A, which could also explain why the peak of concentration

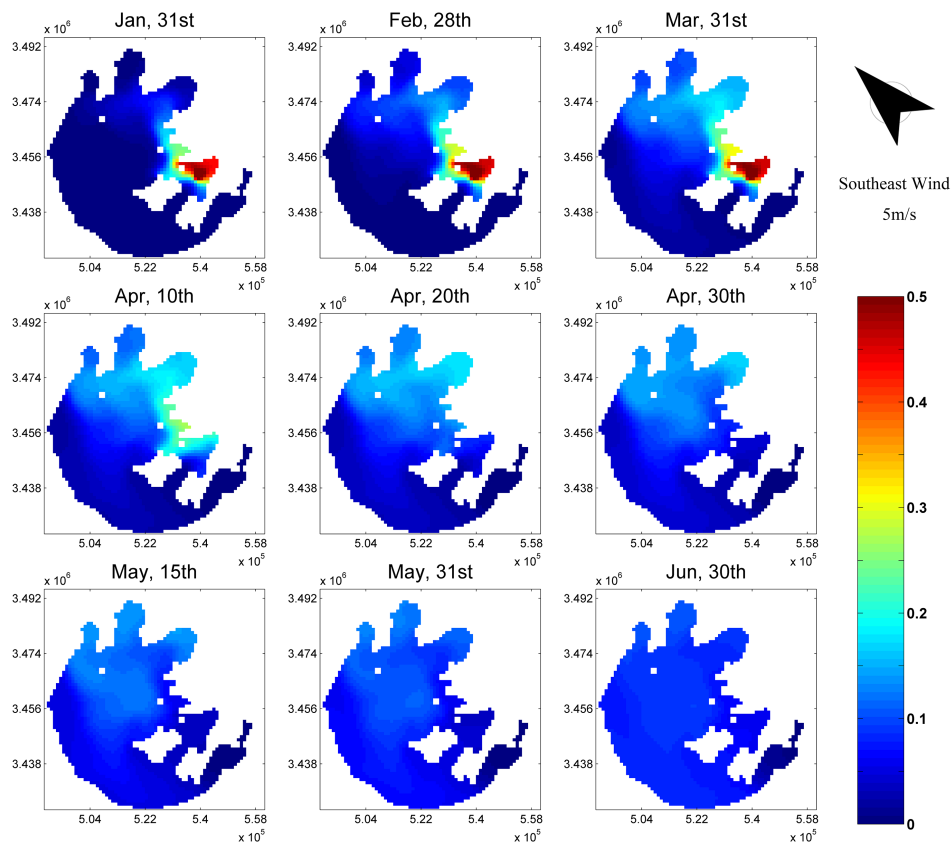


Figure 3.15: Time series of tracer concentration images, with the model driven by constant 5m/s south-east wind. Unit in the figure is kg/m^3 .

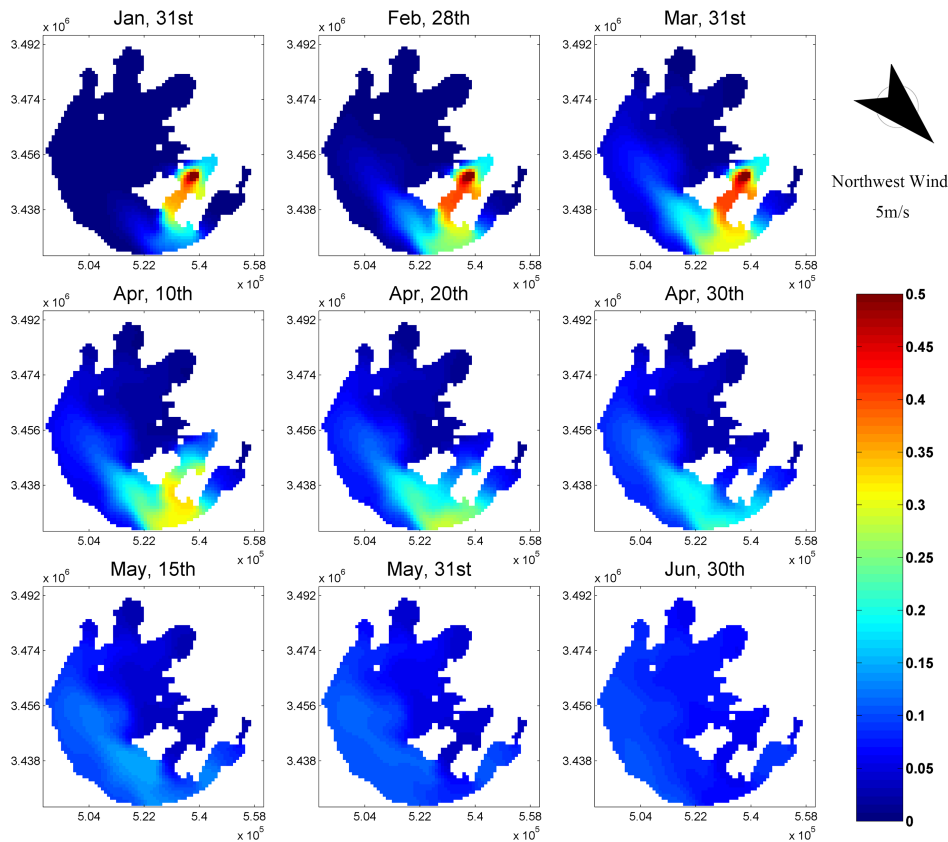


Figure 3.16: Time series of tracer concentration images, with the model driven by constant 5m/s north-west wind. Unit in the figure is kg/m^3 .

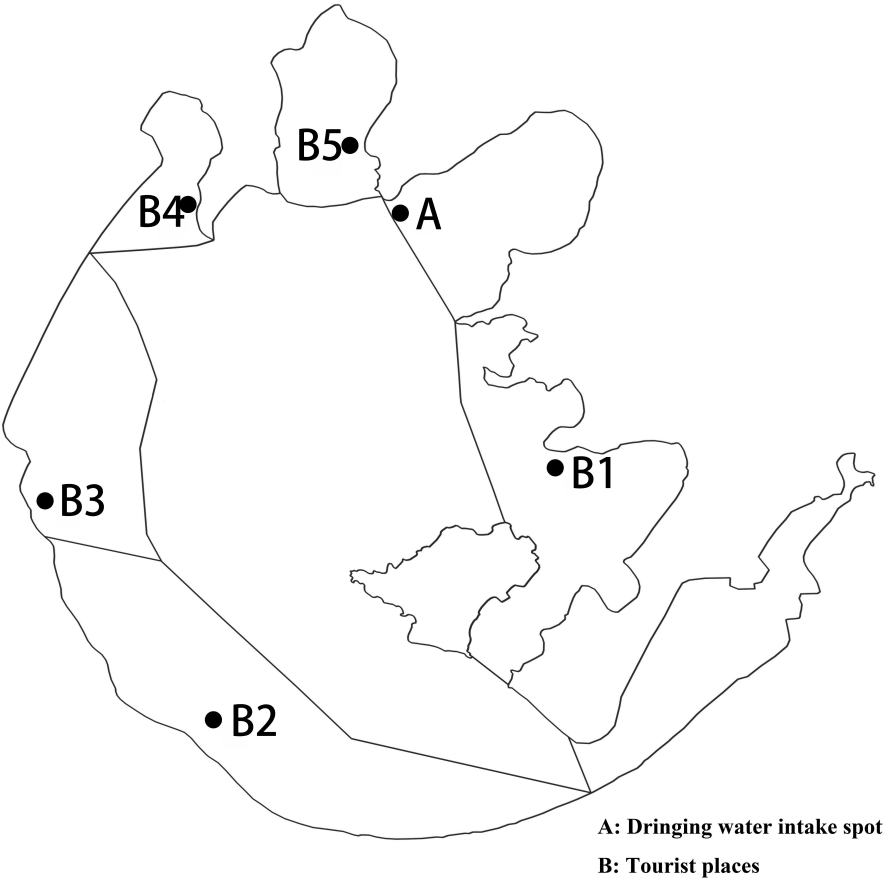


Figure 3.17: Important spots for pollution(tracer) release experiment analysis.

curve of the release of the latter two zones is several days after the release stop time on 31st of March.

With constant northwest wind scenarios, which are represented as blue lines in Figure 3.18, the situation is similar. Tracers from Meiliang Bay reach location A first, however, the distance travelled in this situation is longer than tracer released in Gonghu Bay with southeast wind; due to mixing and diffusion processes, the peak concentration at location A with northwest wind is smaller than that with southeast wind. Water from Zhushan Bay and Center Zone arrives later and introduces delayed concentration peaks. Especially to be noted, tracers released from Dongtaihu Bay show less influence due to longer travel distance and weak hydrodynamics inside Dongtaihu Bay.

For the lake authorities, the analysis of hydrodynamic circulation with tracer experiments under constant wind conditions may provide a quick tool to assess emergency pollution impact on critical areas before carrying out a more complicated hydrodynamic and water quality model.

3.5.4. Is large-scale water transfer effective?

Diluting and flushing the water of Taihu Lake with water transferred and pumped from the Yangtze River has been the largest engineering intervention to improve the water quality in Taihu Lake after 2007. Previous studies with field data collection have been carried out to identify the variation in water quality and biological indices before and after the water transfer. Results show that the effectiveness of the water transfer project remain an issue of concern. Positive effects occurred only in certain parts of Taihu Lake, while in several other areas the water quality even worsened (Hu et al. (2008); Li et al. (2011b); Zhai et al. (2010)).

To investigate the hydrodynamic circulation condition change due to the project, numerical experiments are carried out using the original discharge data of 2008 and the water transfer rate from the literature (Table 1 in (Li et al., 2011(Li et al., 2011a))). The water transfer in 2008 lasted from 23rd Jan to 9th Jun with a total transferred water volume of 870.2 million m^3 , which is around $6.7 \text{ million } m^3/d$.

Model results suggest that, except for Dongtaihu Bay and Gonghu Bay, no significant change in the hydrodynamic circulation condition occurred with and without water transfer. Total discharges of Gonghu Bay and Dongtaihu Bay are shown in Figure 3.19.

For other open cross-sections, such as southwest and northwest, volume exchanges slightly fluctuated but for the entrance cross-sections of semi-closed sub basins like Meiliang Bay, the total discharge remained the same. Model results of total volume exchanges across the cross-sections showed that transferred water neither significantly changed the water amount within each sub basin nor enhanced the volume exchange between sub basins. However, it indeed stimulated the hydrodynamic circulation in Gonghu Bay and Dongtaihu Bay.

Although the water transfer project contributes little to changing the total volume in most sub basins, hydrodynamic circulations still transfer and mix water persistently throughout the lake. Considering that the water transferred from the Yangtze River contains less nutrients or pollution than the average of Taihu Lake,

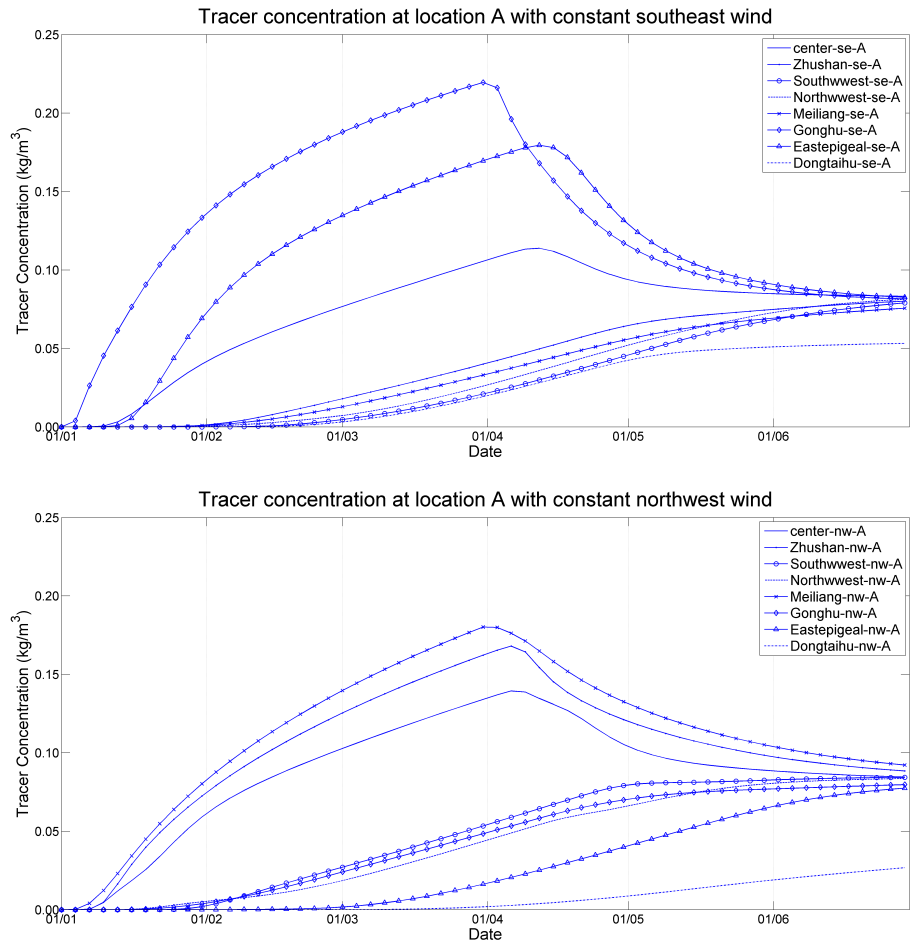


Figure 3.18: Tracer concentration at location A with different tracer release spot, the upper subplot shows tracer concentration with constant 5m/s southeast wind condition while the lower subplot describes the northwest wind condition. To make the plot clearer, data are extracted per 3 days from the model results.

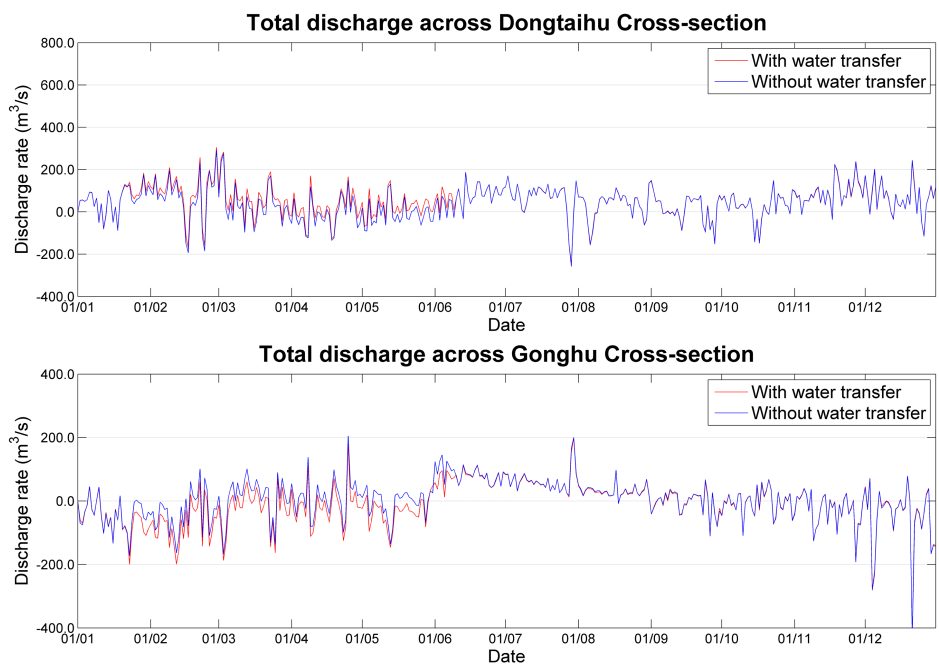


Figure 3.19: Total discharge of Gonghu Bay and Dongtaihu Bay. The red lines refer to the reference case while blue line represents scenarios without water transfer.

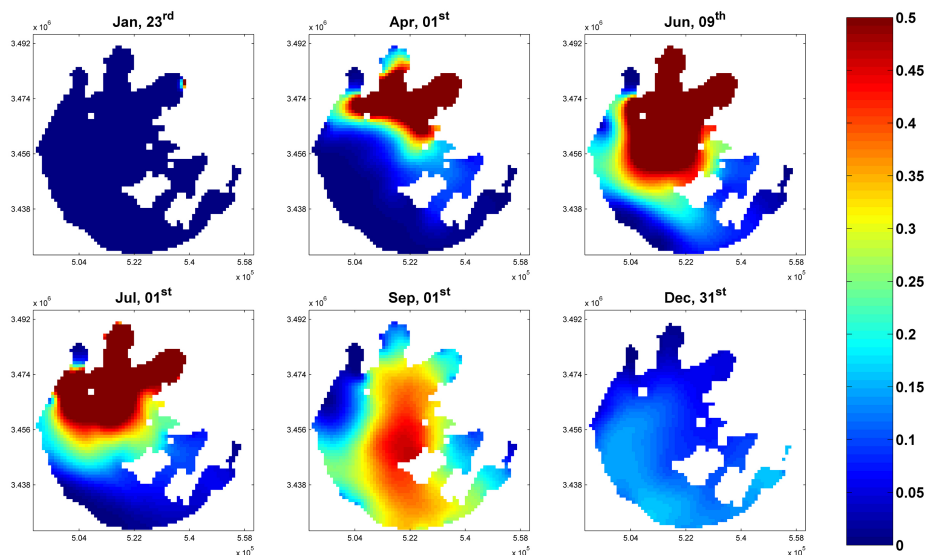


Figure 3.20: Time series of depth-averaged tracer concentration images, unit in map is kg/m^3 .

with the amount of transferred water staying in the sub basins, the nutrient concentration would change consequently. A tracer experiment is conducted to further elucidate the redistribution of transferred water. This scenario lasted for the entire year of 2008, and tracers were continuously released along the Wangyu River boundary at a concentration of $5kg/m^3$ between 23rd Jan and 09th Jun 2008.

Model results are shown in Figure 3.20. As can be observed from the top right sub plot, after 129 days on Jun 9th, a large amount of transferred water had already reached Gonghu Bay, Meiliang Bay and Center Zone. Later the tracers moved southeastwards before they left the lake from Taipu River. To be especially noticed, almost no tracers passed through the entrance of Zhushan Bay, resulting in a tracer concentration of virtually zero inside this sub basin. Volume exchange between Zhushan Bay and other parts of Taihu Lake was more severely blocked, partially due to a weak hydrodynamic circulation near the entrance of the sub basin.

To conclude, the water transfer project in Taihu Lake did not significantly stimulate the hydrodynamic circulation or volume exchange between sub basins. However, tracer scenarios illustrate the project did succeed in redistributing the clearer transferred water throughout the lake, especially in some semi closed sub basins like Meiliang Bay and Dongtaihu Bay.

3.6. Conclusion

Wind induced hydrodynamic circulations and associated transport and mixing processes in large shallow lakes play a significant role in the environmen-

tal and ecological processes. Knowledge of these physical mechanisms helps to understand the eutrophication problems, which are occurring more frequently in large shallow lakes like Taihu Lake. Previous studies emphasized mostly the environmental, biological and ecological aspects of eutrophication problems. However, the driving forces of nutrients transport, algae scums, pollutants mixing, and the underlying physical processes, such as wind- or anthropogenic driven horizontal circulation, have been largely overlooked, but they might be key factors leading to the increasing algae blooms. In this study, hydrodynamic circulation in shallow lakes is defined as the large-scale movement of water in a lake basin. A three-dimensional, numerical Delft3D model of Taihu Lake, driven by steady and/or unsteady wind, river discharge, rainfall and evaporation, is used to quantitatively illustrate the complex hydrodynamic circulation and their effects in transporting and mixing within the lake.

A relative stable circulation pattern is found to be formed after typically 2 days with steady wind, where the overall hydrodynamic circulation structure, i.e. direction, intensity and position, is determined by wind direction, wind speed and initial water level. Vertical variations of horizontal velocity are found to be related to the relative shallowness of water depth. In the shallow marginal area, flow at the bottom and surface layers has the same direction and the surface flow has a higher velocity, while in the deeper area, the bottom flow reverses opposite to the wind direction with a higher velocity. Volume exchange between sub-basins, influenced by wind speed and initial water level, differs due to the complex topography and irregular shape. To a high degree these findings are still valid with unsteady wind as well. Vertical variations in hydrodynamic circulation are found to be very important in explaining the surface accumulation of algae scums in Meiliang Bay in the summer. Vorticity of current velocity, as the key indicator of hydrodynamic circulation, is determined by wind direction, bathymetry gradient and water depths, while the maximum change of velocity vorticity happens when wind direction and bathymetry gradient are perpendicular to each other. Furthermore, we use Lagrangian-based tracer tests to estimate emergency pollution/leakage effects and to evaluate water transfer effects. One emergency pollution leakage point is added to the model to demonstrate the effect on five tourist locations and one drinking water intake point, suggesting that the model application may serve as an operational management tool. The water transfer project shows that even a large-scale water transfer (about 1/5 volume of total lake volume in 138 days from the Yangtze River) does not significantly alter the hydrodynamic circulation and volume exchanges between sub basins, but it succeeds to transport and mix the imported Yangtze River water into the greater part of Taihu Lake area.

This study may well be extended further to provide insight into the spatial and temporal biological process corresponding to wind induced hydrodynamic circulation in Taihu Lake and similar large, shallow lakes to support ecologically sound design and implementation for lake restoration.

4

Hydrodynamic Circulation, Water Age and Water Quality Implication

This chapter has been published in: Liu, S.; Ye, Q.; Wu, S.; Stive, M.J.F. Wind Effects on the Water Age in a Large Shallow Lake. *Water* 2020, 12(5), 1246.

4.1. Introduction

Located in the southeast part of China, Taihu Lake is the 3rd largest fresh water lake in China. Like most large shallow lakes all over the world and as a typical shallow lake around the middle and lower reach of the Yangtze River, Taihu Lake is suffering from the threat of eutrophication (Chen et al., 2003; Janssen et al., 2014; Jin, 2003). Considering the multi-functionality of Taihu Lake, such as supplying drinking water, providing flood control, irrigation, water transport and recreation, the water quality issue and the consequential algae bloom problem cause huge losses to this regional industrial and economic center ever since 1987 (Duan et al., 2009; Guo, 2007; Paerl et al., 2011a; Qin et al., 2010).

The formation of the algae bloom happens when the concentration of algae is high at a particular spot. The growth of the algae population requires the proper temperature, light availability and essential nutrients, such as Nitrogen (N) and Phosphorus (P) (McGowan, 2016). The local government has made many attempts to mitigate the algae bloom, including wetland restoration, water transfer from the Yangtze River, environmental dredging, etc. (He et al., 2013; Li et al., 2013a; Sun et al., 2015). However, these treatments have not achieved the expected goal. Research suggested to apply a nutrient input reduction strategy for Taihu lake's water quality and ecology restoration (Ding et al., 2019; Janssen et al., 2017; Ke et al., 2018; Paerl et al., 2011b; Xu et al., 2015b).

Nutrients release into the lake's water body from two type of sources, namely internal sources from sediment resuspension, and external sources from the connected river network. The previously mentioned studies of input nutrient reduction considered the external sources of nutrient release, which are significantly correlated to the local urbanization around the lake (Deng et al., 2015a). The lake-connected river networks accumulate nutrient from various sources, such as the diffuse sources of agriculture runoff, atmospheric deposition, or point sources of industry waste water and domestic sewage, and transport these into the lake (Bozelli et al., 2009; Chen et al., 2016; Huang et al., 2008; Xu et al., 2018). Nutrient distribution in Taihu Lake varies both spatially and temporally, partially because of the nutrients from the inflow tributaries vary due to local economic structure difference (Wang et al., 2019; Yu et al., 2007). In turn, the uneven distribution caused an inter-annual difference in the location of algae bloom in the lake. During the summer, algae bloom happens in the northern part of the lake, while in the early summer, autumn and sometimes early winter, the algae bloom happens along the southwestern lake region (Zhang et al., 2011). However, these studies usually consider the lake as a whole black box model or as several separate regions for a roughly spatially averaged evaluation without considering the hydrodynamics. Thus, little attention has been paid to the spatial and temporal variations of nutrient distribution inside the waterbody of the lake resulting from the influence of the difference in both external input and physical factors, such as meteorological conditions, and the lake's intrinsic characters before and after the input reduction. Besides, based on hydrodynamic studies more attention should be paid to the effectiveness of stand-alone input nutrient reduction in different sub basins upstream of Taihu Lake.

To quantitatively study the influence of external nutrient input, a time scale is considered valuable, since a certain time is required for the nutrient to transport to a given location and this amount of time is correlated to the hydrodynamics of the lake system (Shen et al., 2011). Considering the nutrient transport from the connected river tributaries into Taihu Lake as point sources, the concept of water age is introduced here as an index to describe the time of the transport of nutrients inside of the lake. Water age is widely used in fresh water- and marine systems to effectively reflect the nutrient transport and mixing process of nutrients, and to provide the spatial and temporal heterogeneity of these processes (de Brye et al., 2013; Li et al., 2011a; Qi et al., 2016). Studies have shown a strong correlation of in situ measured Chl-a concentration and water age distribution of external discharge into shallow lakes, which proves the significance of the existing hydrodynamics (Wu et al., 2014).

In this study, a three-dimensional Delft3D numerical model is setup and used to investigate the transport and mixing of dissolved nutrients in Taihu Lake using the concept of water age. The purpose of this study is to answer the following questions: (1) Is it possible to quantitatively compare the nutrient load from different parts of the catchment river networks to Taihu lake with the concept of water age; (2) How does the meteorological factor wind, which is the largest influencing factor for lake hydrodynamics, impact the transport of nutrient transported from all over the catchment inside the lake?

This chapter is organized as follows. Section 4.2 is the theoretical background describing the water age theory. In the methodology section 4.3, a detailed description of the geographical area, as well as the Delft3D numerical modelling is introduced. In section 4.4, the hydrodynamic results and water age distribution in various scenarios are provided. Then, in section 4.5 discussion and further extensions of this study. Section 4.6 is the conclusion section.

4.2. Theoretical background

Several transport time scales are frequently utilized in hydrodynamic, biological, and water environmental studies for multiple topics like pollution transport tracking, water mass renewal, etc. (Monsen et al., 2002). These time-scales include, for example, water age, flushing time, residence time or transit time, turnover time, exposure time, etc. Each of the transport time scales works within the scope of a certain application (Delhez et al., 2014). In this study, considering the complicated hydrodynamic condition and spatial heterogeneity, the concept of Water Age (WA) is chosen.

The most common water age definition is given as “the time that has elapsed since the particle under consideration left the region in which its age is prescribed as being zero” (Bolin and Rodhe, 1973; Delhez et al., 1999). Thus, particularly in this study, WA is defined as the time elapsed since the tributary water with dissolved nutrient enters the lake water body, with WA is equal to zero at the boundary between the connected river network and the lake water.

Research on WA includes theoretical study, field observation and numerical mod-

elling (Deleersnijder et al., 2001; Jenkins and Clarke, 1976; Johnston et al., 1998; Karstensen and Tomczak, 1998; Pangle et al., 2013; Wunsch, 2002). Considering the applicability and accuracy, a numerical modelling study of WA is suitable under realistic bathymetry and hydrodynamic conditions (de Brye et al., 2013; Li et al., 2013b). There are two widely used numerical approaches for WA calculation in numerical models, namely, the Particle Tracking Method (PTM) (Zhang, 1995), and the Constituent-oriented Age and Residence time Theory (CART) (Chen, 2007; Deleersnijder et al., 2001; Liu et al., 2011). PTM is based on a Lagrangian approach by releasing a large amount of numerical particle tracers and calculate WA from the concentration spectrum. The disadvantage is the high computational cost. While CART is based on the Eulerian method, and thus no numerical particle tracer is required, but the actual transport trajectory is not provided in the model result (Wang et al., 2015). The governing equation for the evolution of the WA concentration distribution function in CART is

$$\frac{\partial c_i}{\partial t} = p_i - d_i - \nabla \cdot (u c_i - K \cdot \nabla c_i) - \frac{\partial c_i}{\partial \tau} \quad (4.1)$$

Where c_i is concentration, t is time, \mathbf{u} is velocity τ is water age number, p_i and d_i are source and sink terms, \mathbf{K} is eddy diffusivity tensor, $-\mathbf{K} \cdot \nabla c_i$ is the diffusive flux. Thus, the mean age at a given location \mathbf{x} is calculated with equation 4.2 based on the assumption that the mean age of a set of water parcels is mass-weighted and, thus, arithmetically averaged.

$$a_i(t, \mathbf{x}) = \frac{\int_0^\infty \tau c_i(t, \mathbf{x}, \tau) d\tau}{\int_0^\infty c_i(t, \mathbf{x}, \tau) d\tau} \quad (4.2)$$

Numerical WA simulation based on PTM is usually combining the hydrodynamic model with a random-walk model of horizontal eddy diffusion for the statistical treatment of turbulent mixing.

Position of a random particle is described by the following function:

$$\vec{x}(t + \Delta t) = \vec{x}(t) + \vec{u}\Delta t + z_n \sqrt{2\vec{K}\Delta t} \quad (4.3)$$

Where $\vec{x}(t)$ is the particle's position at time t , Δt is the time step, \vec{u} is the velocity vector, \vec{K} is the eddy diffusion tensor from hydrodynamic model, and z_n is the random vector normally distributed with unit standard deviation and zero average value.

4.3. Methodology

4.3.1. Numerical model description

Delft3D, an integrated open source modelling software developed by Deltares (Delft, the Netherlands), is used to simulate the hydrodynamics of Taihu Lake and the temporal and spatial varying water age (WA) distribution in this study. In particular its hydrodynamic (FLOW) and water quality (WAQ) modules are applied.

Delft3D-WAQ is a multi-dimensional water quality model framework, which solves the advection-diffusion-reaction equation on a predefined computational grid for a wide range of model sub-stances. D-WAQ simulation includes large numbers of substances and processes. Applications of D-WAQ include, amongst others, the eutrophication of lakes and reservoirs, dissolved oxygen depletion in stratified systems, impact of a sewage outfall on nutrient concentrations and primary production, transport of heavy metals through an estuary, accumulation of organic micro-pollutants in fresh water basins and the emission of greenhouse gases from reservoirs, etc. The hydrodynamic information is derived from the Delft3D-FLOW model Deltares (2005).

The mass balance equation in Delft3D-WAQ is:

$$M_i^{t+\Delta t} = M_i^t + \Delta t \times \left(\frac{\Delta M}{\Delta t} \right)_{Tr} + \Delta t \times \left(\frac{\Delta M}{\Delta t} \right)_p + \Delta t \times \left(\frac{\Delta M}{\Delta t} \right)_s \quad (4.4)$$

Where M_i^t is the mass at the beginning of a time step t , $\left(\frac{\Delta M}{\Delta t} \right)_{Tr}$ is the mass changes by transport including both advective and dispersive transport; $\left(\frac{\Delta M}{\Delta t} \right)_p$ is the mass changes by physical, (bio)chemical or biological processes; $\left(\frac{\Delta M}{\Delta t} \right)_s$ is the mass changes by sources (e.g. waste loads, river discharges).

Mass transport by advection and dispersion in Delft3D-WAQ is:

$$\frac{\partial C}{\partial t} = D_x \frac{\partial^2 C}{\partial x^2} - v_x \frac{\partial C}{\partial x} + D_y \frac{\partial^2 C}{\partial y^2} - v_y \frac{\partial C}{\partial y} + D_z \frac{\partial^2 C}{\partial z^2} - v_z \frac{\partial C}{\partial z} \quad (4.5)$$

Where, $\frac{\partial C}{\partial t}$ is concentration gradient, D_x is dispersion coefficient in x direction, v_x is velocity at x direction.

4.3.2. Age calculation in Delft3D

In the Delft3D model, WA calculation is similar to CART based on the mass concentration ratio of two kinds of tracers, namely the conservative tracer and decayable tracer. The mass of the conservative tracer remains the same amount as at the released time, while the mass of the decayable tracer will decay with time at a given decay rate. The decayable tracers do not need to necessarily exist or be released in the real world; they are a reference to compute the water age in numerical modelling. The mechanism is that the two kinds of tracers will be released at the same time, and since they participate in the advection and diffusion process at the same time, the ratio of their concentration will remain the same at a fixed time. With the decay rate, the water age can be easily achieved. For the conservative tracer, the time derivative of concentration is

$$\frac{\partial c}{\partial t} = \text{advection} + \text{dispersion} + \text{source} \quad (4.6)$$

while for the decayable tracer

$$\frac{\partial c}{\partial t} = \text{advection} + \text{dispersion} + \text{source} - Kc \quad (4.7)$$

where K is the decay rate. The formulation to calculate water age in this study is:

$$ageTr_i = \frac{\ln\left(\frac{dTr_i}{cTr_i}\right)}{RcDecTr_i} \quad (4.8)$$

$$dDecTr_i = RcDecTr_i \times dTr_i$$

Where, $ageTr_i$ is the age of the tracer $i[d]$, cTr_i is the concentration of the conservative tracer $i[gm-3]$; dTr_i is the concentration of the decayable tracer $i[gm-3]$; $RcDecTr_i$ is the first order decay rate constant for the decayable tracer $i[d-1]$; $dDecTr_i$ flux for the decayable tracer $i[gm-3d-1]$.

4.3.3. Model setup

The hydrodynamic section of the Taihu Lake model is developed by (Liu et al., 2018) with Delft3D. This model uses a rectangular grid with a grid resolution of 1000m horizontally and five vertical sigma layers uniformly defined in depth. The model is driven by tributary discharge boundaries and meteorological conditions, like surface wind, evaporation and precipitation. Over 150 tributaries are arranged into 21 groups for simplicity. The simulation time is during the entire year of 2008, with a time step of 10min. Detailed physical and numerical parameter sets are listed in the paper (Liu et al., 2018).

Based on upstream catchment sub basins (Wang et al., 2019) and the boundary condition of the hydrodynamic model (Liu et al., 2018), inflow tributary boundaries are categorized into 3 groups for the WA simulation (Figure 4.1). For each group of boundaries, a set of conservative tracers and decayable tracers are continuously released, with the decay rate of the decayable tracers set to be 0.01/day. The north and northwest boundaries mainly represent the discharges from Jiangsu province (WA1), while the south and southwest boundaries include mountainous river discharges and tributaries from Zhejiang Province (WA2). Northeast boundaries mainly account for water transfer from the Yangtze River (WA3). The WA simulation time step is the same as in the hydrodynamic model, and the model result is recorded at every 6 hours of model time. Note, both inflow and outflow occur in the above mentioned boundaries throughout the year. Tracers released with the outflow boundary condition will be transported out of the model domain and not be included in the WA calculation. Based on Taihu Lake's geometry and hydrological features, the lake is divided into 7 sub basins. For each sub basin, an observation point is set to monitor the WA distribution (Figure 4.1).

4.3.4. Scenarios

The calibrated hydrodynamic model is used to quantitatively investigate the influence from the surrounding river network and wind, focusing on tributary discharges, wind direction and wind speed. A series of numerical scenarios is conducted (Table 4.1). A reference scenario is setup for representing the real tributary discharge and the wind record in 2008 (scenario 1). With the actual boundary discharge conditions and wind directions, wind speed in 2008 downscaled with a ratio

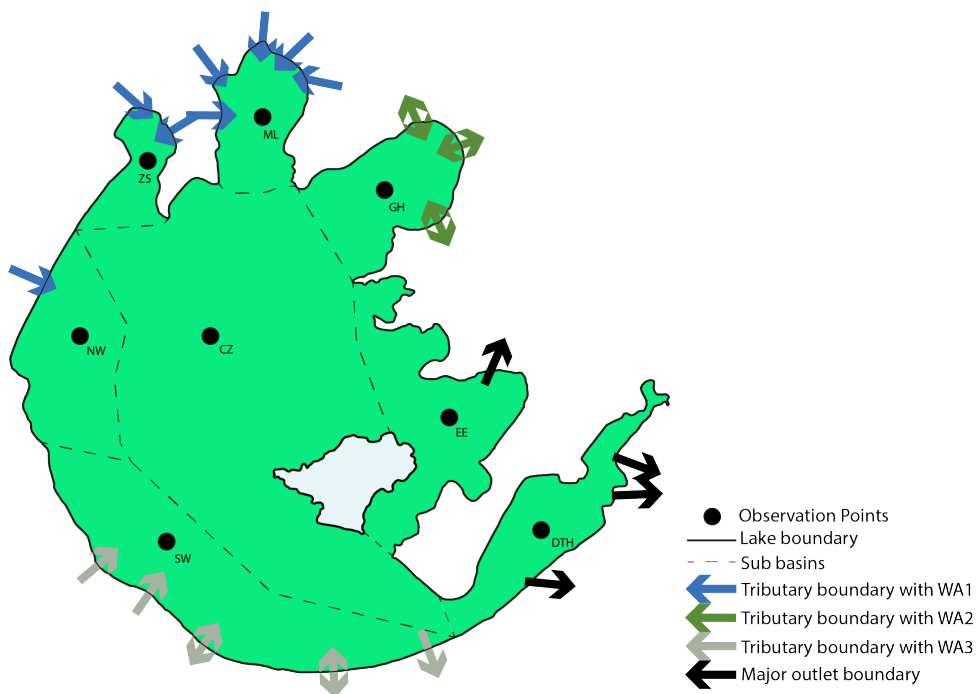


Figure 4.1: Tributary discharge, observation points and sub basins of Taihu Lake. Directions of arrows imply the major inflow/outflow direction of tributary discharge. Abbreviation means names of subbasins, namely, ML: Meiliang Bay; GH: Gonghu Bay; EE: East Epigeal; DTH: Dongtaihu Bay; SW: Southwest Zone; NW: Northwest Zone; ZS: Zhushan Bay; CZ: Central Zone.

0.5 and 0 (scenario 2,3). The other cases are designed to investigate the influence of the prevailing wind and the magnitude of inflow boundary discharge (scenario 4 -11). Further, the influence of all wind directions is studied (scenario 12 - 18). For the constant tributary discharge case, the same amount of water is flowing out of the model domain through the major outlet boundary as the inflow of water.

Table 4.1: Scenarios

| Scenario | Wind | | Discharge for each WA inlet(m^3/s) | | |
|----------|---------------|---------------|--|-----------|-----------|
| | Direction | Speed (m/s) | WA1 | WA2 | WA3 |
| 1 | 2008 data | 2008 data | 2008 data | 2008 data | 2008 data |
| 2 | 0.5*2008 data | 0.5*2008 data | 2008 data | 2008 data | 2008 data |
| 3 | No wind | no wind | 2008 data | 2008 data | 2008 data |
| 4 | SE | 3.5 | 10 | 10 | 10 |
| 5 | SE | 5 | 10 | 10 | 10 |
| 6 | SE | 3.5 | 20 | 20 | 20 |
| 7 | SE | 5 | 20 | 20 | 20 |
| 8 | NW | 3.5 | 10 | 10 | 10 |
| 9 | NW | 5 | 10 | 10 | 10 |
| 10 | NW | 3.5 | 20 | 20 | 20 |
| 11 | NW | 5 | 20 | 20 | 20 |
| 12 | No wind | / | 10 | 10 | 10 |
| 13 | S | 3.5 | 10 | 10 | 10 |
| 14 | SW | 3.5 | 10 | 10 | 10 |
| 15 | W | 3.5 | 10 | 10 | 10 |
| 16 | NW | 3.5 | 10 | 10 | 10 |
| 17 | N | 3.5 | 10 | 10 | 10 |
| 18 | NE | 3.5 | 10 | 10 | 10 |

4.4. Results

4.4.1. Spatial and temporal distribution of WA

Influenced by the time-varying wind field and hydrodynamics, WA distribution for all 3 groups of tracers changed both spatially and temporally. Bottom and surface WA1 distribution at the last time step of scenario 1 is shown in Figure 4.2. Little WA1 vertical difference (~ 0.01 day) between the surface and bottom layer is observed from the model result, as well as in WA2 and WA3. The consistency in vertical WA distribution implies that, although surface and bottom horizontal flow velocity fields differ hugely (Liu et al., 2018), WA is fully mixed in vertically within each time step. WA distribution varies spatially for WA1; the highest WA1 is over 200 days in Dongtaihu Bay, while the lowest WA1 is less than 30 days in Zhushan Bay. The phenomenon could be explained by the difference in distance from the inflow WA1 tributaries. WA1 values near the northern and western part of Taihu

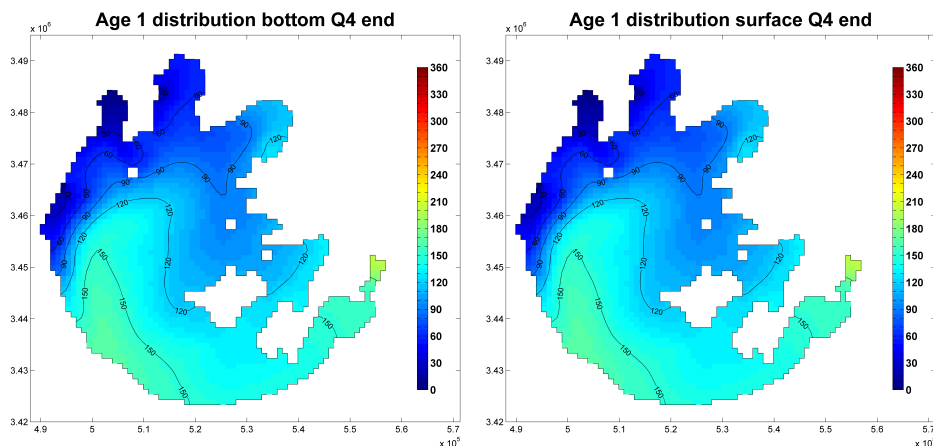


Figure 4.2: WA1 distribution of scenario 1 at the last time step. (Unit: d)

Lake (~ 30–90 days at Zhushan Bay, Meiliang Bay, Gonghu Bay and the northern part of Central Zone) are significantly smaller than the values of the southern and eastern part of the lake (~ 120 –200days at Northwest Zone and Dongtaihu Bay), since the WA1 tributary boundary is located in the northern and western part of the lake.

High temporal heterogeneity is also observed in the model results for WA1 distribution after each quarter of the year in scenario 1 (Figure 4.3). As the time passes since the model's starting time, the maximum WA1 increases. By definition, this value will not exceed the model time passed, but the location with the value varies. At the end of Q1, the maximum value (~ 90days) is located at the east part of the lake; one quarter later, the maximum value (~ 120days) moves to the northeastern part in Gonghu Bay and the northwestern part at Dongtaihu Bay; after another quarter, the maximum value (~ 180days) occurs only in Gonghu Bay in the northeast, and at the end of year, the peak value (~ 200days) lies in Dongtaihu Bay. In contrast, the lowest WA1 value occurs near the WA1 tributary boundary throughout the whole year. Since the tributary boundaries for each WA are located at different locations around Taihu Lake, the distribution of each WA also varies, both spatially and temporally. WA distributions of the final time step in scenario1 are shown in Figure 4.4. For WA1, the northern sub basins (Zhushan Bay, Meiliang Bay, Gonghu Bay and northern part of Central Zone and East Epigeal) have a lower WA1, while the Southwestern Zone and Dongtaihu Bay have a higher WA1. For WA2, WA in the western half of the lake is higher than 240days, implying hardly any water from the WA2 boundary has reached this part of lake. While for WA3, small WA occurs near the western margin of the lake. Beside the distance to the tributary boundaries, the variance in WA distribution could be explained by the value of total discharge through the tributary boundary for each WA group (Figure 4.5). Total discharge for WA2 peaks in June, then becomes almost zero for

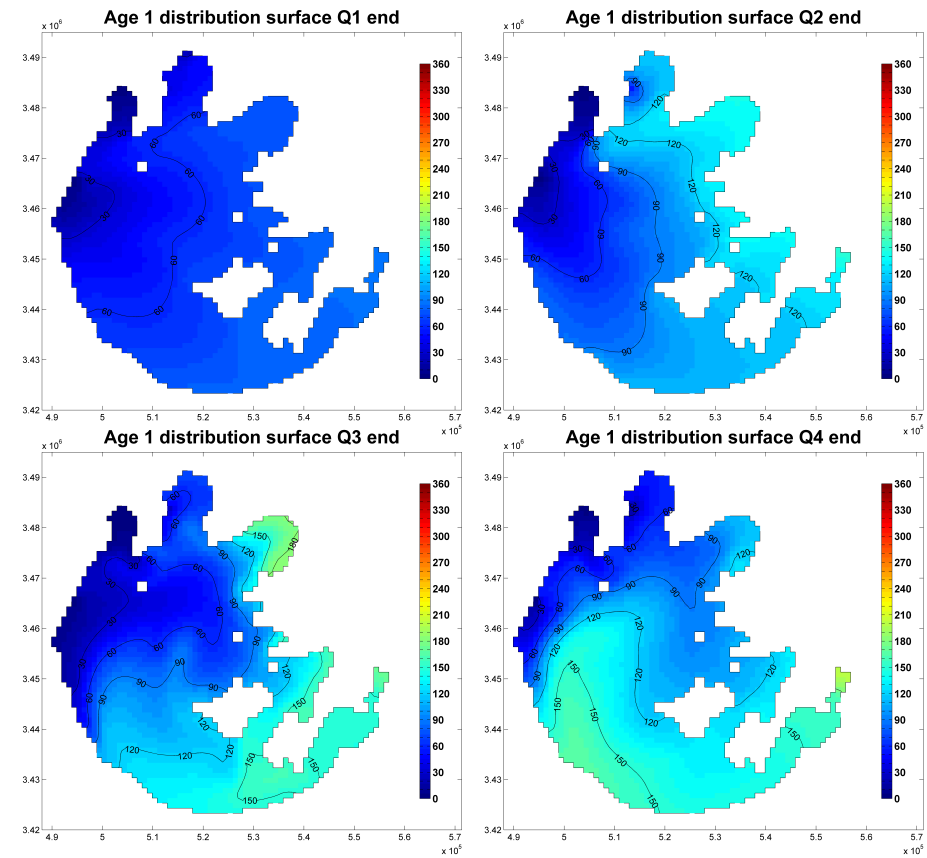


Figure 4.3: WA1 distribution at the end of each quarter

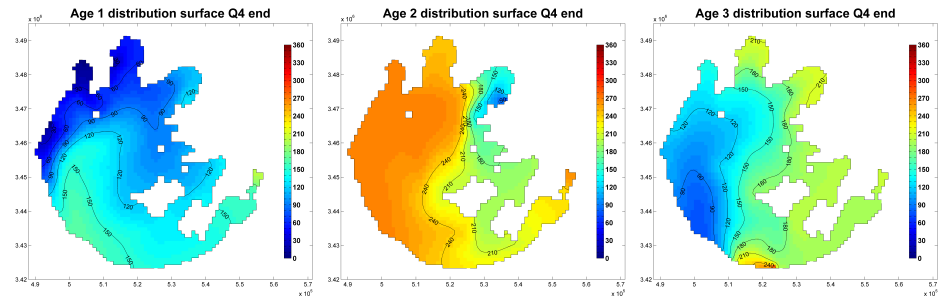


Figure 4.4: WA distribution for scenario 1 at the end of year.

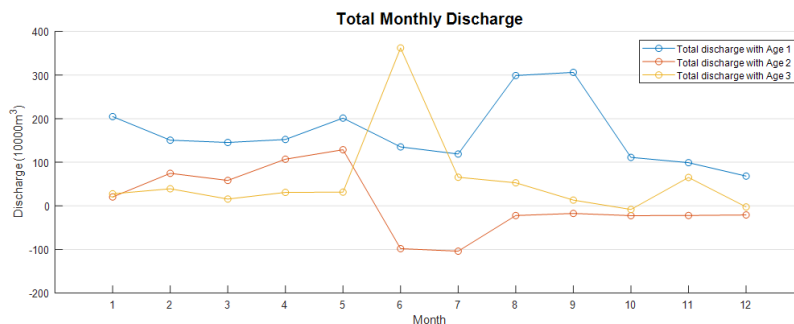


Figure 4.5: Total discharge for each WA discharge

the next 5 months, which could explain the extreme high WA2 in the western half of the lake since water from WA2 barely enters this area. While total discharge for WA1 is always positive and larger than around $100\text{m}^3/\text{s}$, lower WA1 occurs in around half the area of the lake. For WA3, discharge remains negative since June, but since still 2 inflow boundary among WA3 boundary still has positive discharge from mountainous area, area near western margin of the lake still have a smaller WA3. But for all 3 WA, larger value occur in Dongtaihu Bay, suggesting less inflow tributary water enters this sub basin. Possibly it is due to the narrow entrance and elongated geometry of Dongtaihu Bay.

In general, under the influence of time varying inflow discharge, WA distributions show heterogeneity both spatially and temporally.

4.4.2. Wind speed and direction effects

Wind influence on WA is studied by comparing the WA value at the last time step of each steady wind scenario with tributary discharge at $10\text{m}^3/\text{s}$. WA of steady wind for each observation point differs at both the average and range values. This difference could be explained by the influence from hydrodynamics. With steady wind, the horizontal circulation patterns of Taihu Lake differ with wind directions, which in turn influence the advection and mixing processes of inflow tributary discharge. Thus, the corresponding range and average of WA value varies. For example, WA1 distribution within the Southwest Zone ranges from the highest in an east wind condition ($\sim 190\text{days}$) to the lowest with a south wind condition ($\sim 120\text{days}$) with the average WA1 around 140days . While for WA3, the situation is different, the highest WA3 is with a southwest wind ($\sim 120\text{days}$) and the lowest WA is with a north wind ($\sim 70\text{days}$), with the lowest WA of around 100days .

Moreover, in some sub basins where inflow tributary discharge is nearby, wind influence is relatively low, as for example in Gonghu Bay, where WA2 boundaries are adjacent. With 8 wind directions, the range of WA2 is less than 30days , while at the same location the difference between the maximum WA1 and lowest WA1 is larger than 100days . The bias in WA implies that WA2 tributary inflow contributes more to the water retention in Gonghu Bay than WA1 and WA3 tributary discharges.

Beside wind directions, wind speed is also an important factor influencing WA

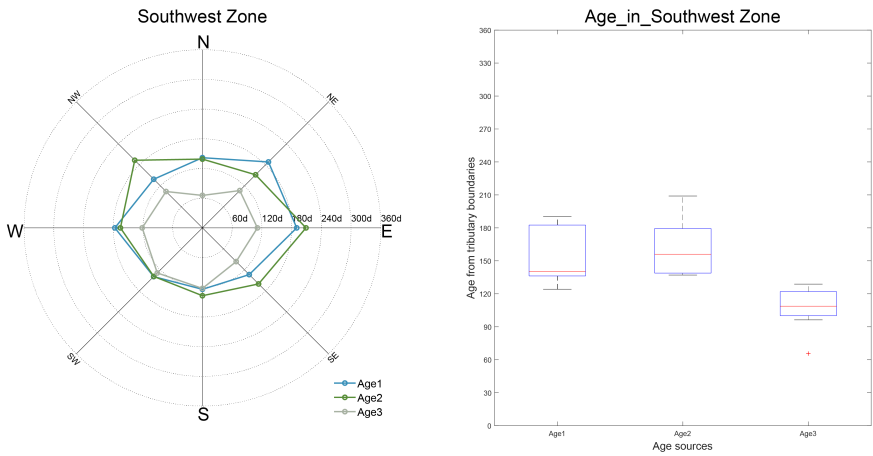


Figure 4.6: WA for Southwest Bay observation point with 8 wind scenarios.

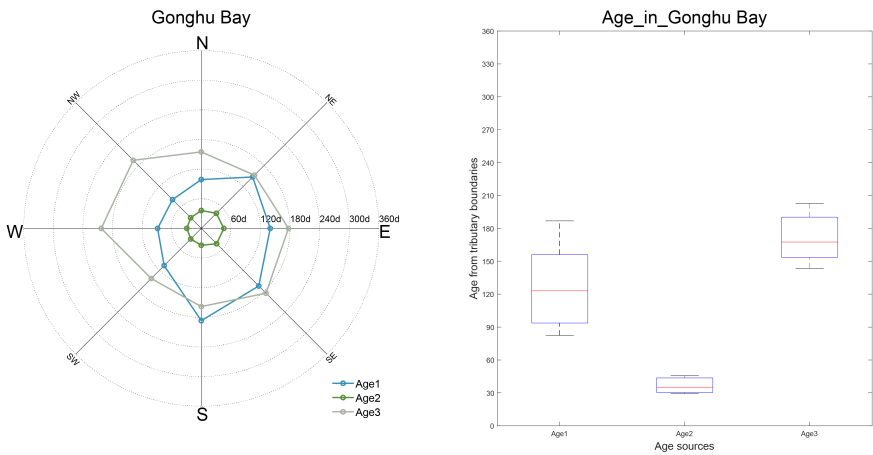


Figure 4.7: WA for Gonghu Bay observation point with 8 wind scenarios.

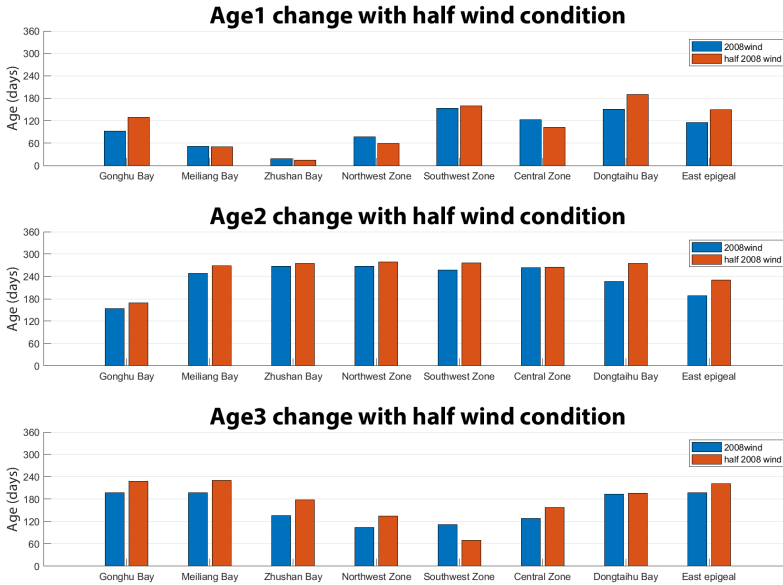


Figure 4.8: Water age comparison between 2008 real wind data scenario and half wind speed scenario.

distribution. In scenario 2, wind speed of the entire simulation is half the wind speed in scenario, which is the real 2008 wind data. As illustrated in the comparison of the model result (Figure 4.8), differences occur for all 3 WA distributions. However, increase or decrease of WA is site-specific and WA-specific. For the Northwest Zone, with half wind, WA1 decreases while WA2 and WA3 increases. But for Gonghu Bay, with half wind, all 3 WA values increase. In general, wind direction and wind speed do influence WA distribution over the whole Taihu Lake. The influence is spatially heterogeneous. Change of wind direction would lead to change on both the average value and the range of WA, while wind speed difference induces a site-specific and age-specific change of the WA value.

4.4.3. Discharge effects

Discharge influence is studied by comparing scenarios with the same wind condition but a different inflow discharge rate. Flow discharge in scenario 4 and scenario 6 are $10\text{m}^3/\text{s}$ and $20\text{m}^3/\text{s}$ in each WA inflow tributary respectively, while the outflow discharge at remaining boundaries are calculated to ensure a mass balance between inflow and outflow. For both scenarios, a steady southeast wind with $3.5\text{m}/\text{s}$ wind speed is set. WA for all 3 WAs of all observation points decreases with a rising tributaries inflow discharge (Figure 4.9), which could be explained by the enhancing hydrodynamics due to more momentum input through the tributary boundaries. The largest WA difference is the WA2 change in East Epigeal

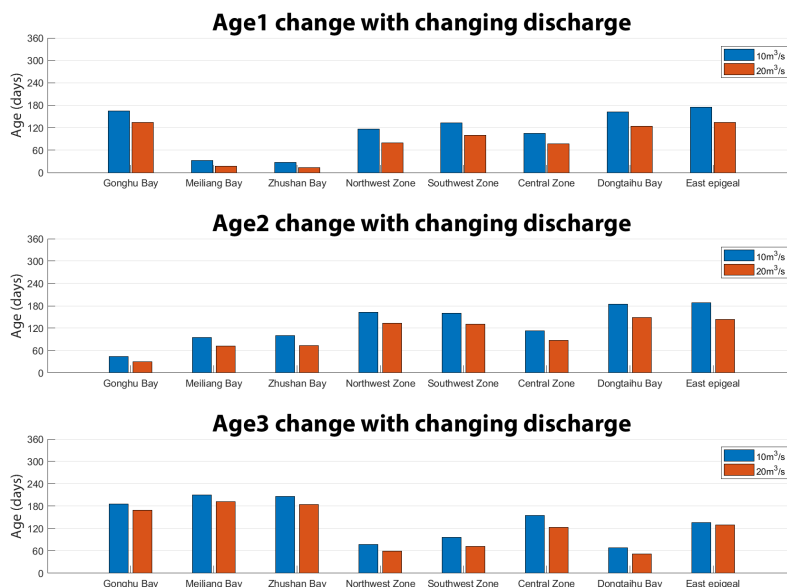


Figure 4.9: Water age comparison between 2008 real wind data scenario and half wind speed scenario.

(~ 45days), while the smallest WA difference is the WA1 change in Zhushan Bay (~ 13days). Again, changes in WA show spatial heterogeneity and that it is WA specific.

Comparing to impact of wind speed and wind direction change, the influence of discharge on WA is smaller. Partially because it is easier to dampen the increasing momentum from tributary discharge when it has penetrated farther into the lake, while wind momentum input through surface shear stress is continuous all over the lake.

4.5. Discussion

4.5.1. Various transport time scales

Transport time scales are frequently adopted in describing the hydrodynamic processes, which transport water and the constituents. Water age is one of the most favorable transport time scales, while the usage of flushing time and residence time is also very common. To extensively adopt transport time scales in large shallow lake studies, understanding the definition and limitations of these time scales is crucial.

Residence time is the time spent by a water parcel or a pollutant to leave the given water body (Delhez et al., 2004). By definition, resident time is location specific value as water age and serves as a complement to water age, since water

age is the duration for a water parcel from the inflow boundary to a given spot, while residence time is the duration from this particular location to the outflow boundary (Monsen et al., 2002). Residence time is commonly used to evaluate the inflow nutrient's further influence inside the water body (Rueda and Cowen, 2005).

Flushing time, on the other hand, is a bulk parameter to describe the exchange of water body. Flushing time is defined as the time it takes to replace all the water in a basin (Bolin and Rodhe, 1973). Flushing time could be seen as the sum of water age and residence time. This concept is frequently used in estuary and lagoon research and the early studies could be traced back to 1950s (Choi and Lee, 2004). The original method to get flushing time is the "tidal prism method", i.e. flushing time is calculated as the ratio of the mass of a scalar to the rate of renewal of the scalar, with the assumption of instantaneously releasing of inflow and thoroughly mixing inside the water body. Another approach considering salt balance is also adopted in previous studies (Miller and McPherson, 1991; Monsen et al., 2002). Further studies have improved the "tidal prism method" to mitigate underestimation due to the idealized assumptions, but the thoroughly mixing assumption is still adopted (Luketina, 1998).

Beside residence time and flushing time, some terminologies like transit time and turn-over time are also found in literature. By definition, turn-over time is identical to flushing time and transit time is the average residence time (Bolin and Rodhe, 1973).

Based on the definition of these transport time scales, the application of these time scales are purpose-oriented. Water age is more suitable when considering the spatial distribution of influence from tributary discharge into the large shallow lake as in this study, while residence time could help to study the dilution of pollution already inside the lake. Flushing time, as the sum of water age and residence time, could be used to indicate the temporal extent and the efficiency of diluted fresh water from external waterbody.

4.5.2. Wind change due to climate change

Terrestrial near-surface wind speed is reported to decrease due to climate change. During the last 30 years, 73% terrestrial stations records average wind speed decline across most of the northern mid-latitudes (McVicar et al., 2012; Stocker et al., 2014; Vautard et al., 2010). For large shallow lakes like Taihu Lake, where wind influences not only the hydrodynamic conditions (Liu et al., 2018), but also the ecological status (Paerl et al., 2011a; Qin et al., 2010), climate change induced wind condition variation and its consequences should be granted more attention.

Nutrient loads in shallow water mainly come from 2 sources, namely the internal sources and the external sources. Albeit low wind speed causes low waves and low corresponding bottom shear stresses, hampering sediment resuspension which is crucial for release of internal nutrient sources, it promotes hypoxia in the bottom layer of the water column, and in turn enhances the nutrient releasing from sediment and counteract the effect of declining resuspension, stimulating the algae growth and finally leading to more severe eutrophication. More effort should be spent on this with numerical models.

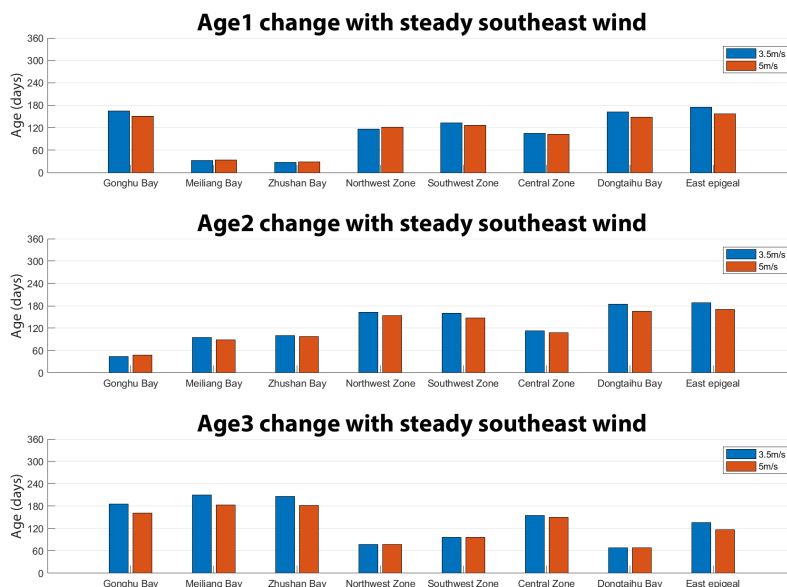


Figure 4.10: WA change with 3.5m/s and 5m/s southeast wind

The combination of summer water level increase and wind speed decrease, (Deng et al., 2018; Ke et al., 2018), is expected to change the distribution of nutrients from external sources in shallow lakes. To illustrate the actual influence of wind speed change, a comparison of model result with steady southeast wind but changing wind speed (scenario 4 and scenario 5) is illustrated (Figure 4.10).

For most observation points, wind speed decline causes an increase in WA values for all 3 WAs. Since less wind speed weakens the wind-induced hydrodynamics in most part of the lake, the advection and mixing processes of incoming water is attenuated. Moreover, increased WA means that external nutrient input would stay longer in the lake, enlarging the chances for cyanobacteria to capture more nutrient and to form an algae bloom (Ji, 2017).

Thus, less wind speed will encourage release of internal source and cause longer duration of external source nutrient inflow, both of which will induce more severe algae bloom and deteriorate of water quality.

4.5.3. Implication of water age on shallow lake management

The initial water age study mainly has two applications: 1. To assess the ventilation rate of semi-closed basins; 2. To infer the horizontal circulation, which focus more on estuary and lagoons (Deleersnijder et al., 2001). Further studies in more broad aqua systems paid more attention on water quality issue such as the efficiency of water transfer (Li et al., 2011a). With climate change and more

complicated nutrient control policy, water age is able to provide more assistance in integrated water quality management of shallow lakes like Taihu Lake.

First, water age analysis would provide help when critical toxins leakage condition happens. With numerical models and meteorological forecasts, water age distribution maps could be generated in minutes. Thus the spatial and temporal spread information of inflow toxins could be provided, and further measures could be decided based on that.

Second, water age analysis would provide information on tributary discharge influence of critical spots, assisting the governance of water quality in a complicated management condition. In this study, three water age groups are chosen corresponding to inflow tributary discharge from three municipalities. Situations become complicated when nutrient control and wastewater treatment involves more stakeholders. And water age analysis could provide essential information to divide the responsibility and help to improve the master plan of Taihu Basin water quality management.

4.6. Conclusions

Impact of tributary discharge inflow from river discharge around Taihu Lake, the 3rd largest fresh water lake in China, is investigated using the concept of water age. Main purposes of this study is to provide quantitative comparison of nutrient loads from different parts of the catchment river networks and to investigate meteorological influence on the advection and mixing process of nutrients from tributary discharge inside the lake body. In this study, the inflow tributaries are divided into three groups based on upstream catchment subbasins and the boundary condition of the hydrodynamic model. Water age is computed using the three-dimensional Delft3D model with Flow and WAQ module.

Model results show both spatial and temporal heterogeneity occurs in all 3 water age groups, which is influenced by both distance to the tributary boundaries and total discharge through tributaries boundary for each water age group. Wind influence on water age is analyzed. Change of wind direction would lead to change on both the average value and range of water age, while wind speed difference induces site-specific and group-specific change of WA value. Water age decreases with rising tributaries inflow discharge, however, the influence of discharge is less significant than that of change of wind.

Various time scales like residence time and flushing time are discussed for clear understanding. Wind speed decline induced by climate change is analyzed on the effect on both internal and external nutrient source release, and influences on both sources would cause water quality to be deteriorated. Lastly, further application of water age is suggested for the more complicated integrated water management on lake basin scale.

5

Interaction between river networks and lakes

5.1. Introduction

5.1.1. Urbanization of Taihu Lake

Taihu Lake river basin, located at the core area of the Yangtze River delta, is the joint location of "Yangtze River Economic Belt" and "The Belt and Road Initiative" (5.1). Scattered in the catchment are big cities including Shanghai, Wuxi, Suzhou and Hangzhou. It is one of the most densely populated and economically developed regions in China. Inside the catchment area nationally leading industries of automobile, metallurgy, chemistry, mechanical electronics and medicine are located. Since the Chinese economic reform, Taihu Lake river basin has entered a phase of rapid urbanization and has become the area with the highest degree of urbanization of China. Up to 2015, the urbanization rate in the river basin reached 80%. With rapid urbanization, the scale of cities increases, the economy develops,



Figure 5.1: The administration division of Taihu Basin

population becomes more dense, wealth is built up and, in turn, the demand of water, electricity, minerals and other resources is gradually increasing (Fan et al., 2017). Attracting growing attention, the resource scarcity has become a hot research topic in the field of changing environment and sustainable development.

As the only megacity in the Taihu Basin, Shanghai's urbanization rate is high. The total GDP and GDP per capita in 2015 increased 9100% and 4100% compared to GDP in 1978. Simultaneously, the road network size increased from 905 km to 18187 km and the cultivated area decreased to half its size. Shanghai's urbanization could be separated into phases, namely, the general growth before 2000 and the

rapid growth after. Compared to Shanghai city, the average value of Taihu Basin shows a similar growing trend. The population density growth rate increased from $10 \text{ km}^2/\text{a}$ during the period of 1978 – 2000 to $26 \text{ km}^2/\text{a}$ after 2000, while the GDP per capita increase rate rose from $905 \text{ ¥}/\text{a}$ to $5714 \text{ ¥}/\text{a}$ ($115 \text{ €}/\text{a}$ to $729 \text{ €}/\text{a}$).

Water has always been a key factor for the Taihu Basin. The Taihu Basin has suffered floods due to the combined effect of a low terrain, a mild slope and tides. Meanwhile, due to the pollution caused by an increasingly dense population and climate change, environmental and water problems occur in Taihu Basin. After the 1991 flood event, the government published 4 master plans to deal with the water related problems, namely, Taihu Basin Flood Control Planning, the Taihu Basin Comprehensive Planning, Taihu Basin Water Resources Comprehensive Planning and Taihu Basin Water Environment Overall Comprehensive Management Plan and its revision. Till 2019, only the investments for the environment have already reached ~ 100 billion RMB (~ 12.5 billion €), but the situation is only slightly better due to excess nutrients in Taihu Basin (Qin et al., 2019).

5.1.2. Water and Energy Status in Taihu Basin

The main water resources in Taihu Basin are coming from the Yangtze River and precipitation. The average annual rainfall of Taihu Basin is 1176 mm (1956 – 2015), of which over 60% in the monsoon season from May to September. Water resources in Taihu Basin are abundant, with an average of yearly locally available surface water to amount to $6.41 \times 10^9 \text{ m}^3$. The total water available ranges from $2.92 \times 10^{10} \text{ m}^3$ to $3.73 \times 10^{10} \text{ m}^3$, of which $\sim 98\%$ is surface water. The annual water demand in Taihu Basin remains stable, ranging from $2.82 \times 10^{10} \text{ m}^3$ to $3.71 \times 10^{10} \text{ m}^3$ during the years from 2001 – 2015. Among the total water demand, the industry claims the largest ratio of water. During the period 2001 – 2015, industry water usage increased from 2001 to 2007, then started to decrease since in 2007 the industrial restructuring strategy was released. Domestic water demand in the same period (2001-2015) gradually increased. The majority of environmental water usage, which cost around 1% of the total water usage, is for urban environment (5.2). Correspondingly, wastewater load increased from 5.1 *billion* in 2001 to 6.4 *billion* in 2015. From 2001 to 2015, water use per person in Taihu Basin decrease from $802 \text{ m}^3/\text{a}$ to $569 \text{ m}^3/\text{a}$ due to increased water use efficiency. However, the concepts of water quality and water quantity remain problematic for Taihu Basin. In 2015 only 27.9% of surface water was considered of good quality. Especially in Taihu Lake, rapid urbanization caused an increased waste water load, moderate eutrophication is occurring in 65.4% of total area, while the remaining area shows a mild eutrophication. The total water demand deficit shows a seasonal variation, and especially in July and August a large amount of water supply is required. The water demand exposes the need to increase the efficiency in water use and management in Taihu Basin's water resources.

The total energy consumption in Taihu Basin kept increasing with the socio-economic development in the region, from 2.76×10^5 tons of standard coal in 2011 to 2.93×10^5 tons of standard coal in 2015. The total energy consumed by Shanghai city amounted to $\sim 40\%$ and by Suzhou city to 30%, respectively. Specifically, from

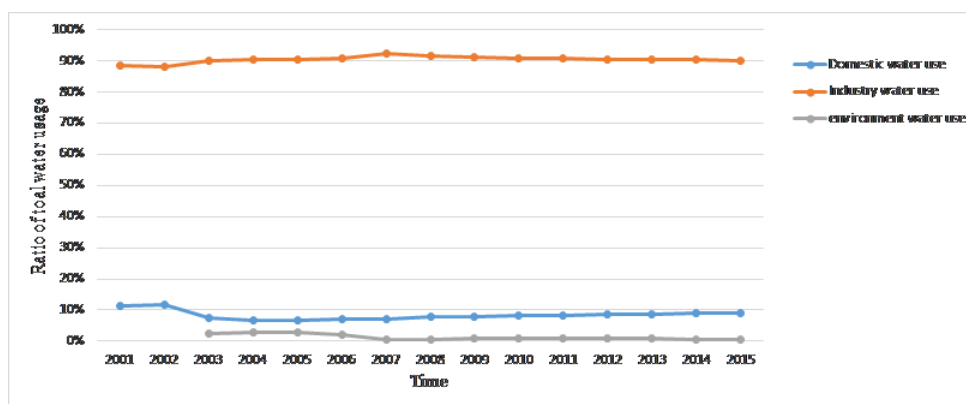


Figure 5.2: Ratio of 3 water use types of total water usage

5

2005 to 2015, the total electricity consumption in Taihu Basin increased at the rate of 5.3% from 266 *billion kWh* to the nearly doubled value of 502 *billion kWh*.

Urbanization is the key reason for the growing demand of water and energy. Although, with increased governance on water use efficiency and industry production efficiency, water use and electricity use per ¥10000 of GDP decreased by 60% and 35% from 2007 to 2015, respectively, a more efficient water and energy usage plan is still required.

5.1.3. Wuxi City: a typical city in the megalopolis of Taihu Basin

Wuxi City, with a population of 4.97 million and a surface area of 4672km², is located along the Yangtze River and to the north of Taihu Lake (5.3). Wuxi City has a history longer than 3000 years, since the end of Shang Dynasty (1600BC to 1046BC). The territory of Wuxi was formed in 1983 after an adjustment of the administrative division of the city.

During the past 30 years, Wuxi has experienced a rapid and ongoing urbanization with a booming population (Table5.1). The urbanization took place after the economic reform in 1978. During the past years, domestic and foreign investments have taken advantage of the geographical position of Wuxi City, its high educated population, its profound cultural accumulation and a stable society (Sun et al., 2019). The economic prosperity has attracted rural labour to migrate into the urban area. In 2019, Wuxi was ranked 13 in the GDP list of Chinese cities, which makes Wuxi a perfect case to study the water-energy plan in Taihu Basin.

The majority of Wuxi City's local water resources are coming from Taihu Lake water, Yangtze River water and rainfall. Both surface water and ground water are used to meet the increasing water demand due to rapid socio-economic development (Xie et al., 2018). Domestic water uses in Wuxi kept increasing with a growing population, while industrial water use rose until the mid-1990s, then decreased due to the shutting down of polluted industries for environmental purposes (Figure



Figure 5.3: Location and administrative division of Wuxi City

Table 5.1: Wuxi population and urbanization rate

| | Total Population | Urban Population | Urbanization Rate |
|------|------------------|------------------|-------------------|
| 1983 | 3.87 million | 0.81 million | 25% |
| 2018 | 4.97 million | 2.63 million | 76% |

* Total Population and urban population here referred to household population while the urbanization rate is calculated with residence population. Data from Wuxi statistical year book 2018.

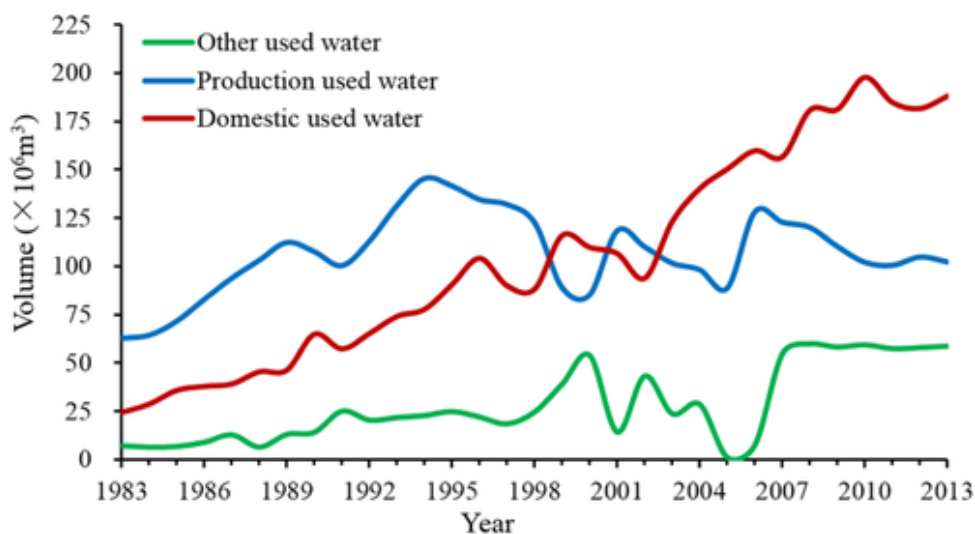


Figure 5.4: Wuxi Water usage from 1983 to 2013

5.4). Specifically in 2010 and 2015, total water use in Wuxi City went up mainly due to the increased water use in fossil-fuel power plants. For water security and a better adaptation for future challenges, Wuxi City has released “Three Red Line management” control plans for the use of water resources in Wuxi City, emphasising the water resources development red line, water use efficiency red line, and water pollution red line.

In the period from 1983 to 2013 energy sources of Wuxi city consisted of raw coal, crude oil and natural gas, all of which were imported from outside regions. Imported from Shanxi and Shandong provinces in China, and other countries, like Australia, coal is the major energy source in Wuxi. Treatment of coal requires a large amount of water and the use of coal should receive special consideration.

5.1.4. Water-energy nexus

A comprehensive and thorough understanding of the interdependency between water and energy, as two essential resources, is required for a more efficient master plan for Taihu Basin. With the urbanization process, society is putting increasing pressures on the environment, which introduces more trade-offs and are a source of potential conflict.

The same topic of the water-energy nexus has attracted attention from both researchers and the public all over the world (Hamiche et al., 2016). Especially for developing countries, of which the urban population is estimated to increase over 50% by 2050 (Dai et al., 2017), the rapid urbanization and climate change reveal the inadequacy in the available resources to supply water, food and energy. The term ‘nexus’, meaning ‘a connection or series of connections linking two or more things’ (Boas et al., 2016), first appeared in the early eighties and nineties, as an

integrated management approach for resource problems under complex situations (Endo et al., 2017). Initially in 1983, the nexus approach was concerned about the interconnections between energy and food, later the concern regarding ecosystems was included. In the mid-eighties, the 'water-energy-agriculture' nexus emerged (Kurian, 2015); then in the early 2000s, researchers started to use the 'Water-Energy-Nexus' (WEN) for the integrated management of water and energy (Al-Masri et al., 2019).

The interdependencies of water and energy are complex. On the one hand, energy challenges the water footprint of energy portfolios and the water quality degradation due to energy production. On the other hand, water challenges energy by the rising water demand due to climate change, water allocation for energy production, the increasing demand of clean hydropower and water reuse (Kurian, 2015). Meanwhile, water conservation and energy production do rely on each other. Water is needed for fuel production, hydropower, and thermal electric cooling. While drinking water production, wastewater treatment, water extraction and transfer, all need energy for the water supply (Kenway et al., 2011). Future energy security relies on water availability and water demands need energy supply.

The nexus approach faces challenges and requires the cooperation of industry, government, and universities to develop local to global scale adaption strategies. Though enormous efforts have been put in the water, food and energy nexus in the past 15 years, about 800 million people are still unsecured in their food supply, have unsafe drinking water, and about 1.2 *billion* people are lacking electricity (Scanlon et al., 2017). There are three important aspects of the nexus study that need further attention. The first (1) is to define proper indices and characteristics to quantify the status of nexus, for example, the water footprint could be used to quantify the human consumptive use of water, including blue water, surface- and ground water, green water, rainfall water, gray water and polluted water. In this way, the global average water footprint could be calculated, which in 2012 was ~ 75% of green water, ~ 10% blue water, ~ 15% of gray water (Hoekstra and Mekonnen, 2012). For each type of energy production, the water footprint is different and should be carefully dealt with. Secondly (2), the widely used term 'scarcity' in economic studies is used as well. Scarcity is defined as the ratio between supply and request/demand. In regard to the scarcity of energy, in mainly oil production (Scanlon et al., 2017), water has been studied independently. However, in this kind of study the time dimension is usually missing. For example, high electricity demands usually happen on days with high temperatures, when the water supply is limited because of draught or excessive evaporation. Thirdly (3), the way to manage the scarcity may include conservation, i.e. to increase the supply, proper storage and transport. All these various aspects add to the comprehension of a possible solution of the whole nexus.

For the rapidly developing area like Taihu Basin the conflict between increased socio-economic needs for water and energy, the fact that the resources are limited and potential environmental pollution have become a serious problem. In this study, we would like to take Wuxi city as an example to demonstrate how to use the water-energy nexus concept to solve this problem and to provide support to the decision

making of water resources related issues. We would like to answer the questions: (1) How to quantitatively generate and access a water allocation scenario of short-term urban planning under rapid urbanization using the concept of water-energy nexus? (2) How to assess the potential environmental damage, based on the Wuxi scenarios, and apply this to the scale of the entire Taihu Basin?

We proceed as follows, first, the methodology is outlined in section 5.2, explaining the numerical tools of WEAP and D-Flow Flexible Mesh; then in section 5.3, scenarios will be provided based on the water-energy nexus; thirdly in section 5.4, hydrodynamic and water quality results will be given and analyzed; in section 5.5 river network characteristics will be discussed; and a conclusion will be provided in section 5.6.

5.2. Methodology

A quantitative approach to study the water quality issue in the river network in Taihu Basin is provided. First, water allocation scenarios are provided and evaluated using WEN model WEAP; then the scenarios are tested in the latest hydrodynamic and water quality model D-Flow Flexible Mesh to represent a large part of the complex river network and of Taihu Lake, focusing on the water quality change due to a planned wastewater treatment plan release.

5.2.1. Water-energy nexus model

The Water Evaluation And Planning system (WEAP), developed by the Stockholm Environment Institute, has been widely adopted in the decision-making support tools to generate and model scenarios linking energy and water (Al-Saidi and Elagib, 2017; Karlberg et al., 2015). This model allows users, based on these scenarios, to improve government of the nexus by considering both water and energy systems and by predicting quantitative cross-sectoral effects on water resource allocation, land-use, energy production and environmental features.

In this study, the integrated model approach is used to predict the water consumption for multi-use in Wuxi City, taking into consideration energy production, focusing on water demand with changing environments resulting from urbanization and industrial development, water use efficiency improvement and energy consumption based on water resource allocation scenarios.

Based on the statistical year book of Wuxi City (2006 – 2015), water use in Wuxi could be categorized into the following: industry water use, domestic water use, agriculture water use, environmental water use and water used in fossil-fuel power plants. There are several methods to calculate water demands including the water quota method, increase rate method, regression analysis method and grey model. Based on data availability and the "Water resource master plan" of Wuxi City requirement, in this study the water quota method is used to calculate the water demand in each scenario.

Domestic water use is derived by

$$WD_n = P_n \times Q_n \times (1 - p)^{-1} \quad (5.1)$$

Where, WD_n is domestic water use, P_n and Q_n are the population and predicted water use per capita, p is the water loss rate of urban pipeline network, and n is the predict year.

Industrial water use is derived by

$$WI_n = M_n \times I_n \quad (5.2)$$

$$M_n = M_o \times (1 - \alpha)^{n-o} \times (1 - \mu_n) / (1 - \mu_o) \quad (5.3)$$

Where WI_n is the industrial water use, M_n is the is the water use per 10000¥of value added of industry, I_n is the value added of industry; α is used to represent water use efficiency and industrial use level, usually between 0.02 and 0.05, α is higher with lower water use efficiency area and lower with higher efficiency area since limited improvement could be made; μ is the water reuse rate, 0 is the reference year and n is the predict year.

According to Jiangsu Province the 13th FYP development plan for the electricity sector, the number of fossil-fuel power plants will remain the same, thus, fossil-fuel power plant water use is designed to be same as year 2015. The fossil-fuel power plant water use is calculated as 5% of the total water needed for fossil-fuel power plant production.

Since the urbanization rate was as high as 74% in 2015, the agriculture water use was relatively low, with a potential of continuous decrease. Based on the water resource report of Wuxi city, the agricultural water use is calculated as:

$$WA_n = AM_n \times A_n \times E_n^{-1} \quad (5.4)$$

Where, WA_n is the water use for agriculture, AM_n is the water use per 10000¥of value added of agriculture, A_n is the value added for agriculture, E_n is the irrigation water efficiency and n is the predict year.

Based on historical data, environmental water use changed little from 2006 to 2015, thus, in the scenario design, we use the maximum value of 0.127 *billionm*³ according to the "Water resource master plan" of Wuxi city.

5.2.2. D-Flow Flexible Mesh

The numerical simulation software used in this research is the world's leading Delft3D Flexible Mesh (DFM) Suite software package. The Delft3D software package is a complete set of numerical simulation tools developed and maintained by Deltares (the Netherlands) for more than 40 years; Delft3D Flexible Mesh Suite is the successor of the structured Delft3D suite. DFM can simulate processes including current, wave, tides, sediment transport, morphology, water quality, ecology and particle tracking, and it is capable of handling the interactions between these processes.

The new generation of computing core Delft3D Flexible Mesh Suite uses finite volume method with unstructured meshing, so it can couple 2D, 3D mesh and 1D generalized water networks in a single model, which is especially suitable for this research concerning both the river network and the lake water in Taihu Basin.

Delft3D Flexible Mesh Suite system solves the incompressible shallow water flow under the assumption of static pressure, namely the Navier-Stokes equation. The continuous equation is:

$$\frac{\partial \zeta}{\partial t} + \frac{\partial [HU]}{\partial \xi} + \frac{\partial [HV]}{\partial \eta} = Q \quad (5.5)$$

where U , V are the vertical average flow velocities along the Cartesian coordinate system.

The momentum equation reads:

$$\frac{\partial u}{\partial t} + u \frac{\partial u}{\partial \xi} + v \frac{\partial u}{\partial \eta} + \frac{\omega}{H} \frac{\partial u}{\partial \sigma} - f v = -g \frac{\partial \zeta}{\partial \xi} + v_H \left(\frac{\partial^2 u}{\partial \xi^2} + \frac{\partial^2 u}{\partial \eta^2} \right) + \frac{1}{H^2} \frac{\partial}{\partial \sigma} \left(v_V \frac{\partial u}{\partial \sigma} \right) + M_\xi \quad (5.6)$$

$$\frac{\partial v}{\partial t} + u \frac{\partial v}{\partial \xi} + v \frac{\partial v}{\partial \eta} + \frac{\omega}{H} \frac{\partial v}{\partial \sigma} + f u = g \frac{\partial \zeta}{\partial \eta} + v_H \left(\frac{\partial^2 v}{\partial \xi^2} + \frac{\partial^2 v}{\partial \eta^2} \right) + \frac{1}{H^2} \frac{\partial}{\partial \sigma} \left(v_V \frac{\partial v}{\partial \sigma} \right) + M_\eta \quad (5.7)$$

where, ζ is water level, u, v are flow velocities.

The transport equation reads:

$$\begin{aligned} \frac{\partial Hc}{\partial t} + \left\{ \frac{\partial [Huc]}{\partial \xi} + \frac{\partial [Hvc]}{\partial \eta} \right\} + \frac{\partial \omega c}{\partial \sigma} = H \left\{ \frac{\partial}{\partial \xi} \left[\frac{D_H}{\sigma_{c0}} \frac{\partial c}{\partial \xi} \right] + \frac{\partial}{\partial \eta} \left[\frac{D_H}{\sigma_{c0}} \frac{\partial c}{\partial \eta} \right] \right\} + \frac{1}{H} \frac{\partial}{\partial \sigma} \left[(D_V) \frac{\partial c}{\partial \sigma} \right] \\ - \lambda_d (d + \zeta) c + S \end{aligned} \quad (5.8)$$

where, c is the pollutant concentration.

5.3. Nexus scenarios

In this study, Wuxi City's water demand forecast is based on data of year 2010, using the water quota method to predict the water demand for various purposes in Wuxi City in 2020 and 2030, respectively. The water consumption indices of year 2010 are provided in Table 5.2. Considering urban development and water efficiency control and based on plans from the municipal to the provincial scale, a total of 10 water demand forecast scenarios are set up from the aspects of urbanization development, industrial structure adjustment, agricultural development, Yangtze River delta megalopolis development, and multi water use efficiency improvement (Table 5.3).

Table 5.2: Water consumption indices of the Wuxi City in 2010 and 2015

| Water consumption indices | 2010 | 2015 |
|---|-------------|-------------|
| Population (million) | 6.37 | 6.5 |
| Value added of industry (billion ¥) | 298.65 | 377.16 |
| Value added of electricity production (billion ¥) | 2.19 | 6.56 |
| Value added of agriculture (billion ¥) | 104.94 | 137.72 |
| Water use per capita (m^3) | 72.12 | 75.28 |
| Water use per 10000¥ of value added of industry (m^3) | 15.6 | 10.43 |
| Water use per 10000¥ of value added of agriculture (m^3) | 778.01 | 637.56 |
| Water use per 10000¥ of value added of electricity production (m^3) | 7417.47 | 3704.41 |
| Leakage percentage (%) | 11.95 | 11.00 |
| Industrial water reuse rate (%) | 78.9 | 80.0 |
| Agriculture water reuse rate (%) | 0.64 | 0.652 |
| Electricity production water reuse rate (%) | 80.71 | 89.37 |

Table 5.3: Scenarios

| Scenarios | Scenario name | Label | Main Assumption | Hypothetical Basis |
|-----------------------|---|-------|--|--|
| Reference scenario | reference scenario | REF | Population growth rate of 0.4% compared to 2010, Value added of industry growth rate of 4.8% | Wuxi city social and economic development bulletin; Wuxi city water resource bulletin; Three red line management control plans for water resources in Wuxi City; |
| Urbanization scenario | Yangtze River Delta Megalopolis development | UBN-1 | Population for 2020 and 2030 to be 7.2 million and 8.5 million, with assumption of | Wuxi City's "13th Five-Year Plan" of Manufacturing Transformation Development Plan |
| | Industrial restructuring | UBN-2 | Value added of industry growth rate of 7% compared to 2010 | Wuxi city's "13th Five-Year Plan (2016-2020) "of Modern Agriculture Development Special Plan |
| | Agriculture development | UBN-3 | Value added of agriculture growth rate of 1.73% compared to 2010 | Jiangsu Province's "13th Five-Year" Electricity Power Development Special Plan |
| | Urbanization development | UBN | UBN-1, UBN-2 and UBN-3 | UBN-1, UBN-2 and UBN-3 |

Table 5.3: (continued)

| Scenarios | Scenario name | Label | Main Assumption | Hypothetical Basis |
|---|-----------------------------|-------|--|---|
| Water use efficiency improvement scenario | Domestic water use | WEF-1 | Annual water consumption per capita decrease rate of 0.71% compared to 2010, leakage percentage for 2020 and 2030 to be 10.8% and 8% | Outline of the 13th Five-Year Plan for National Economic and Social Development in Wuxi City; Three red line management control plans for water resources in Wuxi City; Developed countries level |
| | Industry water use | WEF-2 | Annual water use per 10000¥ of value added of industry decrease at 1.27%; The reuse rates of industrial water use in 2020 and 2030 to be 82% and 90% | Wuxi City's 13th Five-Year Economic and Social Development Plan; Three red line management control plans for water resources in Wuxi City; Developed countries level |
| | Agriculture water use | WEF-3 | Annual water use per 10000¥ of value added of agriculture decrease at 0.28%;Irrigation efficiency coefficient for 2020 and 2030 to be 0.70 and 0.75 | Three red line management control plans for water resources in Wuxi City; Developed countries level |
| | Energy production water use | WEF-4 | Annual water use per 10000¥ of value added of electricity plant decrease 10% and 20% for year 2020 and 2030 compared to 2015 | Wuxi City's 13th Five-Year Economic and Social Development Plan; Three red line management control plans for water resources in Wuxi City; Developed countries level |

Table 5.3: (continued)

| Scenarios | Scenario name | Label | Main Assumption | Hypothetical Basis |
|---------------------------------|---------------------------------|-------|-----------------|--------------------|
| Comprehensive planning scenario | Comprehensive planning scenario | SYN | All above | All above |

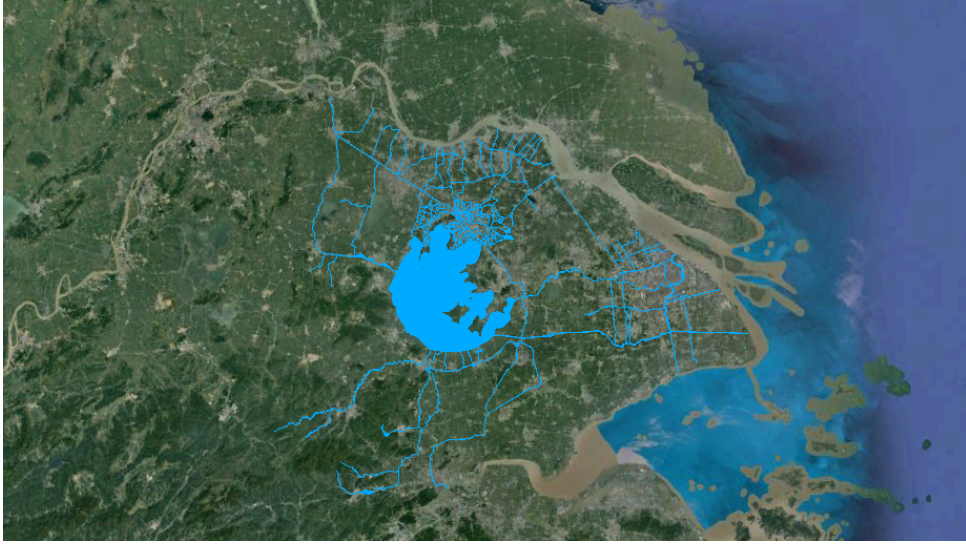


Figure 5.5: Taihu Basin model grid

5.4. Hydrodynamic and water quality model

5.4.1. Model setup

Taihu Basin consists of a complex river network, with river width ranges from $\sim 10m$ to $\sim 700m$. For model efficiency, rivers with a relatively small width are removed from the model. In total 49226 grid cells and 75287 nodes are used for the rivers, where the lake is schematized into 9660 cells and the remainder is used to schematized the river network. The model domain covers the entire Taihu Basin area (Figure 5.5). Specifically, the river network grid is refined for Wuxi city and the adjacent areas (Figure 5.6). The bathymetry data of Taihu Lake is provided by TBA. The topography in the river network is rather scarce. We used 3 different methods to estimate the topography in the river and canals using river width as an input 1) Slope-Break Method (Mersel et al., 2013), 2) power function of width/depth ratio (Andreadis et al., 2013), and 3) Linear function from measurement by (U.S. Army Corps of Engineers, 2004). The computational time is from January 1st of 2008 to December 31st of 2008. In this model study, the changing roughness coefficients are used as: $n = n_0 + n \cdot k(h)$, where $n_0 = 0.012 \sim 0.023$, $n \cdot k(h)$ is a function of water depth. Adaptive time step with average value of 30s to 60s is used. A diffusion coefficient of $1m^2/s$ is used.

The boundary conditions of the river network of the model are divided into two types: the boundaries along Taihu Lake and the boundaries along the Yangtze River and the Qiantang River. Boundaries along Taihu Lake are calculated as the inverse value of the tributary discharge into Taihu Lake, while the boundary conditions along the Yangtze River and the Qiantang River are determined by the corresponding water levels.

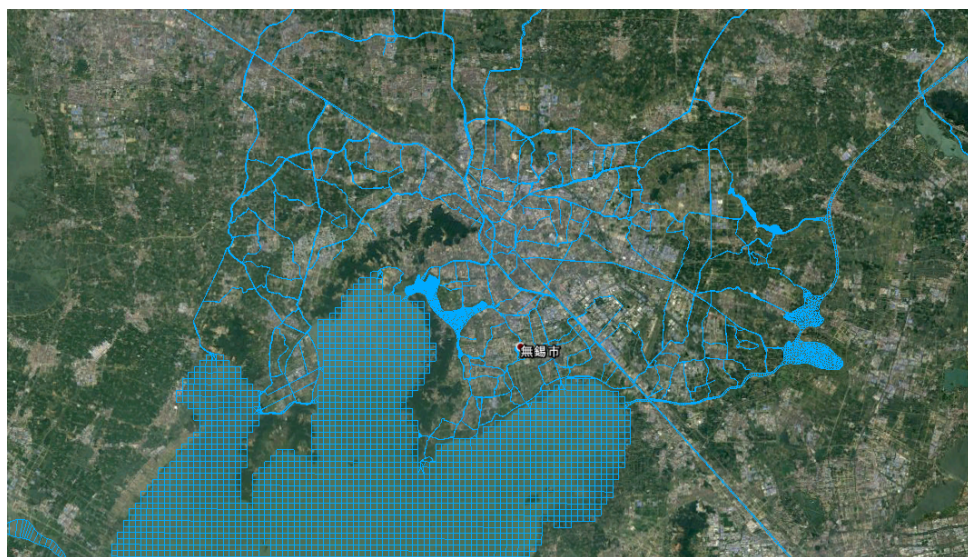


Figure 5.6: Refine of grid of Wuxi city and adjacent area

5

5.4.2. Model calibration and validation

Since hardly any water level measurements can be found in the river network, we used the same data set as in Chapter 3, namely, water levels at 5 points in the lake to calibrate the model. The dataset can be found in TBA website (<http://www.tba.gov.cn:9099/shishiTaihu.aspx>). The positions of the points are shown in Figure 5.7. Water level calibration is shown in chapter 3. The model results do well reflect observed data. The RMSE is within 10cm and the average error is less than 5cm.

5.4.3. Hydrodynamic and water quality scenarios

Based on scenarios provided in section 5.3, the corresponding effluent prediction from the WEAP model is shown in Table 5.4. Based on the various scenarios listed above, corresponding generalizations were made for different water use categories for the model input. The current and future location of electricity power plants are not clearly specified in master plans and based on the assumption that power plant wastewater has little effect on the water quality except a rise in water temperature, the power plant effluent is not considered in this model. The main objective is then the influence of the WWTP effluent on the water quality of the river network.

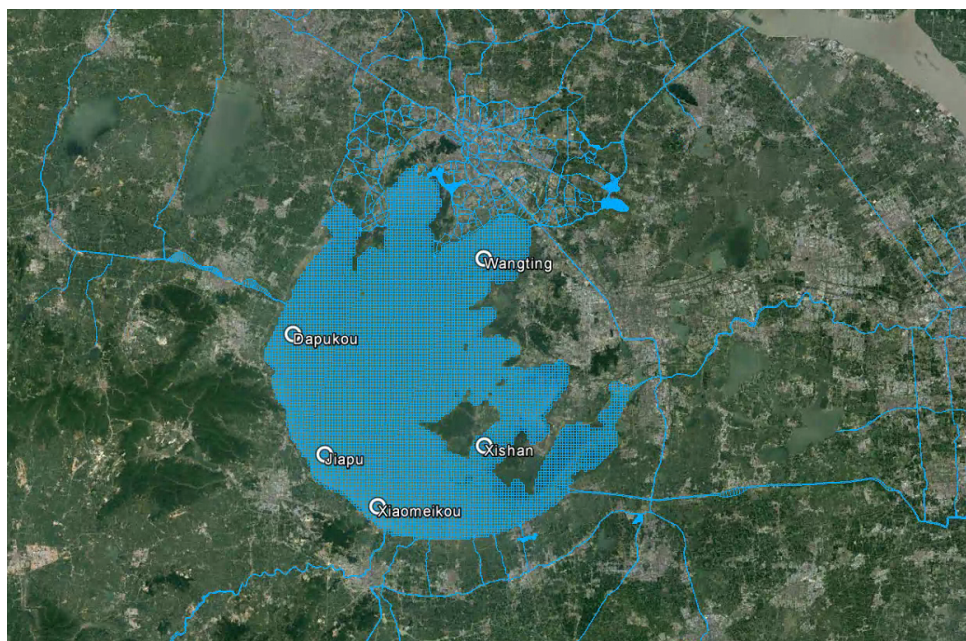


Figure 5.7: Positions of observation points

Table 5.4: Hydrodynamic and water quality scenario

| Scenario index | 2010 | | | | 2015 | | | | 2020 | | | | 2030 | | | |
|----------------|-------|------|------|-------|-------|------|------|-------|-------|------|------|-------|-------|------|------|-------|
| | WC | PPE | AE | WWTPE | WC | PPE | AE | WWTPE | WC | PPE | AE | WWTPE | WC | PPE | AE | WWTPE |
| REF | 34.00 | 3.00 | 2.28 | 4.96 | 42.31 | 2.48 | 2.41 | 5.03 | 44.34 | 2.48 | 2.41 | 5.30 | 47.50 | 2.48 | 2.41 | 5.96 |
| UBN-1 | 34.00 | 3.00 | 2.28 | 4.96 | 42.31 | 2.48 | 2.41 | 5.03 | 44.80 | 2.48 | 2.41 | 5.67 | 48.90 | 2.48 | 2.41 | 7.03 |
| UBN-2 | 34.00 | 3.00 | 2.28 | 4.96 | 42.31 | 2.48 | 2.41 | 5.03 | 44.93 | 2.48 | 3.08 | 5.38 | 50.60 | 2.48 | 3.08 | 6.43 |
| UBN-3 | 34.00 | 3.00 | 2.28 | 4.96 | 42.31 | 2.48 | 2.41 | 5.03 | 45.20 | 2.48 | 2.63 | 5.30 | 50.30 | 2.48 | 3.12 | 5.96 |
| UBN | 34.00 | 3.00 | 2.28 | 4.96 | 42.31 | 2.48 | 2.41 | 5.03 | 46.08 | 2.48 | 2.41 | 5.30 | 54.24 | 4.78 | 2.41 | 5.96 |
| WEF-1 | 34.00 | 3.00 | 2.28 | 4.96 | 42.31 | 2.48 | 2.41 | 5.03 | 44.25 | 2.48 | 2.41 | 5.13 | 47.12 | 2.48 | 2.41 | 5.35 |
| WEF-2 | 34.00 | 3.00 | 2.28 | 4.96 | 42.31 | 2.48 | 2.41 | 5.03 | 44.10 | 2.48 | 2.41 | 5.17 | 46.20 | 2.48 | 2.41 | 5.21 |
| WEF-3 | 34.00 | 3.00 | 2.28 | 4.96 | 42.31 | 2.48 | 2.41 | 5.03 | 44.25 | 2.48 | 2.21 | 5.30 | 47.30 | 2.48 | 2.01 | 5.96 |
| WEF-4 | 34.00 | 3.00 | 2.28 | 4.96 | 42.31 | 2.48 | 2.41 | 5.03 | 41.92 | 2.23 | 2.41 | 5.30 | 42.88 | 1.98 | 2.41 | 5.96 |
| SYN | 34.00 | 3.00 | 2.28 | 4.96 | 42.31 | 2.48 | 2.41 | 5.03 | 42.99 | 2.78 | 2.41 | 5.43 | 46.29 | 3.83 | 2.60 | 5.71 |

* Unit in the table is $10^8 m^3$. Scenario name refer to the index in Table 5.3; **WC**: water consumption; **PPE**: power plant effluent; **AE**: Agriculture effluent; **WWTPE**: wastewater treatment plant effluent,

There are over 20 WWTPs in Wuxi City; the four major WWTP are Lucun, Chengbei, Meicun and Taihuxincheng (Figure 5.8); the locations of the wastewater treatment plants are available on the website of Wuxi Drainage Co., Ltd. (www.wxps.com). Due to lack of data availability, in this study, these four WWTP will be generalized into the model. Daily treated water volume of each WWTP is retrieved from the website. Accordingly, in this study, the proportion of treated water volume is used to estimate the effluent of each WWTP.

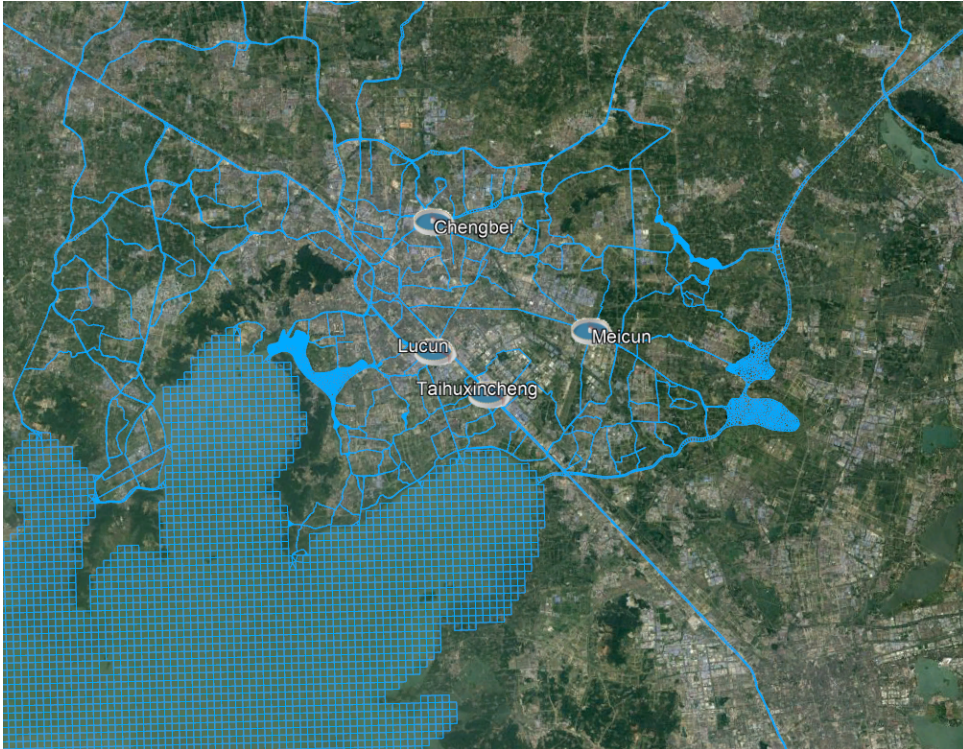


Figure 5.8: Location of 4 major WWTPs in Wuxi city

5.5. Results

5.5.1. Nexus evaluation

The predicted water demand of each category for the designed scenarios is shown in Figure 5.9. Total water resource consumption for Wuxi City in 2020 for all scenarios is smaller than $50 \times 10^8 m^3$, which is the maximum value defined by the three red line management control plans for water resources in Wuxi City. The total water consumption for the urbanization development scenario (UBN) in 2020 is $46.08 \times 10^8 m^3$, which increases by 35.2% compared to 2010. The dramatic increase in the UBN scenario is mainly because the improvement of the water use efficiency is not taken into account. The total water consumption value for the

comprehensive scenario (SYN) that takes all sorts of water use efficiency into account is $42.99 \times 10^8 m^3$, only slightly larger than the 2015 value. The industry water reuse rate increase and the annual water use per 10000 ¥ of value added of industry decrease plays a significant role in relieving Wuxi City's water pressure. As for the

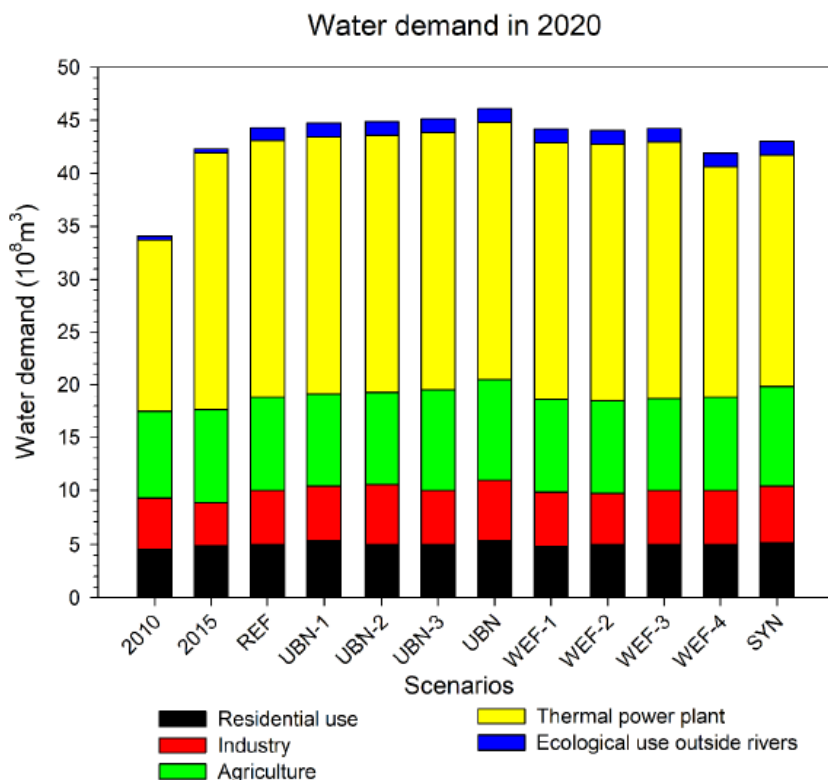


Figure 5.9: Predicted water demands of the Wuxi City in 2020

prediction of Wuxi City in 2030 (Figure 5.10), altogether the total water demands of 3 scenarios, namely the industrial restructuring scenario, agricultural development scenario, and the urbanization development scenario, pass the red line of $50 \times 10^8 m^3$. However, with the water use efficiency increase, the total water demands falls below the red line. Especially for power production, the high water use efficiency shows a significant decrease in water demands (WEF-4). By comparing the prediction for Wuxi city in 2020 and 2030, due to rapid urbanization and industrial development, total water demands will have increased, even if water use per capita, water use of value added of industry and agriculture and power production, leakage percentage, irrigation efficiency, industrial water reuse, and population are taken into account and improved to developed countries level. The key point to stay below the red line of total water demands is to control the water use efficiency and the size of the power plants.

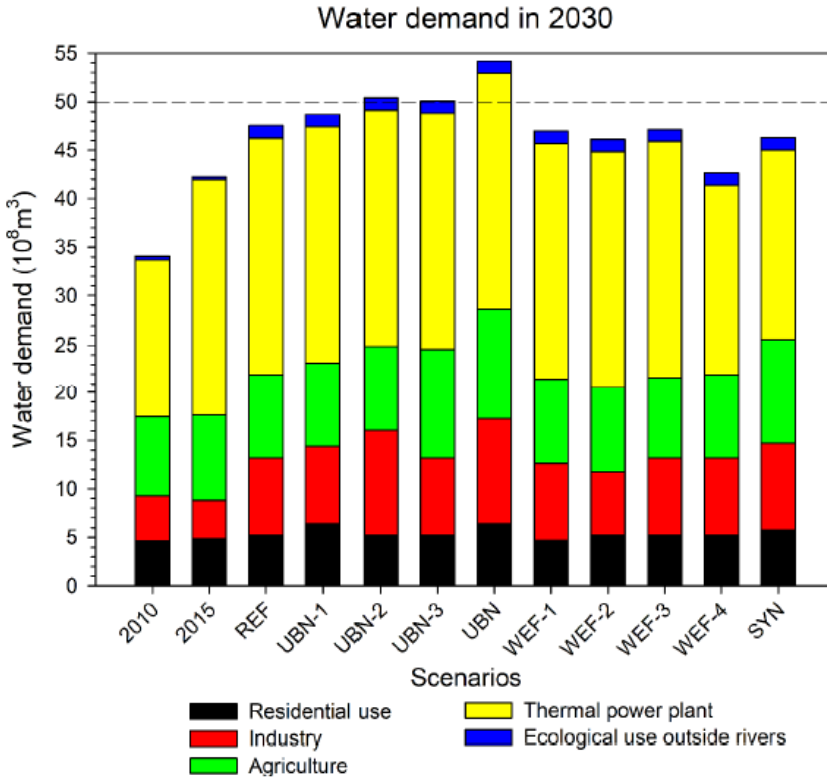


Figure 5.10: Predicted water demands of the Wuxi City in 2030

5.5.2. River network results

The model result is mainly concerned with the local effects of effluent from wastewater treatment plants into the river network. For this, tracers are continuously released at the location of wastewater treatment plants according to the designed scenario. With the spatial and temporal distribution of tracer concentration, the effect of wastewater treatment plant effluents on the local river network could be illustrated at different times for different scenarios. Here, examples of both the 2020 and 2030 prediction with UBN scenario are presented. The illustrated place is the location to the west of the Lucun wastewater treatment plant. Figure 5.11 shows the tracer concentration, while Figure 5.12 and Figure 5.12 shows tracer concentration after 1 month for both the UBN 2020 and the UBN 2030 case. In the tracer concentration maps, different colours represent different concentrations, the more reddish the colour, the higher the particle concentration, the bluer the colour, the lower the particle concentration. From the map it can be observed that after a 1-month simulation time the flow direction of river water in the local river network is mainly west- and southward. Comparing Figure 5.12 and Figure 5.13, differences can be observed. After the 1-month model time, the tracer concentration is higher



Figure 5.11: Tracer concentration at $t = 0$

in the UBN 2030 case. Also, along the river network direction, the amount of tracer particles moving westward and southward also increased in the UBN 2030 case. This is mainly due to the different values of wastewater treatment plant effluent in both scenarios. In the UBN 2020 scenario the total wastewater treatment plant effluent is $5.30 \times 10^8 m^3$, while in UBN 2030 this value increased to $7.49 \times 10^8 m^3$. In the case of different values of wastewater treatment plant effluent, the impact on the local river network environment is different. The more wastewater treatment plant effluent, the more accumulated pollution in the local river network. At the same time, the total wastewater treatment plant effluent within the entire river network will also increase.

5.6. Discussion

5.6.1. Water demand implication

In this study, 10 scenarios of water demand prediction for the years 2020 and 2030 are generated, considering respectively urbanization, water use efficiency, megalopolis development, industrial reconstruction, agricultural development and power production evolution. The conclusion could be drawn that, with urbanization, the water demand is always increasing, but that if water use efficiency, especially power plant water use efficiency, is taken into consideration, the total water demand could be controlled. Conventionally, water resource and energy departments work

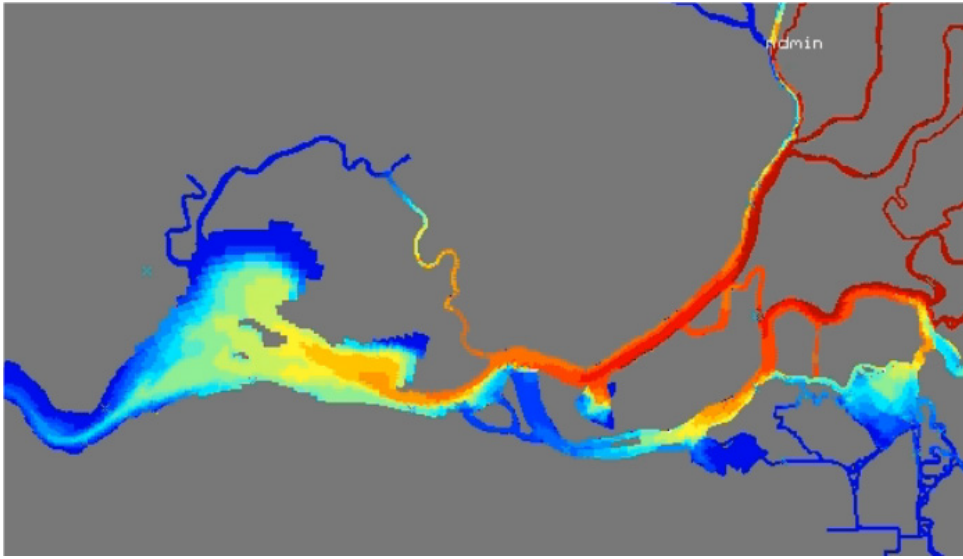


Figure 5.12: Tracer concentration at $t = 1$ month for UBN 2020

separately, ignoring the interdependencies between water resources and energy. Scenarios provided by this study could shed a light on the management of water resource departments to take energy into consideration and present more energy conservative strategies. From an energy production point of view, water use for production takes almost half of the total water consumption. Thermal power plants are no longer favorable according to Wuxi 13th Five-Year Energy Development Plan. Thus, to import energy from other areas to save local water resources could be an option for Wuxi City.

5.6.2. Hydrodynamics of the river network

The river network in Taihu Basin is very complex with a large number of interconnected rivers, serving multiple functions, such as flood control, production water, water supply guarantee, transportation and shipping. Understanding the dynamic characteristics of the river network itself for the comprehensive management of the rivers and lakes in the Taihu Basin is vital. Along the boundary of Taihu Basin flows the Yangtze River and lies Hangzhou Bay with the Beijing-Hangzhou Grand Canal. The river network near the Yangtze River and Hangzhou Bay is affected by the tide and there will be a reciprocating flow at the boundary. The canal water of the river channels to the south of the Beijing-Hangzhou Grand Canal flows into Taihu Lake. The river network of the entire river basin shows the characteristics of a low flow rate and the slow flow of the plain river network. Due to height of the terrain, the flow direction of rivers in the basin is mainly from west to east, and from north to south. However, due to the relative water level of the Yangtze River and Taihu Lake, and the operations of hydraulic structures, i.e. locks, the flow direction

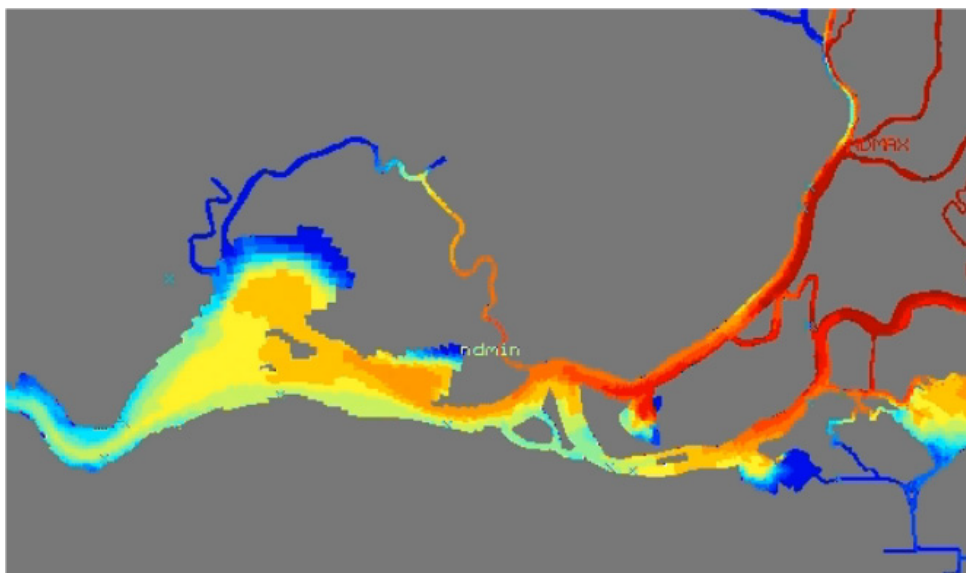


Figure 5.13: Tracer concentration at $t = 1$ month for UBN 2030

of the river is not fixed, and there are often stagnant and backward phenomena. In this model study, due to the lack of data, the artificial gate is not defined, thus the main influencing factor comes from the hydrodynamic characteristics of the river network itself. Please note, that the model is based on the assumption that hydrodynamics would not change much in 2008, 2020 and 2030, but due to climate change and other artificial influences, uncertainty remains in this area. For future related studies, it is recommended to take these aspects into consideration.

5.7. Conclusions

Taihu Basin, located in the southeast part of China, is undergoing rapid urbanization. It has always been one of the most densely populated and economically developed regions in China. With urbanization processes going on, water problems as flooding, water scarcity, and environmental threats increasingly occur in the Taihu Basin. Water problems are interlinked with energy; on the one hand, energy challenges water aspects, such as the water footprint of energy portfolios and water quality degradation due to energy production; on the other hand, water challenges energy by rising water demands due to climate change, water allocation for energy production, increasing demands of clean hydropower and water reuse. The interdependency of water and energy requires more comprehensive management of water resources.

In this study, the Water-Energy-Nexus method is adopted to study the water resource and water environment with the specific consideration of energy in Wuxi city, as an example for Taihu Basin. First, we downscale our study to Wuxi city as

an example of the water allocation scenario using the water-energy nexus method with software WEAP, then we upscale the results as input for the Taihu Basin river network D-Flow Flexible Mesh model. Ten scenarios are designed, based on assumptions of urbanization development, industrial structure adjustment, agricultural development, the Yangtze River delta megalopolis development, and multi water use efficiency improvement. For each scenario, the total water use composed by domestic residential water use, thermal power plant water use, industrial water use, agricultural water use and environmental water use, and the effluent water from thermal power plants, agricultural and wastewater treatment plants are modelled by WEAP and analysed. Then the WEAP model results are used as the input into the hydrodynamic and water quality model D-FLOW Flexible Mesh, to simulate and study the effects of changing water and energy allocation pattern on the environment of the river network using particle tracking model.

The WEAP analysis shows that, due to rapid urbanization and industrial development, the total water demands will increase. However, taking water use efficiency into consideration could help to release the pressure on water demands. Specifically, water use efficiency for energy production and industry has a significant effect on the water demand in the long run. The D-Flow Flexible Mesh model, which is a combination of a quadrilateral and triangular mesh mode, is capable to quantitatively assess the impact of water and energy allocation on the hydrodynamics and water quality during urbanization, covering the entire Taihu Basin including the river network and Taihu Lake. The model simulation results and the water level verification of the five observation points in the lake area indicate that the model can reflect the basic hydrodynamic characteristics of the river network system and provide a reliable basis for the assessment of water and energy allocation scenarios. The results show that, as the degree of urbanization continues to expand over time, wastewater treatment plant effluent will increase, but with high water efficiency scenarios, using the integrated planning of urbanization development, the impact on the hydrodynamic and water environment of the whole system can be mitigated to a large extent.

6

Conclusions and recommendations

6.1. Synthesis

Taihu Lake, as the 3rd largest shallow lake located in the southeastern part of China, near the Yangtze River Delta, is a typical large shallow lake with a surface area of 2338 km² and an average depth of only 1.9 m. Adverse meteorological conditions and increasing waste loads due to rapid urbanization in the surrounding megalopolis, in combination with the typical geometry of Taihu Lake, cause frequent blooming of algae with a disastrous impact on the ecosystem.

Although researchers spent considerable efforts to solve the water problems in Taihu Lake and in the Taihu Basin using chemical and biological methods, the understanding of wind driven hydrodynamic circulation is not yet clearly studied. The complexity of a spatial and temporal varying and changing environment, especially under the pressures of the rapid urbanization, adds to the difficulties of both theoretical analysis and modelling studies. Through this thesis, we aim to provide the knowledge of water driven hydrodynamic circulation in large shallow lakes and its implication on the water quality with a changing environment. Our case is Taihu Lake and Taihu Basin, where a hydrodynamics study on a lake scale, to a lake scale water quality implication and to a basin scale implication is undertaken. Answers to the research questions in Chapter 1 are given below in this concluding chapter.

(1) What is the effect of wind on the spatial and temporal hydrodynamic circulation pattern in Taihu Lake?

Wind induced hydrodynamic circulations and the associated transport and mixing processes in large shallow lakes play a significant role in environmental and ecological processes. In this study, hydrodynamic circulation in shallow lakes is defined as the large-scale movement of water in the lake basin. A three-dimensional, numerical Delft3D model of Taihu Lake, driven by steady and/or unsteady wind, river discharge, rainfall and evaporation, is used to quantitatively illustrate the complex hydrodynamic circulation and the effects in transporting and mixing within the lake.

A stable wind driven circulation pattern is formed after a couple of days with a steady wind, where the overall hydrodynamic circulation structure, including flow direction, intensity and eddy position, is determined by wind direction, wind speed and initial water level. Vertical variations of horizontal velocity component depend on the relative shallowness of the water depth. In the shallow marginal area, flow at the bottom and surface layers has the same direction and the surface flow has a larger velocity, while in the deeper area, the bottom flow reverses opposite to the wind direction with a larger velocity. Vertical variations in hydrodynamic circulation are found very important in explaining the surface accumulation of algae scums in Meiliang Bay in the summer. Volume exchange between sub-basins, influenced by wind speed and initial water level, differs due to the complex topography and irregular shape of the lake. Volume exchange is larger with more open sub-basins; with unsteady wind, these findings are still valid to a high degree.

Vorticity of current velocity, as the key indicator of wind induced hydrodynamic circulation is determined by wind direction, bathymetry gradient and water depths, while the maximum change of velocity vorticity happens when the wind direction and the bathymetry gradient are perpendicular to each other.

Further, Lagrangian-based tracer tests are used to estimate emergency pollu-

tion/leakage effects and to evaluate water transfer effects. A virtual leakage event is simulated on tourism hotspots and drinking water intake points are evaluated, suggesting that the model application may serve as an operational management tool. Then, the water transfer project, shows that even a large scale water transfer (about 1/5 volume of total lake volume in 138 days from the Yangtze River) does not significantly alter the hydrodynamic circulation and the volume exchange pattern between sub basins, but it succeeds to transport and mix the imported Yangtze River water with the majority of water in the Taihu Lake area.

(2) What is the implication of wind induced hydrodynamic circulation on water quality?

The process based hydrodynamic and water quality model Delft3D is used to investigate the wind induced hydrodynamic circulation implication on the water quality of Taihu Lake. Wind induced hydrodynamic circulation transports and mixes nutrients and pollution that dissolved in tributary discharges around Taihu Lake, inducing the spatial and temporal heterogeneity of nutrient distribution. The river network adjacent to Taihu Lake is complex with a large number of river channels. The tributary boundaries are categorized into three groups based on upstream sub basins and the hydrodynamic model. Then, the concept of Water Age is adopted in this study to illustrate wind how affects the transport and mixing process of nutrients.

Model results show that both spatial and temporal heterogeneity occurs with all three water age groups, which is influenced by both distance to the tributary boundaries and by the variance in value of total discharge through the tributary boundary for each WA group. Change of wind direction would lead to changes on both the average value and the range of WA, while wind speed differences induce a site-specific and age-specific change of the WA value. Compared to wind influence, the discharge volume effect is less significant, partially due to the quick dissipation of incoming momentum from tributary boundaries.

Based on the discussion of the definition and the applications of various transport time scales, water age is considered the most suitable time scale to study the wind induced hydrodynamic circulation implications in Taihu Lake. Climate effects are studied with changing wind speeds; a lower wind speed will encourage a release of inner source and cause a longer duration of the outer source nutrient inflow, both of which will induce more severe algae bloom and deteriorate of the quality of the water.

Wind influence on WA is analysed. WA decreased with a rising tributaries inflow discharge, however, the influence of the discharge is smaller than the change of wind.

Various time scales, like residence time and flushing time, are presented for a clear understanding. The effect of a decline in wind speed induced by climate change is analysed on both inner and outer nutrient source release and both influences caused water quality to deteriorate. Lastly, further application of water age is suggested for a more complicated lake basin scale integrated water management.

(3) What is the main hydrodynamic and water quality implication under the changing environment with wind induced hydrodynamic circula-

tion on the catchment scale tributary systems of Taihu Lake?

To study the main hydrodynamic, water quality implication under a changing environment with wind induced hydrodynamic circulation on the catchment scale tributary systems of Taihu Lake, rapid urbanization is assumed to have the most significant influence on the Taihu Basin water system. In this study, the Water-Energy-Nexus method is adopted to study the water resource and water environment in Wuxi City, with the consideration of energy, as an example for Taihu Basin. First, downscaling to the local level of Wuxi City is applied for the water allocation scenario using water-energy nexus method with software WEAP. Subsequently, the results are upscaled as input for the Taihu Basin river network D-Flow Flexible Mesh model. Ten scenarios are designed, based on assumptions of urbanization development, industrial structural adjustment, agricultural development, the development of the Yangtze River delta megalopolis, and improvement of multifunctional water use efficiency. For each scenario, the total water use, composed by the various uses of domestic residential water use, thermal power plant water use, industry water use, agriculture water use, environmental water use, effluent water from thermal power plants, agriculture and wastewater treatment plants, are modelled by WEAP and analysed. Then, the WEAP model results are used as input into the hydrodynamic and water quality model D-FLOW Flexible Mesh, to simulate and study the effects of changing water and energy allocation patterns on the environment of the river network using a particle tracking model.

WEAP analysis showed that due to a rapid urbanization and industrial development, total water demands will increase. However, taking water use efficiency into consideration could help to release the water demand pressure. Specifically, water use efficiency for energy production and industry has a significant effect on water demand in the long run. The D-Flow Flexible Mesh model covering the entire Taihu Basin, including the river network and Taihu Lake, which is a combination of quadrilateral and triangular mesh mode, is capable of quantitatively assess the impact of water and energy allocation on the hydrodynamics and water quality during urbanization. The model simulation results and the water level verification of the five observation points in the lake area indicate that the model can reflect the basic hydrodynamic characteristics of the river network system and provide a reliable basis for the assessment of water and energy allocation scenarios. The results show that, as the degree of urbanization continues to expand over time, wastewater treatment plant effluents will increase, but with sound water efficiency scenarios, using the integrated planning of urbanization development, the impact on the hydrodynamic and water environment of the whole system can be mitigated to the utmost extent.

6.2. Recommendations

This thesis presents a series of studies focusing on wind induced hydrodynamic circulation in large shallow lakes, in this case with the implication of Taihu Lake from a lake scale hydrodynamic study, to a lake scale water quality implication, and to the level of a basin scale implication. However, there are still limitations that need to be improved in future studies.

In this study, research is focused on the entire lake spatial scale and the daily to

yearly temporal scale wind hydrodynamic circulation, mainly considering the transport and mixing of nutrients and pollution. However, smaller scale physical and biological processes are not thoroughly discussed. These processes could influence the formation of algae bloom, the health of lake ecosystem, and the shift of the alternative stable state. For future studies, it is recommended to put more efforts into small-scale hydrodynamics, especially the wave and turbulence influences in large shallow lakes.

In the hydrodynamic model, due to data availability, only one precipitation value is used to represent the whole lake area and only the water level at 5 monitoring stations in the calibration process. With more in situ observations, e.g. flow velocity, precipitation pattern with higher resolution, etc., the model could be more convincing. When using the model to explain the possible reason of algae accumulation, wave effects and the natural vertical movement pattern of algae is missing, as well as the influence of the navigation channel inside Taihu Lake. Future studies are encouraged to study algae bloom with a higher resolution wind and wave data. Further, the model could be used to predict hydrodynamic and water quality changes due to hydraulic structures inside Taihu Lake.

When considering the water age implication on water quality, a strong assumption is made that movement of nutrients and pollutants are assumed as exactly the same as passive tracers, and that the advection and diffusion are the same as water. However, the absorption, dispersion and reaction processes introduced by phytoplankton and macrophytes, etc. are not considered. Future studies are encouraged to involve these processes.

Data availability for the Taihu Basin river network model is still limited. Artificial hydraulic structure operations block river connectivity, which is not included in the model. Future work may include collecting relevant operation records or other human interventions, and analysing the relative importance of it. The model remains a challenge for future study especially under rapid urbanization conditions. Also, detailed water quality information inside the river network is missing in the nexus part of the study, since polluted water may not be directly used as assumed, which should be collected and studied for future model calibration. Possible application of the DFM river network model could be an evaluation tool for small scaled inter basin water transfer projects between cities in the megalopolis of Taihu Basin.

When considering the long term water allocation scenarios in 2020 and 2030, the hydrodynamics used in the model are still the same as in the 2008 model. However, the hydrodynamics could change due to climate change, since meteorological factors have a significant influence on hydrodynamics in this area. Climate change effects on water quality also occur with changing air temperatures, precipitation, wind and solar radiation: an increased air temperature is favoured by algae growth; an extreme precipitation event introduces more nutrients and is a threat for the dilution capacity of large shallow lakes; an extreme wind event influences the internal nutrients release and external nutrient transport; and solar radiation encourages hypoxia. These processes are recommended to be extended in future studies.

Large-scale hydrodynamic processes, such as lake scale topographical gyres,

are not easy to observe and capture, unless in a controlled laboratory environment with physically scaled models. Large scale physically scaled models are common for river and estuaries studies, but few studies and models are adopted for large shallow lakes. Knowledge could be gained from these physical scale models and should be verified with numerical models. Thus, the application of large-scale physical scale models for large shallow lakes is recommend for future studies.



Appendix

A.1. Experiment setup

A.1.1. Flume layout

The, experimental investigation was performed in the wind flume at the hydraulic engineering laboratory of Nanjing Hydraulic Research Institute. The flume is 27m long in total, 1m wide and 1.2m deep (Figure A.1). Top of the flume is covered with by arc-shaped roof made of glass and rubber to ensure air-tightness. Body of the flume is made of steel plate and 1.5m width tempered glass for transparency. Except for the first unit which is the air inlet, the total effective fetch length is 25.5m. Elevation of the bottom is 1.2m to allow enough space for instruments.

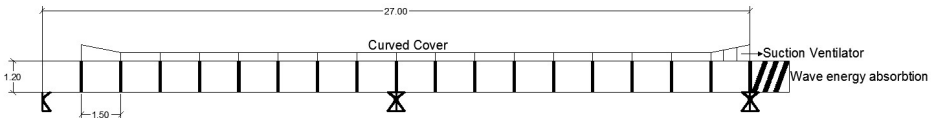


Figure A.1: Side view of the flume

Wind suction ventilator is placed at the end of the flume right at the top of the wave energy absorption (Figure A.2). Wind speed is adjustable and the maximum wind speed it generates inside the flume is 20m/s. A honeycomb-shaped structure is placed at the wind inlet to reduce air turbulence.



Figure A.2: Wave energy absorption at the end of the flume

The flume is further modified in order to create both horizontal circulation and vertical circulation inside the flume. A vertical partition made of plastic grey board along the axis of the flume is setup to divide the flume into two parts, creating two horizontal channel with same width. One channel in the flume is covered with plastic grey board while the other channel is open. At both ends of the flume, a 1.5m width cover is made. (Figure A.3) Thus, the effective fetch length in the flume is now 24m.

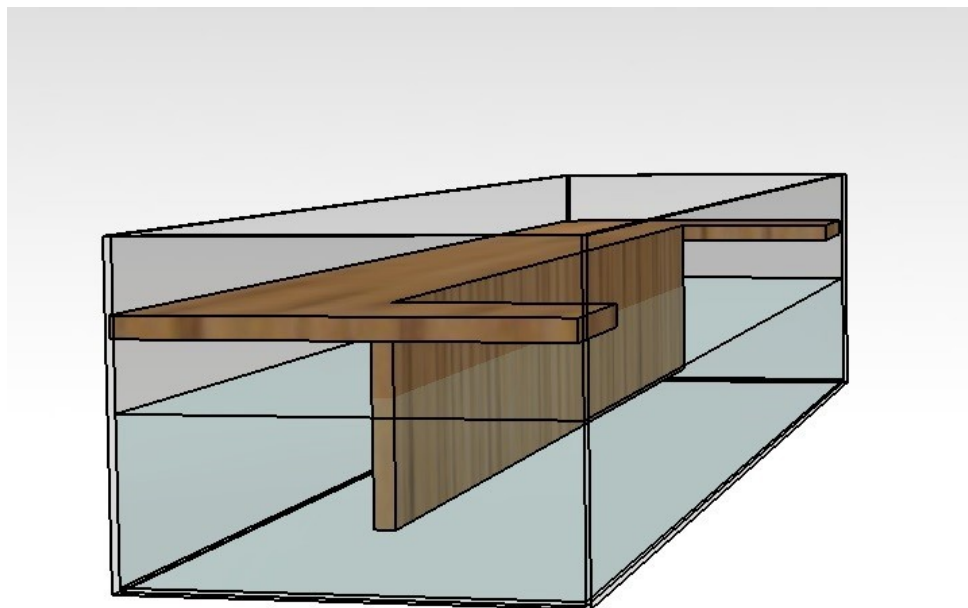


Figure A.3: Modification inside the flume

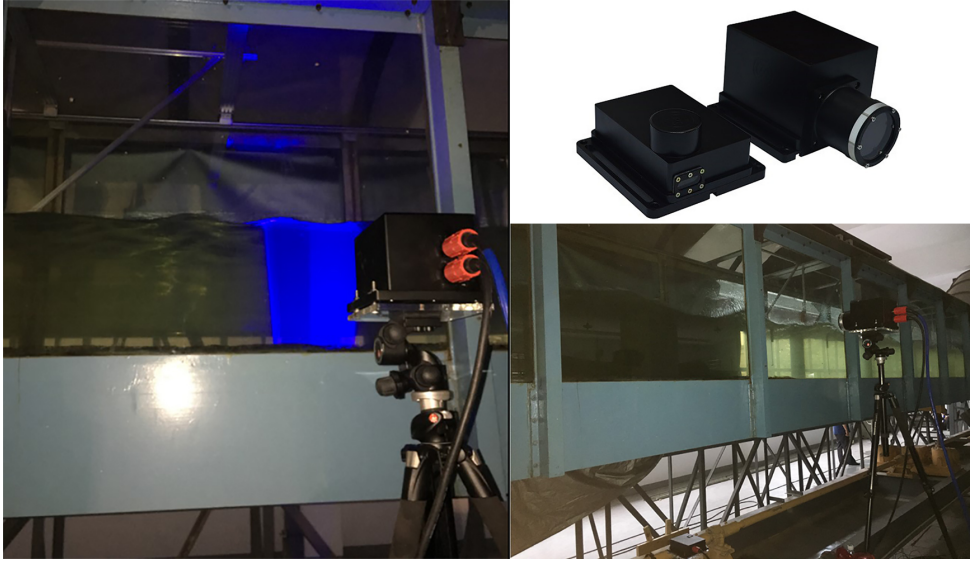


Figure A.4: PIV system working state

A.1.2. Instruments

Three most frequently used current velocity measurement instruments in the flume experiments are the propeller current meter (PC), the electromagnetic velocity meter (EMV), the Acoustic Doppler velocity meter (ADV), the Particle Image Velocimetry (PIV) and the High Speed Video (HSV). The propeller current meter (PC) is not suitable in this flume experiment since the flow structure to be measured is small and is easily disturbed by the propeller. The electromagnetic velocity meter (EMV) is frequently in the flume experiment is TUD. The advantage of the EMV is that it covers a large velocity range and won't be interfered by the temperature and pressure. However, it is very sensitive to vibration and magnetic field nearby. The Acoustic Doppler velocity meter (ADV) can be used to measure the flow velocities without disturbing the flow itself, however, it is more suitable to measure the average flow speed for a single point. The similar Laser Doppler Velocimetry (LDV) is more accurate but more costly.

The Particle Image Velocimetry (PIV) system is used in this experiment to capture the flow velocity field in the vertical plane. (Figure A.4) The fluid is seeded with tracer particles which, for sufficiently small particles, are assumed to faithfully follow the flow dynamics. The PIV system provides instantaneous snapshot of the flow structure and is therefore very applicable for the description and understanding of the large scale unsteady flow.

In this experiment, the PIV laser transmitter is placed under the flume at around 20cm from the edge of the flume and camera is placed on a tripod to match the height of scenarios. The system adopted is capable of make 100 pairs of photos at 10Hz.(A.5)

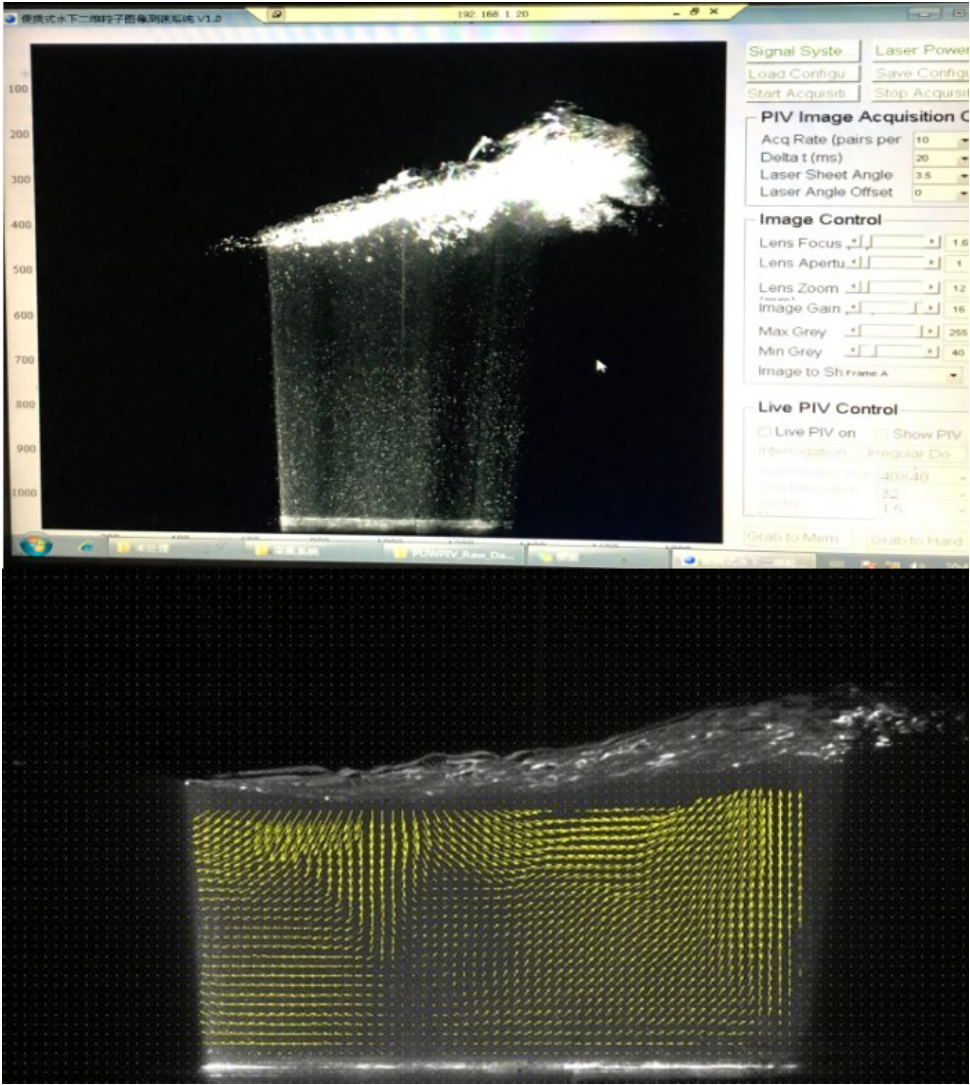


Figure A.5: PIV system example results

A

Altogether 3 wave gauges are used in the experiment, with a 1mm measuring accuracy and a 100 Hz sampling frequency. Model of wind anemometer used in the experiment is Wind Sonic M from GILL(Figure A.6). The wind anemometer covers wind speed from $0 - 60\text{m/s}$ with a 2Hz frequency and has the resolution of 0.01m/s . The wind anemometer is placed above the middle of the open water to measure the wind speed.



Figure A.6: Wind Sonic M

References

- Al-Masri, R. A., Chenoweth, J., and Murphy, R. J. (2019). Exploring the Status Quo of Water-Energy Nexus Policies and Governance in Jordan. *Environmental Science & Policy*, 100(June):192–204.
- Al-Saidi, M. and Elagib, N. A. (2017). Towards understanding the integrative approach of the water, energy and food nexus. *Science of The Total Environment*, 574:1131–1139.
- Allen, M. R., Dube, O. P., and Solecki, W. (2018). IPCC Special Report 2018 - Chapter 1. Technical report.
- Allen, M. R. and Ingram, W. J. (2002). Constraints on future changes in climate and the hydrologic cycle. *Nature*, 419(6903):228–232.
- Andreadis, K. M., Schumann, G. J., and Pavelsky, T. (2013). A simple global river bankfull width and depth database. *Water Resources Research*, 49(10):7164–7168.
- Babiker, M., Bertoldi, P., Buckeridge, M., Cartwright, A., Araos, M., Bakker, S., Bazaz, A., Belfer, E., Benton, T., Coninck, D., Revi, A., Babiker, M., Bertoldi, P., Buckeridge, M., Cartwright, A., Dong, W., Ford, J., Fuss, S., Hourcade, J.-c., Ley, D., Mechler, R., Newman, P., Revokatova, A., Schultz, S., Steg, L., Zhai, P., Pörtner, H.-o., Roberts, D., Skea, J., Shukla, P., Pirani, A., Moufouma-Okia, W., Péan, C., Pidcock, R., Connors, S., Matthews, J., Chen, Y., Zhou, X., Gomis, M., Lonnoy, E., Maycock, T., Tignor, M., and Waterfield, T. (2018). IPCC Special Report 2018 - Chapter 4. Technical report.
- Beklioglu, M., Altinayar, G., and Tan, C. O. (2006). Water level control over submerged macrophyte development in five shallow lakes of Mediterranean Turkey. *Archiv für Hydrobiologie*, 166(4):535–556.
- Beklioglu, M., Meerhoff, M., Davidson, T. A., Ger, K. A., Havens, K., and Moss, B. (2016). Preface: Shallow lakes in a fast changing world. *Hydrobiologia*, 778(1):9–11.
- Bishop, K., Buffam, I., Erlandsson, M., Fölster, J., Laudon, H., Seibert, J., and Temnerud, J. (2008). Aqua Incognita: the unknown headwaters. *Hydrological Processes*, 22(8):1239–1242.
- Boas, I., Biermann, F., and Kanie, N. (2016). Cross-sectoral strategies in global sustainability governance: towards a nexus approach. *International Environmental Agreements: Politics, Law and Economics*, 16(3):449–464.

- Boegman, L., Loewen, M. R., Hamblin, P. F., and Culver, D. A. (2001). Application of a two-dimensional hydrodynamic reservoir model to Lake Erie. *Canadian Journal of Fisheries and Aquatic Sciences*, 58(5):858–869.
- Bolin, B. and Rodhe, H. (1973). A note on the concepts of age distribution and transit time in natural reservoirs. *Tellus*, 25(1):58–62.
- Bozelli, R. L., Caliman, A., Guariento, R. D., Carneiro, L. S., Santangelo, J. M., Figueiredo-Barros, M. P., Leal, J. J., Rocha, A. M., Quesado, L. B., Lopes, P. M., Farjalla, V. F., Marinho, C. C., Roland, F., and Esteves, F. A. (2009). Interactive effects of environmental variability and human impacts on the long-term dynamics of an Amazonian floodplain lake and a South Atlantic coastal lagoon. *Limnologia*, 39(4):306–313.
- Callin, W., Jiangshi, Z., Linghua, T., Jinlong, D., Min, Z., Yuxing, Z., T, U., and H, F. (2000). Rice cultivation at the Neolithic Age in Taihu Valley. *Jiangsu Journal of Agricultural Sciences*, 16(3):129–138.
- Cao, H.-S., Kong, F.-X., Luo, L.-C., Shi, X.-L., Yang, Z., Zhang, X.-F., and Tao, Y. (2006). Effects of Wind and Wind-Induced Waves on Vertical Phytoplankton Distribution and Surface Blooms of *Microcystis aeruginosa* in Lake Taihu. *Journal of Freshwater Ecology*, 21(2):231–238.
- Chen, C., Zhong, J. C., Yu, J. H., Shen, Q. S., Fan, C. X., and Kong, F. X. (2016). Optimum dredging time for inhibition and prevention of algae-induced black blooms in Lake Taihu, China. *Environmental Science and Pollution Research*, 23(14):14636–14645.
- Chen, Q., Zhang, C., Recknagel, F., Guo, J., and Blanckaert, K. (2014). Adaptation and multiple parameter optimization of the simulation model SALMO as prerequisite for scenario analysis on a shallow eutrophic Lake. *Ecological Modelling*, 273:109–116.
- Chen, X. (2007). A laterally averaged two-dimensional trajectory model for estimating transport time scales in the Alafia River estuary, Florida. *Estuarine, Coastal and Shelf Science*, 75(3):358–370.
- Chen, Y., Fan, C., Teubner, K., and Dokulil, M. (2003). Changes of nutrients and phytoplankton chlorophyll-a in a large shallow lake, Taihu, China: an 8-year investigation. *Hydrobiologia*, 506-509(1-3):273–279.
- Chengxin, F., Lu, Z., Jianjun, W., Chaohai, Z., Guang, G., and Sumin, W. (2004). Processes and mechanism of effects of sludge dredging on internal source release in lakes. *Chinese Science Bulletin*, 49(17):1853–1859.
- Choi, K. W. and Lee, J. H. (2004). Numerical determination of flushing time for stratified water bodies. *Journal of Marine Systems*, 50(3-4):263–281.

- Chung, E. G., Bombardelli, F. A., and Schladow, S. G. (2009). Modeling linkages between sediment resuspension and water quality in a shallow, eutrophic, wind-exposed lake. *Ecological Modelling*, 220(9-10):1251–1265.
- Codd, G. A., Lindsay, J., Young, F. M., Morrison, L. F., and Metcalf, J. S. (2005). Harmful Cyanobacteria. In *Harmful Cyanobacteria*, pages 1–23. Springer-Verlag, Berlin/Heidelberg.
- Connor, R., Renata, A., Ortigara, C., Koncagül, E., Uhlenbrook, S., Lamizana-Diallo, B. M., Zadeh, S. M., Qadir, M., Kjellén, M., Sjödin, J., and Others (2017). The united nations world water development report 2017. wastewater: The untapped resource. *The United Nations World Water Development Report*.
- Cooke, G. D., Welch, E. B., Peterson, S., and Nichols, S. A. (2016). *Restoration and management of lakes and reservoirs*. CRC press.
- Dai, J., Wu, S., Han, G., Weinberg, J., Xie, X., Wu, X., Song, X., Jia, B., Xue, W., and Yang, Q. (2017). Water-energy nexus: A review of methods and tools for macro-assessment. *Applied Energy*, (August):0–1.
- Dake, J. M. K. and Harleman, D. R. F. (1969). Thermal stratification in lakes: Analytical and laboratory studies. *Water Resources Research*, 5(2):484–495.
- de Brye, B., de Brauwere, A., Gourgue, O., Delhez, E. J., and Deleersnijder, E. (2013). Reprint of Water renewal timescales in the Scheldt Estuary. *Journal of Marine Systems*, 128:3–16.
- Deleersnijder, E., Campin, J. M., and Delhez, E. J. (2001). The concept of age in marine modelling I. Theory and preliminary model results. *Journal of Marine Systems*, 28(3-4):229–267.
- Delhez, E. J., Campin, J. M., Hirst, A. C., and Deleersnijder, E. (1999). Toward a general theory of the age in ocean modelling. *Ocean Modelling*, 1(1):17–27.
- Delhez, É. J., Heemink, A. W., and Deleersnijder, É. (2004). Residence time in a semi-enclosed domain from the solution of an adjoint problem. *Estuarine, Coastal and Shelf Science*, 61(4):691–702.
- Delhez, É. J. M., de Brye, B., de Brauwere, A., and Deleersnijder, É. (2014). Residence time vs influence time. *Journal of Marine Systems*, 132:185–195.
- Deltares (2005). Delft3D-WAQ Users Manual. Technical report.
- Deng, J., Paerl, H. W., Qin, B., Zhang, Y., Zhu, G., Jeppesen, E., Cai, Y., and Xu, H. (2018). Climatically-modulated decline in wind speed may strongly affect eutrophication in shallow lakes. *Science of The Total Environment*, 645:1361–1370.
- Deng, X., Xu, Y., Han, L., Song, S., Yang, L., Li, G., and Wang, Y. (2015a). Impacts of Urbanization on River Systems in the Taihu Region, China. *Water*, 7(12):1340–1358.

- Deng, Y., Daniele, B., Paolo, F., Angela, M., Andrea, C., Yun, Z., and Antonio, M. (2015b). China's Water Environmental Management Towards Institutional Integration. A Review of Current Progress and Constraints vis-a-vis the European Experience. *Journal of Cleaner Production*.
- Ding, Y., Xu, H., Deng, J., Qin, B., and He, Y. (2019). Impact of nutrient loading on phytoplankton: a mesocosm experiment in the eutrophic Lake Taihu, China. *Hydrobiologia*, 829(1):167–187.
- Duan, H., Ma, R., Xu, X., Kong, F., Zhang, S., Kong, W., Hao, J., and Shang, L. (2009). Two-Decade Reconstruction of Algal Blooms in China's Lake Taihu. *Environmental Science & Technology*, 43(10):3522–3528.
- Ellis, E. (1997). Sustainable Traditional Agriculture in the Tai Lake Region of China. *Agriculture, Ecosystems & Environment*, 61(2-3):177–193.
- Endo, A., Tsurita, I., Burnett, K., and Orencio, P. M. (2017). A review of the current state of research on the water, energy, and food nexus. *Journal of Hydrology: Regional Studies*, 11:20–30.
- Falconer, R. A., George, D. G., and Hall, P. (1991). Three Dimensional Numerical Modelling of Wind-driven Circulation in a Shallow Homogeneous Lake. *Journal of Hydrology*, 124:59–79.
- Fan, J. L., Zhang, Y. J., and Wang, B. (2017). The impact of urbanization on residential energy consumption in China: An aggregated and disaggregated analysis. *Renewable and Sustainable Energy Reviews*, 75(October 2016):220–233.
- Fenocchi, A., Petaccia, G., and Sibilla, S. (2016). Modelling flows in shallow (fluvial) lakes with prevailing circulations in the horizontal plane: limits of 2D compared to 3D models. *Journal of Hydroinformatics*, (May):jh2016033.
- Fragoso, C. R., Motta Marques, D. M., Ferreira, T. F., Janse, J. H., and van Nes, E. H. (2011). Potential effects of climate change and eutrophication on a large subtropical shallow lake. *Environmental Modelling & Software*, 26(11):1337–1348.
- Frey, K. E., Perovich, D. K., and Light, B. (2011). The spatial distribution of solar radiation under a melting Arctic sea ice cover. *Geophysical Research Letters*, 38(22):n/a–n/a.
- Gulati, R. D., Pires, L. M. D., and Van Donk, E. (2008). Lake restoration studies: Failures, bottlenecks and prospects of new ecotechnological measures. *Limnologia*, 38(3-4):233–248.
- Guo, L. (2007). ECOLOGY: Doing Battle With the Green Monster of Taihu Lake. *Science*, 317(5842):1166–1166.

- Häder, D.-P., Kumar, H. D., Smith, R. C., and Worrest, R. C. (2007). Effects of solar UV radiation on aquatic ecosystems and interactions with climate change. *Photochem. Photobiol. Sci.*, 6(3):267–285.
- Hamiche, A. M., Stambouli, A. B., and Flazi, S. (2016). A review of the water-energy nexus. *Renewable and Sustainable Energy Reviews*, 65:319–331.
- He, W., Shang, J., Lu, X., and Fan, C. (2013). Effects of sludge dredging on the prevention and control of algae-caused black bloom in Taihu Lake, China. *Journal of Environmental Sciences*, 25(3):430–440.
- Hilt, S., Gross, E. M., Hupfer, M., Morscheid, H., Mählmann, J., Melzer, A., Poltz, J., Sandrock, S., Scharf, E. M., Schneider, S., and van de Weyer, K. (2006). Restoration of submerged vegetation in shallow eutrophic lakes - A guideline and state of the art in Germany. *Limnologia*, 36(3):155–171.
- Hoekstra, A. Y. and Mekonnen, M. M. (2012). The water footprint of humanity. *Proceedings of the National Academy of Sciences*, 109(9):3232–3237.
- Hu, F., Bolding, K., Bruggeman, J., Jeppesen, E., Flindt, M. R., Van Gerven, L., Janse, J. H., Janssen, A. B. G., Kuiper, J. J., Mooij, W. M., and Trolle, D. (2016). FABM-PCLake - Linking aquatic ecology with hydrodynamics. *Geoscientific Model Development*, 9(6):2271–2278.
- Hu, W. (2016). A review of the models for Lake Taihu and their application in lake environmental management. *Ecological Modelling*, 319:9–20.
- Hu, W., Jørgensen, S. E., and Zhang, F. (2006). A vertical-compressed three-dimensional ecological model in Lake Taihu, China. *Ecological Modelling*, 190(3-4):367–398.
- Hu, W., Zhai, S., Zhu, Z., and Han, H. (2008). Impacts of the Yangtze River water transfer on the restoration of Lake Taihu. *Ecological Engineering*, 34(1):30–49.
- Huang, K., Guo, H., Liu, Y., Zhou, F., Yu, Y., and Wang, Z. (2008). Water environmental planning and management at the watershed scale: A case study of Lake Qilu, China. *Frontiers of Environmental Science & Engineering in China*, 2(2):157–162.
- Huisman, J., Sharples, J., Stroom, J. M., Visser, P. M., Kardinaal, W. E. A., Verspagen, J. M. H., and Sommeijer, B. (2004). CHANGES IN TURBULENT MIXING SHIFT COMPETITION FOR LIGHT BETWEEN PHYTOPLANKTON SPECIES. *Ecology*, 85(11):2960–2970.
- Hullebusch, E. V., Deluchat, V., Chazal, P. M., and Baudu, M. (2002). Environmental impact of two successive chemical treatments in a small shallow eutrophied lake: Part II. Case of copper sulfate. *Environmental Pollution*, 120(3):627–634.

- Hulot, F. D., Rossi, M., Verdier, B., Urban, J. P., Blotti re, L., Madricardo, F., and Decenci re, B. (2017). Mesocosms with wavemakers: A new device to study the effects of water mixing on lake ecology. *Limnology and Oceanography: Methods*, 15(2):154–165.
- Jan ula, D. and Mar  alek, B. (2011). Critical review of actually available chemical compounds for prevention and management of cyanobacterial blooms. *Chemosphere*, 85(9):1415–1422.
- Janssen, A. B., de Jager, V. C., Janse, J. H., Kong, X., Liu, S., Ye, Q., and Mooij, W. M. (2017). Spatial identification of critical nutrient loads of large shallow lakes: Implications for Lake Taihu (China). *Water Research*, 119:276–287.
- Janssen, A. B., Teurlincx, S., An, S., Janse, J. H., Paerl, H. W., and Mooij, W. M. (2014). Alternative stable states in large shallow lakes? *Journal of Great Lakes Research*, 40(4):813–826.
- Jenkins, W. and Clarke, W. (1976). The distribution of ^3He in the western Atlantic ocean. *Deep Sea Research and Oceanographic Abstracts*, 23(6):481–494.
- Jeppesen, E., Kronvang, B., Meerhoff, M., S ndergaard, M., Hansen, K. M., Andersen, H. E., Lauridsen, T. L., Liboriussen, L., Beklioglu, M.,  zen, A., and Olesen, J. E. (2009). Climate Change Effects on Runoff, Catchment Phosphorus Loading and Lake Ecological State, and Potential Adaptations. *Journal of Environment Quality*, 38(5):1930.
- Jeppesen, E., Meerhoff, M., Davidson, T. A., Trolle, D., S ndergaard, M., Lauridsen, T. L., Beklioglu, M., Brucet, S., Volta, P., Gonz lez-Bergonzoni, I., and Nielsen, A. (2014). Climate change impacts on lakes: an integrated ecological perspective based on a multi-faceted approach, with special focus on shallow lakes. *Journal of Limnology*, 73(s1):88–111.
- Jeppesen, E., S ndergaard, M., Meerhoff, M., Lauridsen, T. L., and Jensen, J. P. (2007). Shallow lake restoration by nutrient loading reduction - Some recent findings and challenges ahead. *Hydrobiologia*, 584(1):239–252.
- Ji, Z.-G. (2017). *Hydrodynamics and Water Quality*. John Wiley & Sons, Inc., Hoboken, NJ, USA.
- Jin, X. (2003). Analysis of eutrophication state and trend for lakes in China. *Journal of Limnology*, 62(1s):60.
- Jin, X., Xu, Q., and Huang, C. (2005). Current status and future tendency of lake eutrophication in China. *Science in China. Series C, Life sciences*, 48 Suppl 2(948):948–54.
- Johnston, C., Cook, P., Frape, S., Plummer, L., Busenberg, E., and Blackport, R. (1998). Ground Water Age and Nitrate Distribution Within a Glacial Aquifer Beneath a Thick Unsaturated Zone. *Ground Water*, 36(1):171–180.

- Józsa, J. (2014). On the internal boundary layer related wind stress curl and its role in generating shallow lake circulations. *Journal of Hydrology and Hydromechanics*, 62(1):16–23.
- Karlberg, L., Hoff, H., Amsalu, T., Andersson, K., Binnington, T., Flores-López, F., de Bruin, A., Gebrehiwot, S. G., Gedif, B., zur Heide, F., Johnson, O., Osbeck, M., and Young, C. (2015). Tackling complexity: Understanding the food-energy-environment nexus in Ethiopia's lake TANA sub-basin. *Water Alternatives*, 8(1):710–734.
- Karstensen, J. and Tomczak, M. (1998). Age determination of mixed water masses using CFC and oxygen data. *Journal of Geophysical Research: Oceans*, 103(C9):18599–18609.
- Ke, Z., Xie, P., and Guo, L. (2018). Ecological restoration and factors regulating phytoplankton community in a hypertrophic shallow lake, Lake Taihu, China. *Acta Ecologica Sinica*, 39(1):81–88.
- Kenway, S. J., Lant, P. A., Priestley, A., and Daniels, P. (2011). The connection between water and energy in cities: A review. *Water Science and Technology*, 63(9):1983–1990.
- King, K., Balogh, J., and Harmel, R. (2007). Nutrient flux in storm water runoff and baseflow from managed turf. *Environmental Pollution*, 150(3):321–328.
- Kurian, M. (2015). *Governing the Nexus*. Springer International Publishing, Cham.
- Laval, B., Imberger, J., Hodges, B. R., and Stocker, R. (2003). Modeling circulation in lakes: Spatial and temporal variations. *Limnol. Oceanogr*, 48(3):983–994.
- Le, C., Zha, Y., Li, Y., Sun, D., Lu, H., and Yin, B. (2010). Eutrophication of lake waters in China: Cost, causes, and control. *Environmental Management*, 45(4):662–668.
- Le Moal, M., Gascuel-Oudou, C., Ménesguen, A., Souchon, Y., Étrillard, C., Levain, A., Moatar, F., Pannard, A., Souchu, P., Lefebvre, A., and Pinay, G. (2019). Eutrophication: A new wine in an old bottle? *Science of the Total Environment*, 651:1–11.
- Leira, M. and Cantonati, M. (2008). Effects of water-level fluctuations on lakes: An annotated bibliography. *Hydrobiologia*, 613(1):171–184.
- Lewandowski, J., Meinikmann, K., Nützmann, G., and Rosenberry, D. O. (2015). Groundwater - the disregarded component in lake water and nutrient budgets. Part 2: effects of groundwater on nutrients. *Hydrological Processes*, 29(13):2922–2955.
- Li, Y., Acharya, K., and Yu, Z. (2011a). Modeling impacts of Yangtze River water transfer on water ages in Lake Taihu, China. *Ecological Engineering*, 37(2):325–334.

- Li, Y., Tang, C., Wang, C., Anim, D. O., Yu, Z., and Acharya, K. (2013a). Improved Yangtze River Diversions: Are they helping to solve algal bloom problems in Lake Taihu, China? *Ecological Engineering*, 51:104–116.
- Li, Y., Tang, C., Wang, C., Tian, W., Pan, B., Hua, L., Lau, J., Yu, Z., and Acharya, K. (2013b). Assessing and modeling impacts of different inter-basin water transfer routes on Lake Taihu and the Yangtze River, China. *Ecological Engineering*, 60:399–413.
- Li, Y., Wang, Q., Wu, C., Zhao, S., Xu, X., Wang, Y., and Huang, C. (2011b). Estimation of Chlorophyll a Concentration Using NIR/Red Bands of MERIS and Classification Procedure in Inland Turbid Water. *IEEE Transactions on Geoscience and Remote Sensing*, 50(3):988–997.
- Liu, S. (2013). *Numerical modeling of hydrodynamic circulation in Lake Taihu Sien LIU*. PhD thesis.
- Liu, S., Ye, Q., Wu, S., and Stive, M. (2018). Horizontal Circulation Patterns in a Large Shallow Lake: Taihu Lake, China. *Water*, 10(6):792.
- Liu, W.-C., Chen, W.-B., and Hsu, M.-H. (2011). Using a three-dimensional particle-tracking model to estimate the residence time and age of water in a tidal estuary. *Computers & Geosciences*, 37(8):1148–1161.
- Luketina, D. (1998). Simple Tidal Prism Models Revisited. *Estuarine, Coastal and Shelf Science*, 46(1):77–84.
- Madsen, J. D., Chambers, P. A., James, W. F., Koch, E. W., and Westlake, D. F. (2001). The interaction between water movement, sediment dynamics and submersed macrophytes. *Hydrobiologia*, 444:71–84.
- McGowan, S. (2016). Algal Blooms. In *Biological and Environmental Hazards, Risks, and Disasters*, pages 5–43. Elsevier.
- McVicar, T. R., Roderick, M. L., Donohue, R. J., Li, L. T., Van Niel, T. G., Thomas, A., Grieser, J., Jhajharia, D., Himri, Y., Mahowald, N. M., Mescherskaya, A. V., Kruger, A. C., Rehman, S., and Dinpashoh, Y. (2012). Global review and synthesis of trends in observed terrestrial near-surface wind speeds: Implications for evaporation. *Journal of Hydrology*, 416-417:182–205.
- Mersel, M. K., Smith, L. C., Andreadis, K. M., and Durand, M. T. (2013). Estimation of river depth from remotely sensed hydraulic relationships. *Water Resources Research*, 49(6):3165–3179.
- Miller, R. L. and McPherson, B. F. (1991). Estimating estuarine flushing and residence times in Charlotte Harbor, Florida. via salt balance and a box model. *Limnology and Oceanography*, 36(3):602–612.

- Monsen, N. E., Cloern, J. E., Lucas, L. V., and Monismith, S. G. (2002). A comment on the use of flushing time, residence time, and age as transport time scales. *Limnology and Oceanography*, 47(5):1545–1553.
- Mooij, W. M., Hülsmann, S., De Senerpont Domis, L. N., Nolet, B. A., Bodelier, P. L., Boers, P. C., Dionisio Pires, L. M., Gons, H. J., Ibelings, B. W., Noordhuis, R., Portielje, R., Wolfstein, K., and Lammens, E. H. (2005). The impact of climate change on lakes in the Netherlands: A review. *Aquatic Ecology*, 39(4):381–400.
- Morris, W. and Others (1969). *American heritage dictionary of the English language*. American heritage.
- Moss, B., Mckee, D., Atkinson, D., Collings, S. E., Eaton, J. W., Gill, A. B., Harvey, I., Hatton, K., Heyes, T., and Wilson, D. (2003). How important is climate? Effects of warming, nutrient addition and fish on phytoplankton in shallow lake microcosms. *Journal of Applied Ecology*, 40(5):782–792.
- Moss, B., Stansfield, J., Irvine, K., Perrow, M., and Phillips, G. (1996). Progressive Restoration of a Shallow Lake: A 12-Year Experiment in Isolation, Sediment Removal and Biomanipulation. *The Journal of Applied Ecology*, 33(1):71.
- Murakami, K. (1984). DREDGING FOR CONTROLLING EUTROPHICATION OF LAKE KASUMIGAURA, JAPAN. *Lake and Reservoir Management*, 1(1):592–598.
- Murray-Gulde, C. L., Heatley, J. E., Schwartzman, A. L., and Rodgers, Jr., J. H. (2002). Algicidal Effectiveness of Clearigate, Cutrine-Plus, and Copper Sulfate and Margins of Safety Associated with Their Use. *Archives of Environmental Contamination and Toxicology*, 43(1):19–27.
- Nash, J. E. and Sutcliffe, J. V. (1970). River Flow Forecasting Through Conceptual Models Part I-a Discussion of Principles*. *Journal of Hydrology*, 10:282–290.
- Nations, U. (2018). 2018 revision of world urbanization prospects.
- Nazari-Sharabian, M., Ahmad, S., and Karakouzian, M. (2018). Climate Change and Eutrophication: A Short Review. *Engineering, Technology & Applied Science Research*, 8(6):pp. 3668–3672.
- Nutz, A., Schuster, M., Ghienne, J.-F., Roquin, C., and Bouchette, F. (2018). Wind-driven waterbodies: a new category of lake within an alternative sedimentologically-based lake classification. *Journal of Paleolimnology*, 59(2):189–199.
- Oki, T. (2006). Global Hydrological Cycles and World Water Resources. *Science*, 313(5790):1068–1072.
- Oliver, R. L. (1994). FLOATING AND SINKING IN GAS-VACUOLATE CYANOBACTERIA1. *Journal of Phycology*, 30(2):161–173.

- Paerl, H. W., Hall, N. S., and Calandrino, E. S. (2011a). Controlling harmful cyanobacterial blooms in a world experiencing anthropogenic and climatic-induced change. *Science of the Total Environment*, 409(10):1739–1745.
- Paerl, H. W., Xu, H., McCarthy, M. J., Zhu, G., Qin, B., Li, Y., and Gardner, W. S. (2011b). Controlling harmful cyanobacterial blooms in a hyper-eutrophic lake (Lake Taihu, China): The need for a dual nutrient (N & P) management strategy. *Water Research*, 45(5):1973–1983.
- Pangle, L. A., Klaus, J., Berman, E. S. F., Gupta, M., and McDonnell, J. J. (2013). A new multisource and high-frequency approach to measuring $\delta^2\text{H}$ and $\delta^{18}\text{O}$ in hydrological field studies. *Water Resources Research*, 49(11):7797–7803.
- Pastorok, R. A., Ginn, T. C., and Lorenzen, M. W. (1981). *Evaluation of aeration/circulation as a lake restoration technique*. Environmental Research Laboratory, Office of Research and Development, US Environmental Protection Agency.
- Pécseli, H. L., Trulsen, J. K., and Fiksen, Ø. (2014). Predator-prey encounter and capture rates in turbulent environments. *Limnology and Oceanography: Fluids and Environments*, 4(1):85–105.
- Peperzak, L. (2003). Climate change and harmful algal blooms in the North Sea. *Acta Oecologica*, 24(SUPPL. 1):S139–S144.
- Peters, M. (2006). Inhalation of stable dust extract prevents allergen induced airway inflammation and hyperresponsiveness. *Thorax*, 61(2):134–139.
- Poikane, S., Phillips, G., Birk, S., Free, G., Kelly, M. G., and Willby, N. J. (2019). Deriving nutrient criteria to support 'good' ecological status in European lakes: An empirically based approach to linking ecology and management. *Science of The Total Environment*, 650:2074–2084.
- Prairie, J. C., Sutherland, K. R., Nickols, K. J., and Kaltenberg, A. M. (2012). Biophysical interactions in the plankton: A cross-scale review. *Limnology and Oceanography: Fluids and Environments*, 2(1):121–145.
- Qi, H., Lu, J., Chen, X., Sauvage, S., and Sanchez-Pérez, J.-M. (2016). Water age prediction and its potential impacts on water quality using a hydrodynamic model for Poyang Lake, China. *Environmental Science and Pollution Research*, 23(13):13327–13341.
- QIAN, J., Zheng, S.-s., WANG, P.-f., and Wang, C. (2011). Experimental study on sediment resuspension in taihu lake under different hydrodynamic disturbances. *Journal of Hydrodynamics, Ser. B*, 23(6):826–833.
- Qin, B., Paerl, H. W., Brookes, J. D., Liu, J., Jeppesen, E., Zhu, G., Zhang, Y., Xu, H., Shi, K., and Deng, J. (2019). Why Lake Taihu continues to be plagued with cyanobacterial blooms through 10 years (2007–2017) efforts. *Science Bulletin*, 64(6):354–356.

- Qin, B., Xu, P., Wu, Q., Luo, L., and Zhang, Y. (2007). Environmental issues of Lake Taihu, China. *Hydrobiologia*, 581(1):3–14.
- Qin, B., Zhu, G., Gao, G., Zhang, Y., Li, W., Paerl, H. W., and Carmichael, W. W. (2010). A Drinking Water Crisis in Lake Taihu, China: Linkage to Climatic Variability and Lake Management. *Environmental Management*, 45(1):105–112.
- Qiu, D., Wu, Z., Liu, B., Deng, J., Fu, G., and He, F. (2001). The restoration of aquatic macrophytes for improving water quality in a hypertrophic shallow lake in Hubei Province, China. *Ecological Engineering*, 18(2):147–156.
- Rastogi, R. P., Madamwar, D., and Incharoensakdi, A. (2015). Bloom Dynamics of Cyanobacteria and Their Toxins: Environmental Health Impacts and Mitigation Strategies. *Frontiers in Microbiology*, 6(NOV):1–22.
- Reckien, D., Creutzig, F., Fernandez, B., Lwasa, S., Tovar-Restrepo, M., Mcevoy, D., and Satterthwaite, D. (2017). Climate change, equity and the Sustainable Development Goals: an urban perspective. *Environment and Urbanization*, 29(1):159–182.
- Ren, Y., Pei, H., Hu, W., Tian, C., Hao, D., Wei, J., and Feng, Y. (2014). Spatiotemporal distribution pattern of cyanobacteria community and its relationship with the environmental factors in Hongze Lake, China. *Environmental Monitoring and Assessment*, 186(10):6919–6933.
- Romero, E., Peters, F., and Marrasé, C. (2012). Dynamic forcing of coastal plankton by nutrient imbalances and match-mismatch between nutrients and turbulence. *Marine Ecology Progress Series*, 464:69–87.
- Rueda, F. J. and Cowen, E. A. (2005). Residence time of a freshwater embayment connected to a large lake. *Limnology and Oceanography*, 50(5):1638–1653.
- Rueda, F. J., Schladow, S. G., Monismith, S. G., and Stacey, M. T. (2005). On the effects of topography on wind and the generation of currents in a large multi-basin lake. *Hydrobiologia*, 532(1):139–151.
- Scanlon, B. R., Ruddell, B. L., Reed, P. M., Hook, R. I., Zheng, C., Tidwell, V. C., and Siebert, S. (2017). The food-energy-water nexus: Transforming science for society. *Water Resources Research*, 53(5):3550–3556.
- Scavia, D., David Allan, J., Arend, K. K., Bartell, S., Beletsky, D., Bosch, N. S., Brandt, S. B., Briland, R. D., Daloğlu, I., DePinto, J. V., Dolan, D. M., Evans, M. A., Farmer, T. M., Goto, D., Han, H., Höök, T. O., Knight, R., Ludsin, S. A., Mason, D., Michalak, A. M., Peter Richards, R., Roberts, J. J., Rucinski, D. K., Rutherford, E., Schwab, D. J., Sesterhenn, T. M., Zhang, H., and Zhou, Y. (2014). Assessing and addressing the re-eutrophication of Lake Erie: Central basin hypoxia. *Journal of Great Lakes Research*, 40(2):226–246.
- Scheffer, M. (2004). *Ecology of Shallow Lakes*, volume 68. Springer Netherlands, Dordrecht.

- Scheffer, M., Carpenter, S., Foley, J. a., Folke, C., and Walker, B. (2001). Catastrophic shifts in ecosystems. *Nature*, 413(6856):591–596.
- Schindler, D. W. (2012). The dilemma of controlling cultural eutrophication of lakes. *Proceedings of the Royal Society B: Biological Sciences*, 279(1746):4322–4333.
- Schoen, J. H., Stretch, D. D., and Tirok, K. (2014). Wind-driven circulation patterns in a shallow estuarine lake: St Lucia, South Africa. *Estuarine, Coastal and Shelf Science*, 146:49–59.
- Shen, J., Yuan, H., Liu, E., Wang, J., and Wang, Y. (2011). Spatial distribution and stratigraphic characteristics of surface sediments in Taihu Lake, China. *Chinese Science Bulletin*, 56(2):179–187.
- Shuwen, Y., Hui, Y., Lulu, Z., Jun, X., and Zhenping, W. (2011). Water quantity and pollutant fluxes of inflow and outflow rivers of Lake Taihu, 2009. *Journal of Lake Sciences*, 23(6):855–862.
- Sierp, M. T., Qin, J. G., and Recknagel, F. (2009). Biomanipulation: a review of biological control measures in eutrophic waters and the potential for Murray cod *Maccullochella peelii peelii* to promote water quality in temperate Australia. *Reviews in Fish Biology and Fisheries*, 19(2):143–165.
- Simionato, C. G., Dragani, W., Meccia, V., and Nuñez, M. (2004). A numerical study of the barotropic circulation of the Río de la Plata estuary: Sensitivity to bathymetry, the Earth's rotation and low frequency wind variability. *Estuarine, Coastal and Shelf Science*, 61(2):261–273.
- Smith, D. R., King, K. W., and Williams, M. R. (2015). What is causing the harmful algal blooms in Lake Erie? *Journal of Soil and Water Conservation*, 70(2):27A–29A.
- Smith, S. D. and Banke, E. G. (1975). Variation of the sea surface drag coefficient with wind speed. *Quarterly Journal of the Royal Meteorological Society*, 101(429):665–673.
- Smith, V., Tilman, G., and Nekola, J. (1999). Eutrophication: impacts of excess nutrient inputs on freshwater, marine, and terrestrial ecosystems. *Environmental Pollution*, 100(1-3):179–196.
- Stocker, T. F., Qin, D., Plattner, G.-K., Tignor, M., Allen, S. K., Boschung, J., Nauels, A., Xia, Y., Bex, V., Midgley, P. M., and Others (2014). *Climate Change 2013 - The Physical Science Basis*. Cambridge University Press, Cambridge.
- Strand, J. A. and Weisner, S. E. (2001). Dynamics of submerged macrophyte populations in response to biomanipulation. *Freshwater Biology*, 46(10):1397–1408.
- Strub, P. T. and Powell, T. M. (1986). Wind-driven surface transport in stratified closed basins: Direct versus residual circulations. *Journal of Geophysical Research*, 91(C7):8497.

- Strub, P. T. and Powell, T. M. (1987). Surface temperature and transport in Lake Tahoe: inferences from satellite (AVHRR) imagery. *Continental Shelf Research*, 7(9):1001–1013.
- Su, W., Ye, G., Yao, S., and Yang, G. (2014). Urban land pattern impacts on floods in a new district of China. *Sustainability (Switzerland)*, 6(10):6488–6508.
- Sun, W., Chen, W., and Jin, Z. (2019). Spatial Function Regionalization Based on an Ecological-economic Analysis in Wuxi City, China. *Chinese Geographical Science*, 29(2):352–362.
- Sun, X., Xiong, S., Zhu, X., Zhu, X., Li, Y., and Li, B. L. (2015). A new indices system for evaluating ecological-economic-social performances of wetland restorations and its application to Taihu Lake Basin, China. *Ecological Modelling*, 295:216–226.
- U.S. Army Corps of Engineers (2004). UpperMississippi River SystemFlow Frequency Study: Final Report.
- Vautard, R., Cattiaux, J., Yiou, P., Thépaut, J. N., and Ciais, P. (2010). Northern Hemisphere atmospheric stilling partly attributed to an increase in surface roughness. *Nature Geoscience*, 3(11):756–761.
- Wang, H., Guo, X., Liu, Z., and Gao, H. (2015). A comparative study of CART and PTM for modelling water age. *Journal of Ocean University of China*, 14(1):47–58.
- Wang, M., Strokal, M., Burek, P., Kroeze, C., Ma, L., and Janssen, A. B. (2019). Excess nutrient loads to Lake Taihu: Opportunities for nutrient reduction. *Science of The Total Environment*, 664:865–873.
- WANG, X.-l., LU, Y.-l., HAN, J.-y., HE, G.-z., and WANG, T.-y. (2007). Identification of anthropogenic influences on water quality of rivers in Taihu watershed. *Journal of Environmental Sciences*, 19(4):475–481.
- Whitehead, P. G., Wilby, R. L., Battarbee, R. W., Kernan, M., and Wade, A. J. (2009). A review of the potential impacts of climate change on surface water quality. *Hydrological Sciences Journal*, 54(1):101–121.
- Williamson, C. E., Zepp, R. G., Lucas, R. M., Madronich, S., Austin, A. T., Ballaré, C. L., Norval, M., Sulzberger, B., Bais, A. F., McKenzie, R. L., Robinson, S. A., Häder, D.-P., Paul, N. D., and Bornman, J. F. (2014). Solar ultraviolet radiation in a changing climate. *Nature Climate Change*, 4(6):434–441.
- Willmott, C. J. (1981). On the validation of models. *Physical Geography*, 2(2):184–194.
- Wu, L., Gao, J. E., Ma, X. Y., and Li, D. (2015). Application of modified export coefficient method on the load estimation of non-point source nitrogen and phosphorus pollution of soil and water loss in semiarid regions. *Environmental Science and Pollution Research*, 22(14):10647–10660.

- Wu, T., Qin, B., Zhu, G., Luo, L., Ding, Y., and Bian, G. (2013). Dynamics of cyanobacterial bloom formation during short-term hydrodynamic fluctuation in a large shallow, eutrophic, and wind-exposed Lake Taihu, China. *Environmental Science and Pollution Research*, 20(12):8546–8556.
- Wu, Z., Lai, X., Zhang, L., Cai, Y., and Chen, Y. (2014). Phytoplankton chlorophyll a in Lake Poyang and its tributaries during dry, mid-dry and wet seasons: a 4-year study. *Knowledge and Management of Aquatic Ecosystems*, (412):06.
- Wüest, A. and Lorke, A. (2003). Small Scale Hydrodynamics in Lakes. *Annual Review of Fluid Mechanics*, 35(1):373–412.
- Wunsch, C. (2002). Oceanic age and transient tracers: Analytical and numerical solutions. *Journal of Geophysical Research*, 107(C6):3048.
- Xie, X., Jia, B., Han, G., Wu, S., Dai, J., and Weinberg, J. (2018). A historical data analysis of water-energy nexus in the past 30 years urbanization of Wuxi city, China. *Environmental Progress & Sustainable Energy*, 37(1):46–55.
- Xu, H., Paerl, H. W., Qin, B., Zhu, G., Hall, N. S., and Wu, Y. (2015a). Determining Critical Nutrient Thresholds Needed to Control Harmful Cyanobacterial Blooms in Eutrophic Lake Taihu, China. *Environmental Science & Technology*, 49(2):1051–1059.
- Xu, J., Chen, Y., Zheng, L., Liu, B., Liu, J., and Wang, X. (2018). Assessment of Heavy Metal Pollution in the Sediment of the Main Tributaries of Dongting Lake, China. *Water*, 10(8):1060.
- Xu, X., Li, W., Fujibayashi, M., Nomura, M., Nishimura, O., and Li, X. (2015b). Asymmetric response of sedimentary pool to surface water in organics from a shallow hypereutrophic lake: The role of animal consumption and microbial utilization. *Ecological Indicators*, 58:346–355.
- Yang, S.-Q. and Liu, P.-W. (2010). Strategy of water pollution prevention in Taihu Lake and its effects analysis. *Journal of Great Lakes Research*, 36(1):150–158.
- Yang, X., Wei, X., Xu, X., Zhang, Y., Li, J., and Wan, J. (2019). Characteristics of Dissolved Organic Nitrogen in the Sediments of Six Water Sources in Taihu Lake, China. *International Journal of Environmental Research and Public Health*, 16(6):929.
- Yao, H., Li, W., and Qian, X. (2015). Identification of major risk sources for surface water pollution by risk indexes (RI) in the multi-provincial boundary region of the taihu basin, China. *International Journal of Environmental Research and Public Health*, 12(8):10150–10170.
- You, B. S., Zhong, J. C., Fan, C. X., Wang, T. C., Zhang, L., and Ding, S. M. (2007). Effects of hydrodynamics processes on phosphorus fluxes from sediment in large, shallow Taihu Lake. *Journal of Environmental Sciences*, 19:1055–1060.

- Yu, G., Xue, B., Lai, G., Gui, F., and Liu, X. (2007). A 200-year historical modeling of catchment nutrient changes in Taihu basin, China. *Hydrobiologia*, 581(1):79–87.
- Yu, Y., Wang, X., Yang, D., Lei, B., Zhang, X., and Zhang, X. (2014). Evaluation of human health risks posed by carcinogenic and non-carcinogenic multiple contaminants associated with consumption of fish from Taihu Lake, China. *Food and chemical toxicology : an international journal published for the British Industrial Biological Research Association*, 69:86–93.
- Zarzuelo, C., Díez-Minguito, M., Ortega-Sánchez, M., López-Ruiz, A., and Losada, M. T. (2015). Hydrodynamics response to planned human interventions in a highly altered embayment: The example of the Bay of Cádiz (Spain). *Estuarine, Coastal and Shelf Science*, 167:75–85.
- Zhai, S., Hu, W., and Zhu, Z. (2010). Ecological impacts of water transfers on Lake Taihu from the Yangtze River, China. *Ecological Engineering*, 36(4):406–420.
- Zhang, H., Culver, D. A., and Boegman, L. (2008). A two-dimensional ecological model of Lake Erie: Application to estimate dreissenid impacts on large lake plankton populations. *Ecological Modelling*, 214(2-4):219–241.
- Zhang, H., Hu, W., Gu, K., Li, Q., Zheng, D., and Zhai, S. (2013). An improved ecological model and software for short-term algal bloom forecasting. *Environmental Modelling & Software*, 48:152–162.
- Zhang, L., Li, K., Liu, Z., and Middelburg, J. J. (2010). Sedimented cyanobacterial detritus as a source of nutrient for submerged macrophytes (*Vallisneria spiralis* and *Elodea nuttallii*): An isotope labeling experiment using ^{15}N . *Limnology and Oceanography*, 55(5):1912–1917.
- Zhang, Q., Jiang, T., Gemmer, M., and Becker, S. (2005). Precipitation, temperature and runoff analysis from 1950 to 2002 in the Yangtze basin, China / Analyse des précipitations, températures et débits de 1950 à 2002 dans le bassin du Yangtze, en Chine. *Hydrological Sciences Journal*, 50(1):65–80.
- Zhang, X.-Y. (1995). *Ocean outfall modeling—interfacing near and far field models with particle tracking method*. PhD thesis, Massachusetts Institute of Technology.
- Zhang, Y., Lin, S., Qian, X., Wang, Q., Qian, Y., Liu, J., and Ge, Y. (2011). Temporal and spatial variability of chlorophyll a concentration in Lake Taihu using MODIS time-series data. *Hydrobiologia*, 661(1):235–250.
- Zheng, S.-s., WANG, P.-f., Wang, C., and Hou, J. (2015). Sediment resuspension under action of wind in Taihu Lake, China. *International Journal of Sediment Research*, 30(1):48–62.
- Zhou, J., Qin, B., Casenave, C., Han, X., Yang, G., Wu, T., Wu, P., and Ma, J. (2015). Effects of wind wave turbulence on the phytoplankton community composition in large, shallow Lake Taihu. *Environmental Science and Pollution Research*, 22(16):12737–12746.

Curriculum Vitæ

Sien LIU

Sien Liu was born on 20th of Jan 1989 in Nanjing, Jiangsu Province in China. He started his undergraduate at Hohai University in Nanjing, China, majoring Harbour, Waterway and Coastal Engineering from 2007 to 2011. After obtaining his BSc. Degree in 2011, he was granted "TU Delft Excellence Scholarship" and went to Technology University of Delft, the Netherlands, for his MSc. Degree in Hydraulic Engineering, major in Coastal Engineering. In 2014, he continued his study in Technology University of Delft, the Netherlands as a PhD candidate with "CSC scholarship" and "Het Lamminga Fonds", following the supervision of Prof. Marcel Stive, Prof. Zhengbing Wang and Dr. Qinghua Ye.

List of Publications

1. **Liu, S.**, Ye, Q., Wu, S., & Stive, M. J. (2018). Horizontal circulation patterns in a large shallow lake: Taihu Lake, China. *Water*, 10 (6), 792.
2. **Liu, S.**, Ye, Q., Wu, S., & Stive, M. J. (2020). Wind Effects on the Water Age in a Large Shallow Lake. *Water*, 12 (5), 1246.
3. Janssen, A. B., de Jager, V. C., Janse, J. H., Kong, X., **Liu, S.**, Ye, Q., & Mooij, W. M. (2017). Spatial identification of critical nutrient loads of large shallow lakes: implications for Lake Taihu (China). *Water research*, 119, 276-287.
4. Van Gerven, L., Brederveld, R. J., de Klein, J. J., ...**Liu, S.**, ... & Jeuken, M. (2015). Advantages of concurrent use of multiple software frameworks in water quality modelling using a database approach. *Fundamental and Applied Limnology/Archiv fur Hydrobiologie*, 186(1-2), 5-20.

Acknowledgements

The past years in TU Delft have been a great memory for which I'm very grateful. During the period, I have shared my time with many people who contribute to my research and my life. This thesis could not be possible to complete without the support and guidance from them and I wish to acknowledge at this time.

Doing a PhD is not only knowledge gaining process, but also the way to be a better person. First, I would like to express my sincere thanks to my promotor, Prof. Marcel Stive, not only for providing me this opportunity to study in TU Delft, but also to let me know how scientific researchers devote their enthusiasm to their works. Your expertise, passion and guidance always shed light on my studies when I feel confused. Your unlimited trust and encouragement during all these years always kept me optimistic, both about research and life. I'm also very thankful for letting me the freedom to do research that I would like to do even it is already not in the field of coastal engineering. Sometimes I just feel I'm too lucky to have you as my promoter.

I would like to address my special thanks to Dr. Qinghua YE. We have been supervisor and student ever since I was a master student back to 8 years ago. You are always there, encouraging, pushing and guiding me. Your valuable comments and insightful discussion not only help with this thesis, but also widen my research from many perspectives. When I am not confident about my studies, you are always the first one to give me confidence. Sometimes we work till everyone else has left the faculty building but you never complain. You also help me a lot with my life, thank you a lot for being my supervisor, Qinghua.

I would like also to thank Prof. Wang to be my promoter, for your kindly support for me to gain financial support from Lamminga funds. Your rigorous attitude toward scientific research always encourage me to forge ahead for a scientific career. We didn't have much discussion about my work, but every time we talked, I just felt more inspired and confident to move on with my study.

Next, I gratefully acknowledge Professor Shiqiang Wu from Nanjing Hydraulic Research Institute for the help during my research. You give me a lot of help with the opportunity to take part in the joint China-Dutch-Sweden research program about Water Energy Nexus. Discussion with you provides a lot of insights and perspectives on my research.

I would also like to thank Jiangyu Dai, Xinghua Xie for the discussion of Water Energy Nexus projects, and Lei Yu for the assistance in experiments. My great acknowledgment is extended to my colleagues from TU Delft and friends in Delft. Thanks, Mariette van Tilburg for reviewing my manuscripts. I've learned a lot from your revisions. I thank Anh, Runxiang, Yujian, Hassan and Su as office roommates, talks between us always inspire me both from research and life perspectives. Special thanks also goes to our Chinese student lunch team, Peng Yao, Min Su, Lixia Niu,

Yang Zhou, Rong Zhang, Qian Ke, Chunyan Zhu, Jiangliang Lin, Kuai Yu, Lian Liu, Yuning Zhang, and Zaiyang Zhou. Talks during lunch and spare time we spent together is really relaxing and gives me a lot of good memories. Special thanks to my dearest friends, Mengyang Li, Shuai Lv, Xiuhan Chen, and Sida Liu, for sharing the enjoyable moments with me.

I would like to give my special thanks and express my heartfelt appreciation to my families for their unconditional love and full support: my grandparents, my parents, my uncle and aunt. Their love always accompanied me and provided me with spiritual power. Finally, I acknowledge the financial support from "the China Scholarship Council (CSC)", "Het Lamminga Fonds" and funds from NHRI and Deltares.

Sien Liu
October 2019